2-DIMENSIONAL "PARTICLE-IN-A-BOX" PROBLEMS IN QUANTUM MECHANICS

Part I: Propagator & eigenfunctions by the method of images

Nicholas Wheeler, Reed College Physics Department
July 1997

Introduction. All strings make the same music, and support the same physics, because all strings have the same shape. The vibrational physics of a drumhead is, on the other hand, shape-dependent—whence Mark Kac' famous question: "Can one hear the shape of a drum?"[1] Relatedly, all instances of the quantum mechanical "particle-in-a-box" problem are, in the one-dimensional case, scale-equivalent to one another, but higher-dimensional instances of the same problem are (in general) inequivalent.

Though the one-dimensional box-problem yields quite readily to exact closed-form analysis—the simplest (but only the simplest!) aspects of which can be found in every quantum text—the higher-dimensional problem ($N \geq 2$) is in most of its aspects analytically intractable except in certain special cases. In previous work[2] I have identified a class of cases that yield to analysis by what might be called the "quantum mechanical method of images." I undertake the present review of the essentials of that work partly to make it more readily available to students of quantum mechanics, but mainly to be responsive to an expressed need of my colleague Oz Bonfim, who speculates that some of my results may be relevent to his own work in connection with the so-called "Bohm interpretation of quantum mechanics."[3] I have also an ulterior motivation,

[1] Amer. Math. Monthly **73**, 1 (1966). This classic paper is reprinted in *Mark Kac: Selected Papers on Probability, Number Theory & Statistical Physics* (1979)

[2] FEYNMAN FORMALISM FOR POLYGONAL DOMAINS (1971–1976); CIRCULAR BOXES & RIGID WAVEPACKETS (1977–1980).

[3] See P. R. Holland, *The Quantum Theory of Motion: An Account of the de Broglie-Bohm Causal Interpretation of Quantum Mechanics* (1993).

which will from time to time serve invisibly to shape my remarks: I plan soon to examine aspects of the problem of doing quantum mechanics in *curved* space, and imagine some of this material to stand preliminary to some of that.

1. Review of the one-dimensional box problem. A mass point m is confined by infinite forces to the interior $0 \leq x \leq a$ of an interval, within which it moves freely. The "infinite square well potential potential" standardly associated with this problem

$$U(x) = \begin{cases} \infty & x < 0 \\ 0 & 0 \leq x \leq a \\ \infty & a < x \end{cases}$$

is such a singular object as to be (though it can be considered to be the endpoint of a limiting process) in reality scarcely more than a figure of speech, a mnemonic for remembering conditions which we are prepared to impose "by hand" upon the wave function. The time-independent Schrödinger reads

$$\psi''(x) = -k^2\psi(x) \quad \text{with} \quad k \equiv \sqrt{\frac{2mE}{\hbar^2}}$$

and the physically acceptable solutions are required

- to be continuous
- to vanish outside the interval $[0, a]$
- to be normalized.

An elementary argument leads fairly immediately to the familiar eigenfunctions

$$\psi_n(x) = \sqrt{\frac{2}{a}} \sin k_n x \quad \text{with} \quad k_n \equiv \frac{n\pi}{a} \quad : \quad n = 1, 2, 3, \ldots \tag{1}$$

and to the associated energy eigenvalues

$$E_n = \frac{\hbar^2}{2m} k_n^2 = \mathcal{E}\, n^2 \quad \text{with} \quad \mathcal{E} \equiv \frac{h^2}{8ma^2} \tag{2}$$

Here as generally, the connection between quantum statics and quantum dynamics is established by the (Green's function or) "propagator," which is assembled from static data

$$K(x, t; y, 0) = \sum_{n=1}^{\infty} e^{-\frac{i}{\hbar} E_n t} \psi_n(x) \psi_n^*(y) \tag{3}$$

but permits one (in the absence of intervening measurement processes) to write

$$\psi(x, 0) \longrightarrow \psi(x, t) = \int K(x, t; y, 0) \psi(y, 0)\, dy \tag{4}$$

in description of the temporal evolution of the initial state $\psi(x, 0)$. If, in particular, $\psi(x, 0) = \psi_n(x)$ then it follows from (4) by the orthonormality of the eigenfunctions ($\int \psi_m^*(y) \psi_n(y)\, dy = \delta_{mn}$) that

$$\psi(x, t) = e^{-\frac{i}{\hbar} E_n t} \psi(x, 0) \quad \text{and} \quad |\psi(x, t)|^2 \text{ is } t\text{-independent}$$

but in less specialized cases $\psi(x,t)$ does not simply "buzz harmonically" (like a string in one of its harmonic modes) and the probability density $|\psi(x,t)|^2$ is launched into actual motion. Asymptotically we expect to lose all knowledge of the initial state of the system, and to obtain

$$|\psi(x)|^2 \xrightarrow[t\to\infty]{} 1/a$$

Returning now from generalities to the specifics of the particle-in-a-box problem at hand, one has only to introduce (1) and (2) into (3) to obtain

$$K(x,t;y,0) = \frac{2}{a}\sum_{n=1}^{\infty} \sin n\pi\frac{x}{a}\cdot\sin n\pi\frac{y}{a}\cdot\exp\Big\{-\frac{i}{\hbar}\mathcal{E}n^2t\Big\} \tag{5.1}$$

$$= \frac{1}{a}\sum_{n=1}^{\infty} \underbrace{2\sin n\xi\cdot\sin n\zeta}\cdot\exp\Big\{-i\beta n^2\Big\}$$

$$= \cos n(\xi-\zeta) - \cos n(\xi+\zeta)$$

$$= \frac{1}{a}\sum_{n=1}^{\infty} e^{-i\beta n^2}\cos n(\xi-\zeta) - \frac{1}{a}\sum_{n=1}^{\infty} e^{-i\beta n^2}\cos n(\xi+\zeta) \tag{5.2}$$

where the dimensionless variables ξ, ζ and β are defined

$$\xi \equiv \pi x/a \qquad \zeta \equiv \pi y/a \qquad \beta \equiv \mathcal{E}t/\hbar \tag{6}$$

Further progress is greatly facilitated by the observation that we have at this point established contact with the inexhaustibly rich *theory of theta functions*.[4] These functions come to us in four flavors, but it is only in $\vartheta_3(z,q)$ that—as it turns out—we have specific interest, so I will drop the identifying subscript. By definition[5]

$$\vartheta(z,\tau) = 1 + 2\sum_{n=1}^{\infty} q^{n^2}\cos 2nz \qquad \text{with} \qquad q = e^{i\pi\tau} \tag{7}$$

[4] This theory is the creation of C. G. Jacobi (1804–1851), and was presented to the world in his youthful *Fundamenta nova theoriae functionum ellipticum* (1829). The theory was originally devised as an aid to the development of what are now called "Jacobian elliptic functions" (see, for example, Chapter 16 of Abramowitz & Stegun), but is now recognized to have intimate connections with virtually the whole of higher analysis; Richard Bellman, in his wonderful little book *A Brief Introduction to Theta Functions*, has provided a valuable survey of the field, in all its incredible variety.

[5] See Abramowitz & Stegun **16.27** or Bellman's §2. Confusingly, some sources (see, for example, *Encyclopedic Dictionary of Mathematics* (1987) p. 529, or Magnus & Oberhettinger, p. 98) adopt—as did I in the old material upon which I base the present discussion—the variant definition

$$\vartheta(z,\tau) = 1 + 2\sum_{n=1}^{\infty} q^{n^2}\cos 2n\pi z$$

in which notation (5.2) reads

$$K(x,t;y,0) = \tfrac{1}{2a}\big[\vartheta\big(\tfrac{\xi-\zeta}{2},-\tfrac{\beta}{\pi}\big)-1\big] - \tfrac{1}{2a}\big[\vartheta\big(\tfrac{\xi+\zeta}{2},-\tfrac{\beta}{\pi}\big)-1\big]$$
$$= \tfrac{1}{2a}\big[\vartheta\big(\tfrac{\xi-\zeta}{2},-\tfrac{\beta}{\pi}\big) - \vartheta\big(\tfrac{\xi+\zeta}{2},-\tfrac{\beta}{\pi}\big)\big] \tag{8}$$

Bellman remarks in his §4 that “the theta functions satisfy a host of recondite transformation formulas”[6] of which “one of the most fascinating” reads

$$\vartheta(z,\tau) = A\cdot\vartheta\Big(\frac{z}{\tau},-\frac{1}{\tau}\Big) \qquad \text{where} \qquad A \equiv \sqrt{i/\tau}\, e^{z^2/i\pi\tau} \tag{9}$$

Concerning this simple-looking formula—which some authors call “Jacobi’s imaginary transformation”—Bellman writes that it

> *has amazing ramifications in the fields of algebra, number theory, geometry, and other parts of mathematics. In fact, it is not easy to find another identity of comparable significance. We shall make some effort in coming pages to justify this apparently extravant statement.*

My own effort in coming pages may serve to demonstrate that (9) has important applications also to quantum mechanics, where it encapsulates the relationship between the standard (Hamiltonian) formalism and Feynman’s (Lagrangian based) sum-over-paths formalism.

It follows by $2\cos 2nz = e^{i2nz} + e^{-i2nz}$ from (7) that

$$\vartheta(z,\tau) = \sum_{-\infty}^{\infty} e^{i(\pi\tau n^2 - 2nz)}$$
$$= \sqrt{i/\tau}\, e^{z^2/i\pi\tau}\cdot\sum_{-\infty}^{\infty}\exp\Big\{-i\Big(\frac{\pi n^2}{\tau}+\frac{2nz}{\tau}\Big)\Big\} \quad \text{by (9)}$$
$$= \sqrt{\tfrac{i}{\tau}}\sum_{-\infty}^{\infty}\exp\Big\{-\frac{i\pi}{\tau}\Big(\frac{z}{\pi}+n\Big)^2\Big\} \tag{10}$$

Returning with this result to (8) we have

$$K(x,t;y,0) = \sqrt{\tfrac{-i\pi}{4a^2\beta}}\sum_{-\infty}^{\infty}\Big[\exp\Big\{\frac{i\pi^2}{\beta}\Big(\frac{\xi-\zeta}{2\pi}+n\Big)^2\Big\} - \exp\Big\{\frac{i\pi^2}{\beta}\Big(\frac{\xi+\zeta}{2\pi}+n\Big)^2\Big\}\Big]$$
$$= \sqrt{\tfrac{m}{iht}}\sum_{-\infty}^{\infty}\Big[\exp\Big\{\frac{i}{\hbar}\frac{m(x-y+2an)^2}{2t}\Big\} - \exp\Big\{\frac{i}{\hbar}\frac{m(x+y+2an)^2}{2t}\Big\}\Big] \tag{11}$$
$$= \sqrt{\tfrac{m}{iht}}\exp\Big\{\frac{i}{\hbar}\frac{m}{2}\frac{(x-y)^2}{t}\Big\} + \text{infinite sum of similar terms} \tag{12}$$

It is to facilitate interpetation of the isolated term—and by extension of the others—that I digress now to review some aspects of the classical/quantum dynamics of an *unconstrained* free particle.

---

[6] For a representative sample see p. 99 of Magnus & Oberhettinger.

Hamilton's Principle assigns dynamical significance to the spacetime path (or paths)

$$x(t) \quad : \quad (x,t) \xleftarrow[\text{path}]{\qquad\qquad} (y,0)$$

which extremize the action functional

$$S[\text{path}] \equiv \int_0^t L\big(\dot{x}(t'), x(t')\big)\, dt'$$

S[dynamical path] is a (possibly multiple-valued) function of the endpoints

$$S(x,t;y,0) \equiv S[(x,t) \xleftarrow[\text{dynamical path}]{\qquad\qquad} (y,0)]$$

called the "2-point action function" (or sometimes by me, in my admittedly idiosyncratic terminology, the "dynamical action"). $S(x,t;\bullet,\bullet)$ is a solution of the Hamilton-Jacobi equation

$$H(S_x, x) + S_t = 0$$

where $S_x \equiv \partial S/\partial x$, $S_t \equiv \partial S/\partial t$. For a free particle one has $L(\dot{x},x) = \frac{1}{2}m\dot{x}^2$ so Hamilton's principle supplies $m\ddot{x} = 0$ of which the (solitary) solution is

$$x(t') = y + vt' \quad \text{with} \quad v \equiv \frac{x-y}{t} \quad : \quad (x,t) \xleftarrow[\text{unconstrained free motion}]{\qquad\qquad} (y,0)$$

The "dyanamical action" function for such a system is given therefore by

$$S_{\text{free}}(x,t;y,0) = \int_0^t \tfrac{1}{2}mv^2\, dt' = \frac{m}{2}\frac{(x-y)^2}{t} \tag{13.1}$$

and is a solution of

$$\frac{1}{2m}\Big(\frac{\partial S}{\partial x}\Big)^2 + \frac{\partial S}{\partial t} = 0$$

The so-called "Van Vleck determinant"

$$D(\boldsymbol{x},t;\boldsymbol{y},0;) \equiv \det\left\|\frac{\partial^2 S}{\partial x^i \partial y^j}\right\|$$

—which figures importantly in the higher-dimensional generalization[7] of the material here under review—reduces in the present instance to the simple expression

$$D_{\text{free}} = -\frac{m}{t} \tag{13.2}$$

Equations (13) put us in position to recognize that the term which stands isolated on the right side of (12) can be written

$$\begin{aligned}\sqrt{\tfrac{m}{iht}}\exp\Big\{\frac{i}{\hbar}\frac{m}{2}\frac{(x-y)^2}{t}\Big\} &= \sqrt{\tfrac{i}{\hbar}D_{\text{free}}}\cdot\exp\Big\{\frac{i}{\hbar}S_{\text{free}}(x,t;y,0)\Big\} \\ &= K_{\text{free}}(x,t;y,0) \\ &= \int_{-\infty}^{+\infty} e^{-\frac{i}{\hbar}E(p)t}\psi_p(x)\psi_p^*(y)\, dp \end{aligned} \tag{14}$$

[7] See Chapter I, p.88 of QUANTUM MECHANICS (1967).

where $E(p) \equiv \frac{1}{2m}p^2$ and $\psi_p(x) \equiv \frac{1}{\sqrt{h}}\exp\left\{\frac{i}{\hbar}px\right\}$ refer familiarly to the standard quantum mechanics of a free particle.

Look now to the classical mechanics of a *confined* free particle. For such a system there exist *multiple* dynamical paths $(x,t) \longleftarrow (y,0)$, which is to say: the action functional S[path] possesses multiple extrema; in addition to the "direct" path there are "n-bounce paths" of two types—those that bounce first off the barrier at $x = 0$ and those that bounce first off the barrier at $x = a$. Details relating to the design of that infinitude of dynamical paths is greatly facilitated by the "barber shop construction" known as the "method of images" (see Figures 1 & 2). It emerges that paths are classified most usefully not by their handedness (i.e., by whether the first bounce is left or right) but by their parity (i.e., by whether the number of bounces experienced by the particle is even or odd), for this reason:

$$\begin{aligned}
\text{paths of } \textit{even parity} \text{ have lengths} &= |x - y + 2na| \quad : \quad n = 0, \pm1, \pm2, \ldots \\
\text{paths of } \textit{odd parity} \text{ have lengths} &= |(x - y + 2na) + 2(a - x)| \\
&= |x + y + 2na| \quad : \quad n = 0, \pm1, \pm2, \ldots
\end{aligned}$$

It makes sense on these grounds to speak of "the even/odd path of order n," and it makes tentative good sense, on the basis of (13.1), to write

$$\begin{aligned}
S[\text{even path of order } n] &= \frac{m}{2}\frac{(x - y + 2na)^2}{t} \\
S[\text{ odd path of order } n] &= \frac{m}{2}\frac{(x + y + 2na)^2}{t}
\end{aligned}$$

in which notation (11) assumes the following very striking form:

$$\begin{aligned}
K(x,t;y,0) &= \sqrt{\frac{m}{iht}}\sum_{n=-\infty}^{\infty}\left\{e^{\frac{i}{\hbar}S[\text{even path of order } n]} - e^{\frac{i}{\hbar}S[\text{odd path of order } n]}\right\} \\
&= \sum_{\text{all paths}}(-)^{\text{number of reflections}}\sqrt{\frac{m}{iht}}\,e^{\frac{i}{\hbar}S[\text{classical path}]} \qquad (15)
\end{aligned}$$

The result just achieved raises this obvious question: Why the minus sign? It is in the first place a clear implication of (11) that the minus sign is essential if we are to achieve

$$K(x,t;y,0) = 0 \ \text{ when either } x \text{ or } y \text{ lies at either endpoint}$$

Its presence admits, however, of interpretation on other grounds. Suppose the classical action were to exhibit a jump discontinuity

$$S \longrightarrow S + \Delta S$$

at each reflection point. We would then recover (15) if it were the case that

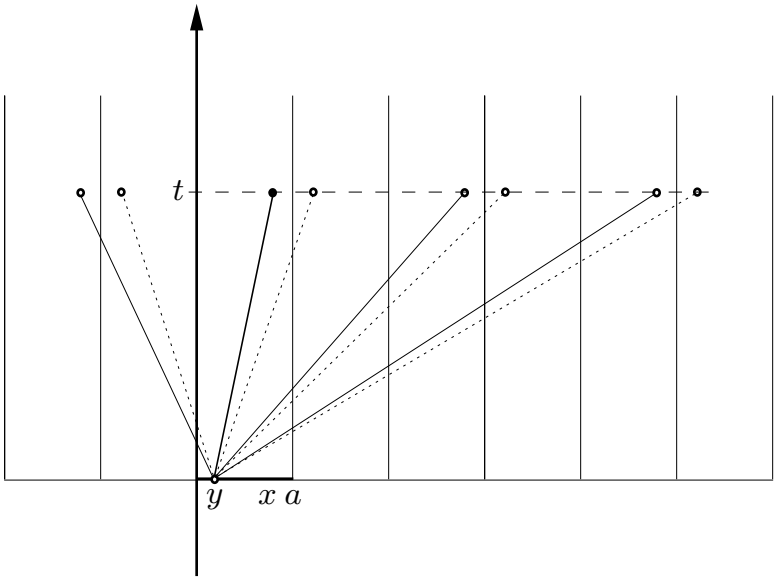

FIGURE 1: *Spacetime diagram in which reflected free particle paths are displayed as straight paths from the source point* $(y, 0)$ *to various "images" of the target point* (x, t)*. Note how paths that involve an even number of bounces are distinguished from those that involve an odd number.*

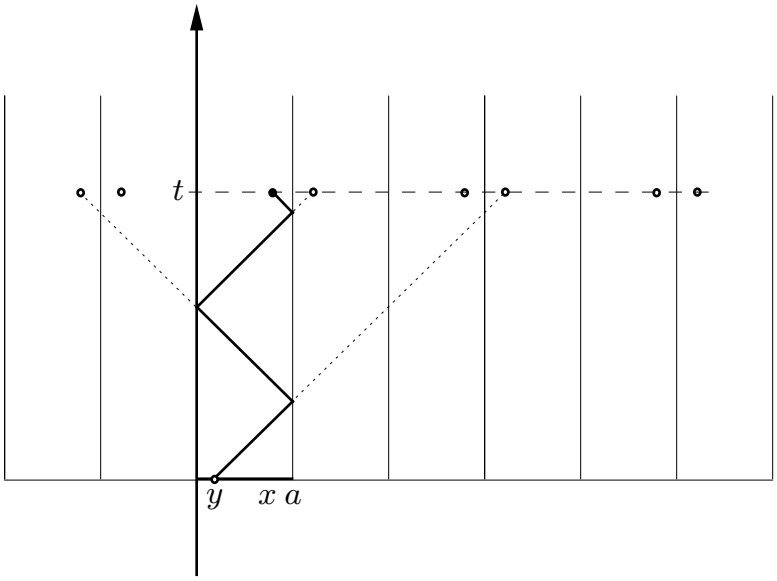

FIGURE 2: *Representation of the construction by which fictitious image paths give rise in physical spacetime to multiply reflected paths.*

$\frac{i}{\hbar}\Delta S = i(1+2n)\pi$, which entails (here n is any positive or negative integer, not to be confused with the n we have used to identify paths)

$$\Delta S = (n + \tfrac{1}{2})h \tag{16}$$

Such a result would be rendered intelligible if, proceeding in reference to the following figure, we were to require that the shaded region have area given by

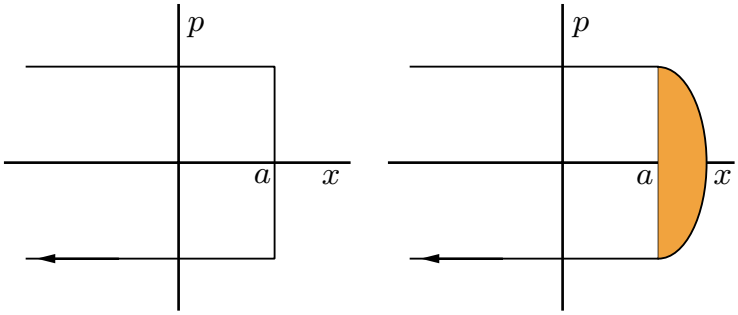

FIGURE 3: *The figures are drawn on phase space. The figure on the left represents the collision of a particle with an idealized barrier of infinite stiffness. On the right the particle penetrates a certain distance into a relatively more physical (because relatively "soft") barrier.*

the Bohr-Sommerfeld quantization condition[8]

$$\oint p\,dx = (n + \tfrac{1}{2})h$$

Though this little argument is certainly not conclusive, it is, I think, powerfully suggestive.

One is reminded in this general connection that light, when reflected from a medium of higher index of refraction, experiences a 180° phase advance (but no such phase advance when the index of refraction is lower). The analogy is, however, not precise: When a classical particle enters a region of discontinuously higher potential its momentum decreases ($p = \sqrt{2mE} \mapsto \sqrt{2m(E-U)}$) but the phase velocity $u = E/p$ of the associated ψ-wave $\psi(x,t) \sim \exp\{\frac{i}{\hbar}[px - Et]\}$

[8] See Max Jammer, *The Conceptual Development of Quantum Mechanics* (1966), §3.1; J. B. Keller, "Correct Bohr-Sommerfeld Quantum Conditions for Nonseparable Systems," Annals of Physics **4**,180 (1958). Near the theoretical foundations of this topic—and of phase-skip phenomena generally—lies that branch of asymptotic analysis having to do with what is called "Stokes' phenomenon;" for an excellent review of the subject and its applications see J. Heading, *An Introduction to Phase-Integral Methods* (1962).

increases, meaning that the "mechanical index of refraction" has become (not higher but) lower. And in "classically forbidden regions" where $U > E$ the index of fraction becomes actually imaginary (refraction becomes absorption).It is, therefore, for multiple reasons that the optical experience fails to illuminate the quantum situation.

If we agree to include reflective jump-discontinuities in our definition of the classical action

$$\begin{aligned} S[\text{classical reflective path}] = S[\text{equivalent image path}] \\ + (\text{number of reflections}) \cdot \Delta S \end{aligned} \tag{17}$$

with $\Delta S = (n+\frac{1}{2})h$, then (15) admits of the following even simpler formulation:

$$K(x,t;y,0) = \sum_{\text{all paths}} \sqrt{\tfrac{m}{iht}}\, e^{\frac{i}{\hbar} S[\text{classical reflective path}]} \tag{18}$$

2. Miscellaneous comments and anticipatory remarks. If we were, on some grounds, authorized to accept (18) as our starting point, then we could—working backwards from the equation (11) that spells out the detailed meaning of (18)—recover (5.1), from which we could simply *read off* the eigenfunctions $\psi_n(x)$ and eigenvalues E_n which were at (1) and (2) found to be characteristic of the one-dimensional box problem. This, in a nutshell, is the program that will lead us to the exact eigenfunctions/eigenvalues of a specialized class of non-separable two-dimensional box problems.

Precisely such authorization was in fact provided by Feynman's celebrated observation[9] that the propagator can be developed

$$K(x,t;y,0) = \sum\!\!\!\!\!\!\int e^{\frac{i}{\hbar} S[\text{path}]}\, \mathcal{D}[\text{path}] \tag{19}$$

provided the "sum-over-paths" is suitably defined. Here the summation process is intended to embrace "all paths"—which we may, in a manner of speaking, take to mean "all Hamiltonian comparison paths" (which Feynman thus gave physical work to do)—but Feynman himself was well aware from the outset that (19) entails[10]

$$K(x,t;y,0) \sim (\text{normalization factor}) \cdot e^{\frac{i}{\hbar} S[\text{classical path}]}$$

in the classical limit $\hbar \downarrow 0$, and that this "semi-classical approximation" becomes exact when the particle moves freely (as it does also when the particle is

[9] "Space-time approach to non-relativistic quantum mechanics," Rev. Mod. Phys. **20**, 367 (1948); R. P. Feynman & A. R. Hibbs, *Quantum Mechanics and Path Integrals* (1965).

[10] The argument—which Feynman himself only sketched—entails use of a functional generalization of the so-called "method of stationary phase."

harmonically bound). We can therefore regard (18) to be a direct implication of the Feynman formalism, in its simplest manifestation.

During the winter of 1953/54 Born and Einstein engaged in vigorous debate concerning the statistical interpretation of quantum mechanics. Record of that debate—in which Born and Einstein took the one-dimensional particle-in-a-box problem as their theoretical "laboratory"—was published in 1971,[11] and came at that time to my attention. I learned that Wolfgang Pauli had been apprised of the substance of the debate, and in December of 1955 had written to Born as follows:

> *I had used the mathematics of the example of the mass point between two walls, and of the wave-packets that belong to it, in my lectures in such a way that the transformation formula of the theta-function comes into play. But that is a mere detail.*

Pauli's remark stimulated Born to return to the problem, and it was from the resulting publication[12] that I gained my first exposure to the theory of theta functions (concerning which Born himself drew inspiration from an old paper of P. Ewald[13] in which Jacobi's transformation formula enters into discussion of the electrostatic fields in crystals). When, in the winter/spring of 1971/72, Richard Crandall and I developed the material outlined in §1 we imagined ourselves to be breaking new ground in one—but only one—respect: Born had all the essential physics in hand, but his eye on a different ball (see below), and seems not to have appreciated that his work had anything to do with ideas that had been put forward by Feynman (whom he does not cite). For Crandall and me the connection with the Feynman formalism was, on the other hand, the principal point of interest, and a point we found ourselves in position quickly to make precise. But we were, as we ultimately discovered, not the first to do so; in 1951/51 Pauli lectured at the ETH in Zürich on "Feldquantisierung," and took advantage of the occasion to present one of the first critical accounts of the then-new Feynman formalism. German-language notes from those lectures circulated fairly widely (and should have been known to Born), but they became available in English translation only in 1973, when they were published by MIT under the title *Pauli Lectures on Physics, Volume 6: Selected Topics in Field Quantization*. In the final pages of that volume (at p. 170 in §30: "The Path Integral Method") one encounters discussion of "the example—interesting in its own right—of a particle in a one-dimensional box" wherein Pauli, writing in reference to what he calles the "method of images," deftly

[11] *The Born-Einstein Letters: Correspondence between Albert Einstein and Max & Hedwig Born from* 1916 *to* 1955*, with Commentaries by Max Born*. The letters in question (N°105–111) appear on pp. 205–216. Three letters, bearing on the substance of this debate, which Born received subsequently from Pauli appear on pp. 217–225.

[12] M. Born & W. Ludwig, "Zur Quantenmechanik des kräftefreien Teilchens," Z. für Physik **150**, 106 (1958).

[13] "Die Berechnung optischer und elektrostatischer Gitterpotentiale," Ann. Phys. **64**, 253 (1921).

encapsulates essentially all that Crandall and I had to say. And, as came later to my attention, the mathematical method employed by Pauli was—as it refers not to the Schrödinger equation but to the heat equation—old even when Pauli wrote: Chapter III of A. Sommerfeld's *Partial Differential Equations in Physics* (1949)—which should also have been familiar to Born—is devoted to "Boundary Value Problems in Heat Conduction," and its §16 ("Linear Heat Conductors Bounded on Both Ends") presents all the essentials of the argument devised by Pauli and Crandall/Wheeler, though for obvious physical reasons it contains no reference to any analog of "classical motion."

I digress to describe the issue which was of such distractingly preeminent interest to Born. A particle-in-a-box is initially localized, in the sense that both Δx and $\Delta v = \frac{1}{m}\Delta p$ are small. How—asymptotically in time—does that localization become lost, and the distribution $|\psi(x,t)|^2$ become flat? The following figure captures the classical essence of their idea. So far as concerns

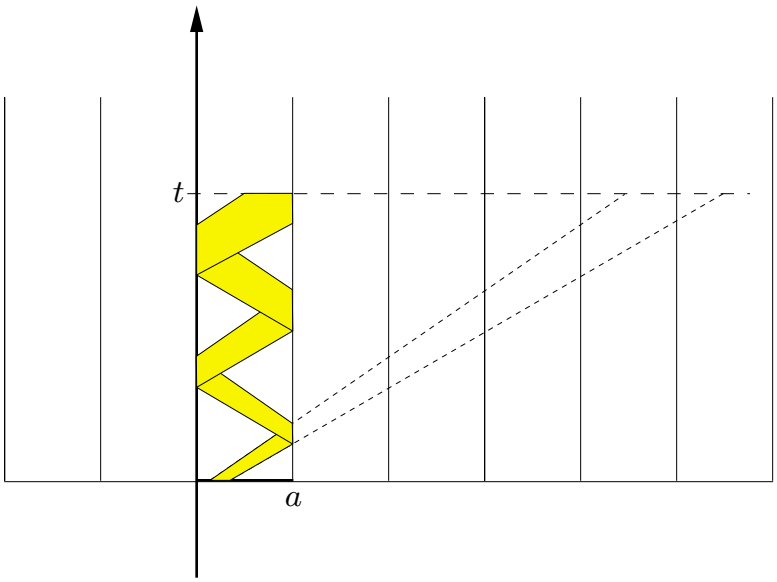

FIGURE 4: *Spacetime diagram of the classical representation of the mechanism by which initial localization information becomes lost.*

the quantum aspects of the problem, Born & Ludwig begin with the pretty observation that if $g(x)$ is defined on the unbounded line (where it describes, let us suppose, a localized wavepacket), then

$$G(x) \equiv \sum_{n=-\infty}^{\infty} g(x+2na) \quad : \quad \text{convergence assumed}$$

is periodic ($G(x) = G(x+2a)$) and

$$\Psi(x) \equiv G(x) - G(-x)$$

is simultaneously periodic and odd, from which it follows that $\Psi(0) = \Psi(a) = 0$ automatically (i.e., for all such functions $g(x)$); the function $\Psi(x)$ describes what might be called a "boxed wavepacket." Born & Ludgwig concentrate on the illustrative case of a "launched Gaussian"

$$g(x) = \sqrt{\tfrac{1}{\sigma_0\sqrt{2\pi}}}\exp\Big\{-\big(\tfrac{x-x_0}{2\sigma_0}\big)^2 + \tfrac{i}{\hbar}mv(x-x_0)\Big\}$$

Such a wavepacket possesses initially minimal dispersion ($\Delta x \cdot \Delta p = \frac{1}{2}\hbar$ with $\Delta x = \sigma_0$), but with the passage of time the dispersion grows

$$\sigma(t) = \sqrt{1 + (\hbar t/2m\sigma_0^2)^2}$$

and in the characteristic time

$$\tau \sim \frac{a}{\frac{1}{m}\Delta p} = 2ma\sigma_0/\hbar$$

becomes as broad as the box. Thus prepared, Born & Ludwig introduce the nomenclature (here $p_n \equiv \hbar k_n = hn/2a$)

$$K(x,t;y,0) = \begin{cases} \text{righthand side of (5.2): the "wave representation"} \\ \text{righthand side of (11): the "particle representation"} \end{cases}$$

$$= \begin{cases} \frac{1}{2a}\sum_{-\infty}^{\infty}\Big[\exp\Big\{\frac{i}{\hbar}\big[p_n(x-y) - \frac{1}{2m}p_n^2 t\big]\Big\} - \exp\Big\{\frac{i}{\hbar}\big[p_n(x+y) - \frac{1}{2m}p_n^2 t\big]\Big\}\Big] \\ \sqrt{\frac{m}{iht}}\sum_{-\infty}^{\infty}\Big[\exp\Big\{\frac{i}{\hbar}\frac{m(x-y+2an)^2}{2t}\Big\} - \exp\Big\{\frac{i}{\hbar}\frac{m(x+y+2an)^2}{2t}\Big\}\Big] \end{cases}$$

—the equivalence of which they establish by appeal to the "Poisson summation formula"[14] (i.e., by in effect reconstructing the proof of Jacobi's transformation formula (9))—and advocate the position that

- the particle representation pertains when $t \ll \tau$
- the wave representation pertains when $t \gg \tau$
- in general one should write something like

$$K(x,t;y,0) = e^{-t/\tau}K_{\text{particle}}(x,t;y,0) + (1-e^{-t/\tau})\,K_{\text{wave}}(x,t;y,0)$$

This idea—which Born & Ludwig admit to having appropriated from an idea put forward by Ewald in quite another connection—does conform to an insight fundamental to the Feynman formalism

> *Quantum mechanics becomes semi-classical*
> *in the short-time approximation.*

but might appear to represent something of a swindle, insofar as it advocates a "distinction without a difference." But consider the point to which Bellman has drawn attention in his §10:

[14] See R. Courant & D. Hilbert, *Methods of Mathematical Physics* (1953), pp. 74–77. The heavy details of Born & Ludwig's argument are developed in §5 of FEYNMAN FORMALISM FOR POLYGONAL DOMAINS (1971–1976).

It is an implication of Jacobi's formula (10) that (set $\tau = it/\pi$ and $z = 0$)

$$f(t) \equiv \sum_{-\infty}^{\infty} e^{-tn^2} = \sqrt{\tfrac{\pi}{t}} \sum_{-\infty}^{\infty} e^{\pi^2 n^2/t}$$

While the left and right sides of the preceding equation are identically equal, they are *not computationally identical!* Suppose, for example, we wanted to evaluate $f(.01)$. Working from the sum on the left, it follows from

$$e^{-25} \approx 10^{-10.8}$$

that we would (since $n^2/100 = 25$ entails $n = 50$) have to keep about 50 terms to achieve 10-place accuracy. Working, on the other hand, from the sum on the right, we have

$$\sqrt{\tfrac{\pi}{t}} \sum_{-\infty}^{\infty} e^{\pi^2 n^2/t} = \sqrt{100\pi}(1 + 2\underbrace{e^{-100\pi^2}} + \cdots)$$
$$\approx 10^{-434}$$

and have achieved accuracy to better than 400 places with only two terms! The situation would be reversed if we were to evaluate $f(100)$. This, I think, is the insight that Born & Ludwig were laboring to promote.

The "method of images" has applications to electrostatics, the theory of heat, optics, acoustics, classical/quantum mechanics... but prior to the physics in any application stands the mathematical problem of describing—of describing in terms most aptly suited to the intended application—the rule according to which points in the physical domain become associated with points in signed "images" of that domain:

$$\text{physical point} \quad \longmapsto \quad \text{signed "images" of that point} \tag{20}$$

In the one-dimensional case that has been our exclusive concern thus far the ramification process (20) is so exceptionally simple as to be describable in many distinct ways: One might simply write

$$x \text{ on physical interval} \quad \longmapsto \quad 2an \pm x, \text{ with parity of the sign} \tag{21}$$

or one might look to (for example) any of the diagramatic devices presented in Figure 5. These and similar constructions acquire some of their interest from the circumstance that when generalized to two or more dimensions (where geometrical considerations come non-trivially into play) they tend to speak to different issues, and to acquire distinct kinds and degrees of utility. The following remarks are intended to illustrate distinctions of the sort that arise and acquire importance in the 2-dimensional case:

It is evident (see Figure 6) even in the absence of formal proof that, in the one-dimensional case, when an inteval somersaults from one position to another it arrives always with the same orientation; to say the same thing another way:

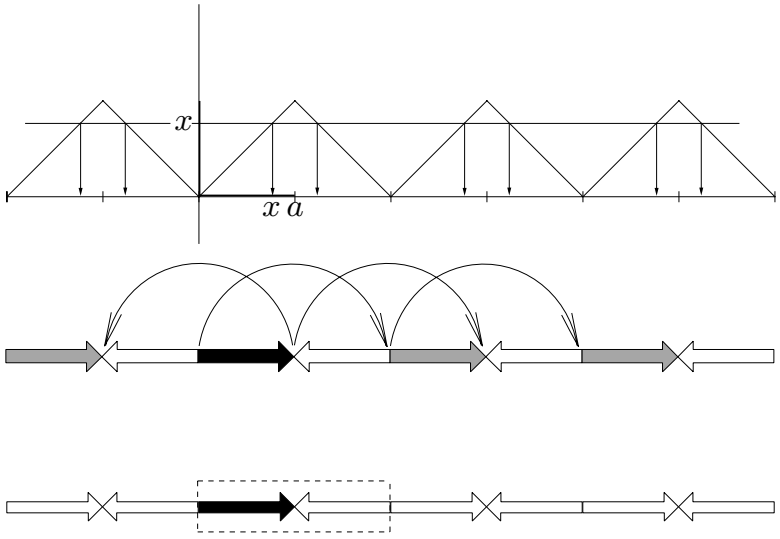

FIGURE 5: *Three representations of (20), as it pertains to image construction in the one-dimensional case. The top diagram can be read as a graph of (21); notice that while* $\longleftarrow\!\shortmid$ *is a many-one function,* $\shortmid\!\longrightarrow$ *has the one-many character typical of what I call a “ramification.” In the middle diagram the physical interval ramifies by “somersaulting” up and down the real line, achieving what I call a “reflective tesellation of the line.” In the bottom figure the physical interval is conjoined with one of its reflective images to produce a (boxed) “fundamental unit,” which is then translated in steps of length* $2a$*.*

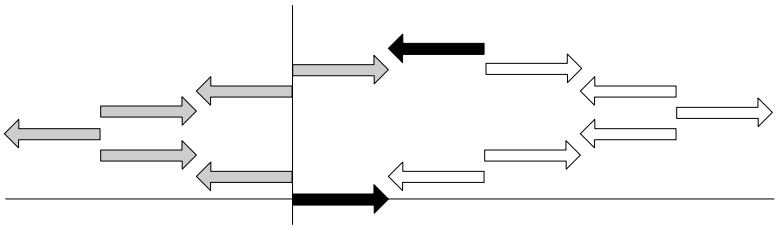

FIGURE 6: *Alternative somersault excursions (grey and white) with identical endpoints (black) achieve terminal orientations that are invariable identical; unambiguous parity assignments are therefore possible.*

somersault excursions of every design—provided only that they begin and end “at home”—preserve orientation. The same, less obviously, can be said of the equilateral trangles that tesselate the plane, as is implicit in Figure 7. The same, however, can *not* be said of the hexagonal tesellations of the plane; the

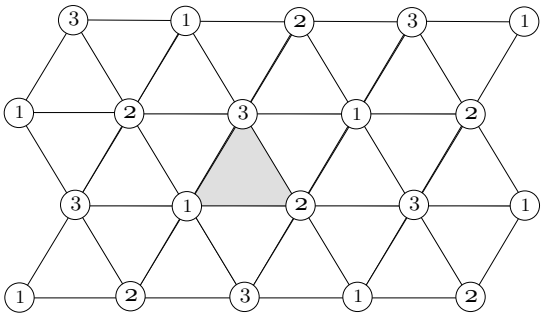

FIGURE 7: *Reflective tesselation of the plane by an equilateral triangle. Triangles of six types are in evidence—three Δ-triangles, corresponding to the even permutations of $\{1, 2, 3\}$, and three ∇-triangles, corresponding to the odd permutations. Reflective radiation of the shaded triangle of the plane assigns unambiguous parity and orientation to every triangle on the tesselated plane.*

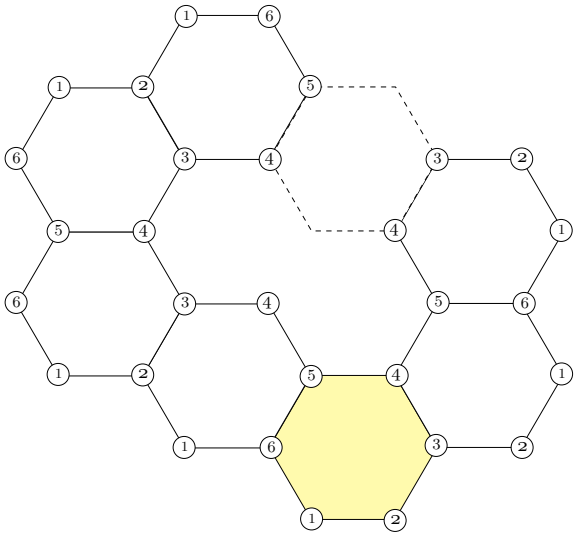

FIGURE 8: *The shaded hexagon moves reflectively by two distinct routes to the dashed position, where it arrives with path-dependent orientation. It is not possible, by reflective radiation of the shaded hexigon, to assign unambiguous parity and orientation to other hexagons on the tesselated plane.*

source of the problem becomes immediately evident when one reflectively walks a hexagon around a vertex: one finds that on the third move the hexagon returns to its original position with permuted vertices and reversed parity, but that on the sixth move (second time around) it is restored to its original configuration.

In a sense that I will not attempt at this point to make precise, the hexagonal tesselation lives on the *double* plane. Relatedly but more obviously: it is not possible to color a hexagonal map using only two colors. We have touched here on a geometrical distinction that has deep quantum mechanical ramifications, as will emerge.

It is amusing to notice—though not immediately germaine to the quantum mechanical work ahead of us—that when a *tetrahedron* (imagine its four sides to be of different colors, and the mode of locomotion to be “rolling about an edge”) is used to decorate the plane with triangles, one obtains (see Figure 9) a 4-color tesselation with the remarkable property that *the color and orientation of every triangle is unambiguously determined* (which is to say: a path-independent implication of the starting position/orientation of the tetrahedron). Somewhat

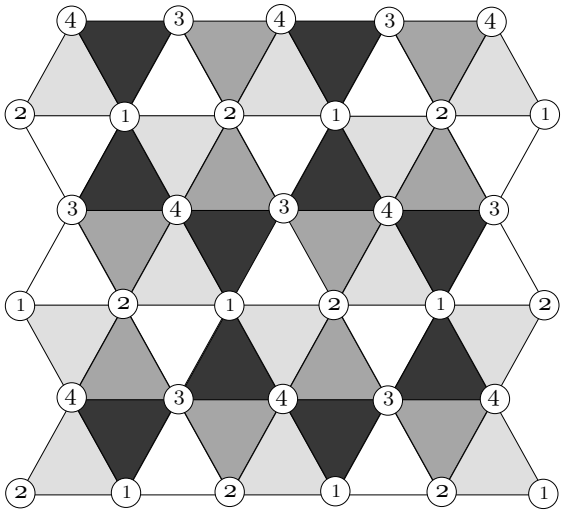

FIGURE 9: *The 4-color tesselation generated by the tetrahedron that sat originally on its white* Δ*-face. All* Δ*-triangles have the same parity, and all* ∇*-triangles have the opposite parity. A tetrahedron can sit on* Δ *in 12 ways, and on* ∇ *in another 12; of those 24 orientations, only eight are realized in the figure.*

surprisingly, the square tesselation generated by a rolling cube fails to display similar self-consistency properties. When these pretty facts were brought to the attention of readers of *American Mathematical Monthly*[15] one problem-solver observed that a rolling cube can assume only 12 of its 24 possible orientations, but that a rolling icosahedron can assume any of its 60 possible orientations.

[15] Advanced Problem 6388, proposed by N. Wheeler & Howard Straubing, Amer. Math. Monthly **89**, 338 (1982). The solution (**90**, 712 (1983)), by J. W. Grossman and twelve others, proceeds directly from information evident in Figure 9.

3. Two approaches to the quantum physics of a particle in a rectangular box. Let our mass point m be confined now to the interior of the rectangular region

$$R \quad : \quad \{0 \leq x_1 \leq a_1; 0 \leq x_2 \leq a_2\}$$

where $x \equiv \{x_1, x_2\}$ refer to an inertial Cartesian coordinatization of the plane. We have

$$\nabla^2\psi(x) = -k^2\psi(x) \quad \text{with} \quad k \equiv \sqrt{\frac{2mE}{\hbar^2}} \quad : \quad x \in R$$

and require $\psi(\partial R) = 0$. Standardly[16] one proceeds by separation of variables, writing $\psi(x_1, x_2) = f(x_1) \cdot g(x_2)$. Easily—since the work was done already in the one-dimensional case: see again (1) and (2)—one obtains the normalized eigenfunctions

$$\psi_{n_1 n_2}(x_1, x_2) = \sqrt{\frac{4}{a_1 a_2}} \sin\left(\frac{n_1\pi}{a_1}x_1\right) \cdot \sin\left(\frac{n_2\pi}{a_2}x_2\right) \tag{22}$$

and finds the associated energy eigenvalue to be given by

$$E_{n_1 n_2} = \mathcal{E}_1 n_1^2 + \mathcal{E}_2 n_2^2 \quad \text{with} \quad \mathcal{E}_1 \equiv \frac{h^2}{8ma_1^2} \quad \text{and} \quad \mathcal{E}_2 \equiv \frac{h^2}{8ma_2^2} \tag{23}$$

Here $\{n_1, n_2\} \in \{1, 2, 3, \ldots\}$ and $a_1 a_2$ is just the *area* of the box R. I propose, however, to proceed non-standardly—by illustrative 2-dimensional application of the method of images.

It is by implicit reference to the tesselated plane (see Figure 10) that one designs the "bank shots" of classical billiards, and it is from (18) that we acquire interest in the *totality* of such "classical reflective paths" $(\boldsymbol{x}, t) \longleftarrow\!\!\!\!\!- (\boldsymbol{y}, 0)$. It is computationally useful—and in more complicated cases essential—to be somewhat circumspect when setting up the "sum-over-paths" to which (18) speaks; in Figure 11 the physical box has been joined with three of its reflective images to form what I call the "fundamental unit." All the "reflective" aspects of the problem have been absorbed into the design of the fundamental unit, and tesselation of the plane has been achieved (no further somersaulting required) by *translation* of the fundamental unit. Introduction of the fundamental unit permits one to write

$$\sum_{\text{all image points}} = \sum_{\text{translations}} \quad \sum_{\substack{\text{image points within} \\ \text{fundamental unit}}}$$

Elaborating upon notation introduced in Figure 12, let the coordinates of the

[16] See, for example, §**5.3** of D. Griffiths, *Introduction to Quantum Mechanics* (1994).

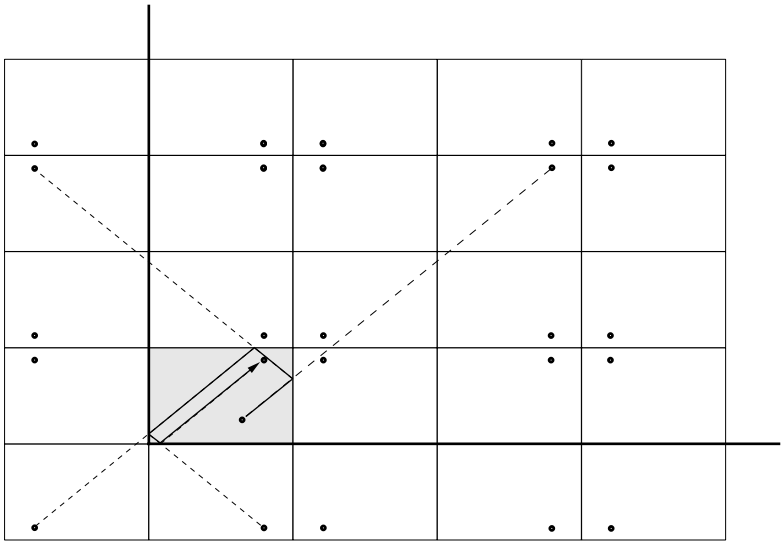

FIGURE 10: *In classical billiards one uses the tesselated plane to construct (compare Figure 2) individual“bank shots.” In quantum billiards one acquires interest in the totality of such reflective paths.*

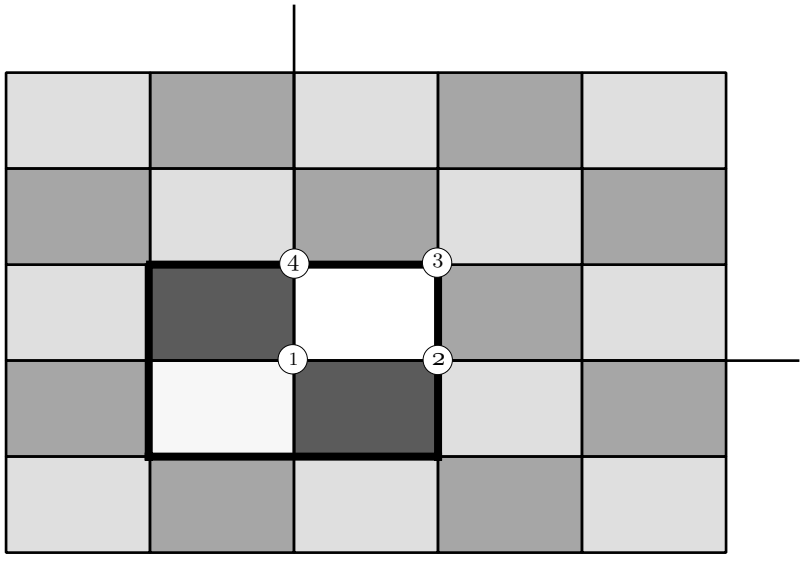

FIGURE 11: *The physical rectangle (white) is joined with three of its reflective images to form the “fundamental unit” (outlined), and tesellation of the plane is achieved by translation of the fundamental unit. See again the bottom diagram in Figure 5.*

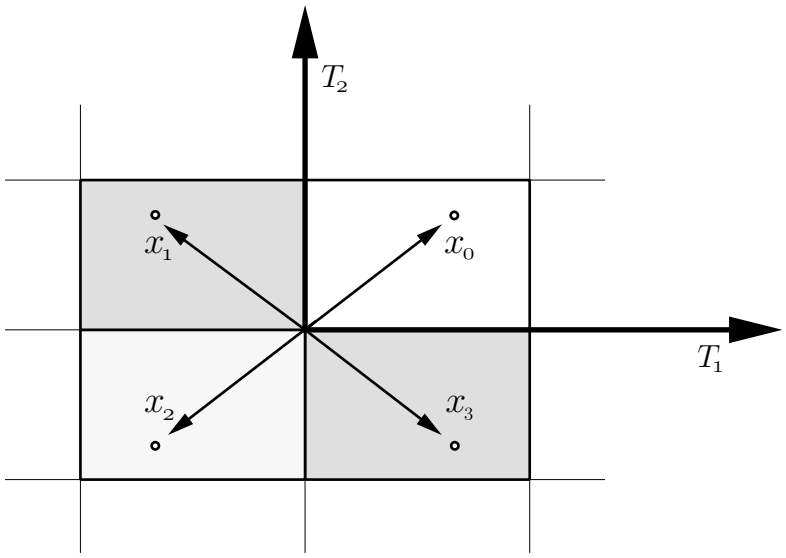

FIGURE 12: *The "fundamental unit" and associated notations.*

"target point" within the physical box be notated

$$\boldsymbol{x} \equiv \boldsymbol{x}_0 = \begin{pmatrix} x_1 \\ x_2 \end{pmatrix}$$

Then

$$\boldsymbol{x}_1 = \begin{pmatrix} -x_1 \\ +x_2 \end{pmatrix}$$

$$\boldsymbol{x}_2 = \begin{pmatrix} -x_1 \\ -x_2 \end{pmatrix}$$

$$\boldsymbol{x}_3 = \begin{pmatrix} +x_1 \\ -x_2 \end{pmatrix}$$

describe the locations of the "fundamental image points" (image points within the fundamental unit) and we can in the general case write

$$\boldsymbol{x} = \boldsymbol{x}_\alpha + n_1 \boldsymbol{T}_1 + n_2 \boldsymbol{T}_2 \tag{24}$$

The numbers $\alpha \in \{0, 1, 2, 3\}$ and $\{n_1, n_2\} \in \{\ldots, -2, -1, 0, +1, +2, \ldots\}$ serve jointly to identify each individual image point, while

$$\boldsymbol{T}_1 \equiv \begin{pmatrix} 2a_1 \\ 0 \end{pmatrix} \quad \text{and} \quad \boldsymbol{T}_2 \equiv \begin{pmatrix} 0 \\ 2a_2 \end{pmatrix} \tag{25}$$

are "translation vectors" that serve to describe the periodicity of the tesselation. Image points with $\alpha \in \{0, 2\}$ have even parity (which is to say: they give rise, by the construction of Figure 10, to paths with an even number of reflection points), while those with $\alpha \in \{1, 3\}$ have odd parity; in short, one can—by notational contrivance—write

$$\text{parity} = (-)^\alpha$$

The squared length of the line drawn from a point $\boldsymbol{y}$ in the physical box to the image point (24) can be described

$$|\boldsymbol{x}_{\text{image point}} - \boldsymbol{y}|^2 = \boldsymbol{S}\cdot\boldsymbol{S} + 2\big(n_1\boldsymbol{S}\cdot\boldsymbol{T}_1 + n_2\boldsymbol{S}\cdot\boldsymbol{T}_2\big) + n_1n_1\boldsymbol{T}_1\cdot\boldsymbol{T}_1 + 2n_1n_2\boldsymbol{T}_1\cdot\boldsymbol{T}_2 + n_2n_2\boldsymbol{T}_2\cdot\boldsymbol{T}_2$$

with
$$\boldsymbol{S} \equiv \boldsymbol{S}_\alpha \equiv \boldsymbol{x}_\alpha - \boldsymbol{y} \tag{26}$$

giving
$$= \boldsymbol{S}\cdot\boldsymbol{S} + 2\,\boldsymbol{n}\cdot\mathbb{T}\boldsymbol{v} + \boldsymbol{n}\cdot\mathbb{T}\boldsymbol{n}$$

where
$$\mathbb{T} \equiv \begin{pmatrix} \boldsymbol{T}_1\cdot\boldsymbol{T}_1 & \boldsymbol{T}_1\cdot\boldsymbol{T}_2 \\ \boldsymbol{T}_2\cdot\boldsymbol{T}_1 & \boldsymbol{T}_2\cdot\boldsymbol{T}_2 \end{pmatrix} \quad \text{and} \quad \boldsymbol{v} = \boldsymbol{v}_\alpha \equiv \mathbb{T}^{-1}\begin{pmatrix} \boldsymbol{S}\cdot\boldsymbol{T}_1 \\ \boldsymbol{S}\cdot\boldsymbol{T}_2 \end{pmatrix} \tag{27}$$

entail (I return to the semi-miraculous proof in a moment) $\boldsymbol{S}\cdot\boldsymbol{S} = \boldsymbol{n}\cdot\mathbb{T}\boldsymbol{v}$; we are led thus, by quite a general line of argument, to this pretty result:

$$|\boldsymbol{x}_{\text{image point}} - \boldsymbol{y}|^2 = (\boldsymbol{v}+\boldsymbol{n})\cdot\mathbb{T}(\boldsymbol{v}+\boldsymbol{n}) \tag{28}$$

Concerning that "semi-miraculous proof": we proceed from the observation that the symmetric matrix $\mathbb{T}$ can be developed $\mathbb{T} = \mathbb{C}^\intercal\mathbb{C}$ where $\mathbb{C}$ is the square matrix into which the $\boldsymbol{T}_i$ enter as the column vectors:

$$\mathbb{C} \equiv \|\boldsymbol{T}_1\ \boldsymbol{T}_2\|$$

The non-singularity of $\mathbb{C}$ is assured by the linear independence of $\boldsymbol{T}_1$ and $\boldsymbol{T}_2$. Let $\overline{\boldsymbol{T}}_1$ and $\overline{\boldsymbol{T}}_2$ be the *row* vectors that enter into the description of $\mathbb{C}^{-1}$:

$$\mathbb{R} \equiv \mathbb{C}^{-1} \equiv \left\| \begin{matrix} \overline{\boldsymbol{T}}_1 \\ \overline{\boldsymbol{T}}_2 \end{matrix} \right\|$$

The statement $\mathbb{R}\mathbb{C} = \mathbb{I}$ amounts to an assertion that the bases $\{\overline{\boldsymbol{T}}_1, \overline{\boldsymbol{T}}_2\}$ and $\{\boldsymbol{T}_1, \boldsymbol{T}_2\}$ are "bi-orthogonal:"[17] $\overline{\boldsymbol{T}}_i\boldsymbol{T}_j = \delta_{ij}$. From the familiar matrix-theoretic fact that left inverses are also right inverses (together with the symmetry of the identity $\mathbb{I}$) we have $\mathbb{R}\mathbb{C} = \mathbb{C}\mathbb{R} = \mathbb{C}^\intercal\mathbb{R}^\intercal = \mathbb{R}^\intercal\mathbb{C}^\intercal = \mathbb{I}$. Moreover $\mathbb{T}^{-1} = \mathbb{R}\mathbb{R}^\intercal$. In these notations we have $\boldsymbol{v} \equiv \mathbb{T}^{-1}\mathbb{C}^\intercal\boldsymbol{S} = \mathbb{R}\boldsymbol{S}$, giving $\boldsymbol{v}\cdot\mathbb{T}\boldsymbol{v} = \boldsymbol{S}\cdot\mathbb{R}^\intercal\mathbb{C}^\intercal\mathbb{C}\mathbb{R}\boldsymbol{S} = \boldsymbol{S}\cdot\boldsymbol{S}$, as claimed.

The dynamical action associated with motion to an image point can now be described rather elegantly as follows:

$$S(\boldsymbol{x}_\alpha + n_1\boldsymbol{T}_1 + n_2\boldsymbol{T}_2, t; \boldsymbol{y}, 0) = \frac{m}{2}\frac{(\boldsymbol{v}+\boldsymbol{n})\cdot\mathbb{T}(\boldsymbol{v}+\boldsymbol{n})}{t} + \Delta S \tag{29}$$

where the value of ΔS entails $e^{\frac{i}{\hbar}\Delta S} = (-)^\alpha$. The argument that brought us to (29) is quite general in its main features; it is by specialization of $\mathbb{T}$ and $\boldsymbol{v}_\alpha$ that one obtains results specific to (in particular) the rectangular box problem.

[17] The former is known to crystalographers as the "reciprocal basis."

That I will do in good time. But to move efficiently beyond this point I now digress to review an ...

4. Outline of a theory of theta functions of several variables. The subject of what Bellman calls "multidimensional theta functions" is taken up in his §61 and surveyed in the final eight pages of the monograph cited in Footnote 4, and is sometimes encountered in physical applications (see the paper by Ewald cited in Footnote 13). For notational and other reasons I find it convenient, however, to proceed from scratch.[18] Looking first to the one-dimensional pattern of our argument...

Let $g(x)$ be defined on the unbounded line, and so well-behaved that

$$G(x) \equiv \sum_{-\infty}^{\infty} g(x+n)$$

exists (i.e., that the series converges).[19] Noting the periodicity of $G(x)$

$$G(x) = G(x+1)$$

we write

$$= \sum_{k=-\infty}^{\infty} g_k \, e^{2\pi i k x}$$

$$g_k = \int_0^1 G(y) e^{-2\pi i k y} \, dy$$

$$= \sum_{n=-\infty}^{\infty} \int_0^1 g(y+n) e^{-2\pi i k y} \, dy$$

$$= \int_{-\infty}^{+\infty} g(y) e^{-2\pi i k y} \, dy$$

to obtain[20]

$$\sum_{n=-\infty}^{\infty} g(x+n) = \sum_{n=-\infty}^{\infty} e^{2\pi i n x} \int_{-\infty}^{+\infty} g(y) e^{-2\pi i n y} \, dy \tag{30}$$

In the particular case $g(x) = e^{-ax^2}$ we have

$$\sum_{n=-\infty}^{\infty} e^{-a(x+n)^2} = \sum_{n=-\infty}^{\infty} e^{2\pi i n x} \int_{-\infty}^{+\infty} e^{-(ay^2+2by)} \, dy \quad \text{with} \quad b \equiv i\pi n \tag{31}$$

---

[18] The following material has been adapted from p. 129 *et seq* of "Two particles in a 1-box; one particle in a 2-box" in FEYNMANISM FOR POLYGONAL DOMAINS (1971–1976).

[19] We note that a similar idea—applied there to a different objective—was encountered already at the bottom of p. 11.

[20] At $x = 0$ the following equation becomes precisely the "Poisson summation formula;" see again Footnote 14.

But the Gaussian integral has a familiar value

$$\int_{-\infty}^{+\infty} e^{-(ay^2+2by)}\,dy = \sqrt{\frac{\pi}{a}}e^{b^2/a} \quad : \quad \Re(a) > 0$$

so we have—as a particular implication of (31)—

$$\sum_{-\infty}^{\infty} e^{-a(x+n)^2} = \sqrt{\frac{\pi}{a}}\sum_{-\infty}^{\infty} e^{2\pi i n x - \pi^2 n^2/a}$$

Equivalently

$$\sum_{-\infty}^{\infty} e^{-(\pi^2/a)n^2 - 2\pi i x n} = \sqrt{\frac{a}{\pi}}e^{-ax^2}\sum_{-\infty}^{\infty} e^{-an^2-2axn}$$

which by notational adjustment

$$a = \frac{i\pi}{\tau} \quad \text{and} \quad x = \frac{z}{\pi}$$

reads

$$\underbrace{\sum_{-\infty}^{\infty} e^{i(\pi\tau n^2 - 2nz)}}_{\equiv\,\vartheta(z,\tau)\quad\text{according to (10)}} = \sqrt{i/\tau}\,e^{z^2/i\pi\tau}\cdot\sum_{-\infty}^{\infty}\exp\Big\{-i\Big(\frac{\pi n^2}{\tau}+\frac{2nz}{\tau}\Big)\Big\}$$

We have, in short, been led to an expression which by one interpretation serves to *motivate the definition* of the theta function $\vartheta(z,\tau)$, and have at the same time obtained a proof of the fundamental identity (9). And we have done so in a way that admits straightforwardly of multivariable generalization:

Let $g(x_1, x_2, \ldots, x_p)$ be some nice function of several variables, and form the multiply-periodic function

$$G(x_1, x_2, \ldots, x_p) \equiv \sum_{\boldsymbol{n}} g(x_1 + n_1, x_2 + n_2, \ldots, x_p + n_p)$$

The argument that gave (30) gives

$$\sum_{\boldsymbol{n}} g(\boldsymbol{x}+\boldsymbol{n}) = \sum_{\boldsymbol{n}} e^{2\pi i\,\boldsymbol{n}\cdot\boldsymbol{x}}\int_{-\infty}^{+\infty} g(\boldsymbol{y})e^{-2\pi i\,\boldsymbol{n}\cdot\boldsymbol{y}}\,dy_1dy_2\cdots dy_p \tag{32}$$

In the particular case $g(\boldsymbol{x}) = e^{-\boldsymbol{x}\cdot\mathbb{A}\,\boldsymbol{x}}$ (the matrix can without loss of generality be assumed to be symmetric, and by explicit assumption its eigenvalues all lie on the right half-plane) we have

$$\sum_{\boldsymbol{n}} e^{-(\boldsymbol{x}+\boldsymbol{n})\cdot\mathbb{A}\,(\boldsymbol{x}+\boldsymbol{n})} = \sum_{\boldsymbol{n}} e^{2\pi i\,\boldsymbol{n}\cdot\boldsymbol{x}}\int_{-\infty}^{+\infty} e^{-(\boldsymbol{y}\cdot\mathbb{A}\,\boldsymbol{y}+2\boldsymbol{b}\cdot\boldsymbol{y})}\,dy_1dy_2\cdots dy_p$$

with $\boldsymbol{b} \equiv i\pi\boldsymbol{n}$. Drawing now upon the famous "multidimensional Gaussian integral formula"[21]

$$\int_{-\infty}^{+\infty} e^{-(\boldsymbol{y}\cdot\mathbb{A}\boldsymbol{y}+2\boldsymbol{b}\cdot\boldsymbol{y})}\, dy_1 dy_2 \cdots dy_p = \sqrt{\frac{\pi^p}{\det \mathbb{A}}}\, e^{\boldsymbol{b}\cdot\mathbb{A}^{-1}\boldsymbol{b}} \tag{33}$$

we obtain—as a particular implication of (32)—

$$\sum_{\boldsymbol{n}} e^{-(\boldsymbol{x}+\boldsymbol{n})\cdot\mathbb{A}(\boldsymbol{x}+\boldsymbol{n})} = \sqrt{\frac{\pi^p}{\det \mathbb{A}}} \sum_{\boldsymbol{n}} e^{2\pi i \boldsymbol{n}\cdot\boldsymbol{x} - \pi^2 \boldsymbol{n}\cdot\mathbb{A}^{-1}\boldsymbol{n}} \tag{34}$$

Equivalently[22]

$$\begin{aligned}\sum_{\boldsymbol{n}} e^{-\pi^2\boldsymbol{n}\cdot\mathbb{B}\boldsymbol{n} - 2\pi i \boldsymbol{n}\cdot\boldsymbol{x}} &= \frac{1}{\sqrt{\pi^p \det \mathbb{B}}} \sum_{\boldsymbol{n}} e^{-(\boldsymbol{x}+\boldsymbol{n})\cdot\mathbb{B}^{-1}(\boldsymbol{x}+\boldsymbol{n})} \\ &= \frac{1}{\sqrt{\pi^p \det \mathbb{B}}}\, e^{-\boldsymbol{x}\cdot\mathbb{B}^{-1}\boldsymbol{x}} \sum_{\boldsymbol{n}} e^{-\boldsymbol{n}\cdot\mathbb{B}^{-1}\boldsymbol{n} - 2\boldsymbol{x}\cdot\mathbb{B}^{-1}\boldsymbol{n}}\end{aligned}$$

which by notational adjustment[23]

$$\mathbb{B} = \frac{1}{i\pi}\mathbb{W} \quad \text{and} \quad \boldsymbol{x} = \frac{\boldsymbol{z}}{\pi}$$

reads

$$\underbrace{\sum_{\boldsymbol{n}} e^{i(\pi\boldsymbol{n}\cdot\mathbb{W}\boldsymbol{n} - 2\boldsymbol{n}\cdot\boldsymbol{z})}}_{\equiv\, \vartheta(\boldsymbol{z},\mathbb{W}) \quad \text{by proposed definition}} = \sqrt{\frac{i^p}{\det \mathbb{W}}}\, e^{-i\frac{1}{\pi}\boldsymbol{z}\cdot\mathbb{M}\boldsymbol{z}} \sum_{\boldsymbol{n}} e^{-i(\pi\boldsymbol{n}\cdot\mathbb{M}\boldsymbol{n} + 2\boldsymbol{n}\cdot\mathbb{M}\boldsymbol{z})} \tag{35}$$

In this notation (35) becomes

$$\vartheta(\boldsymbol{z},\mathbb{W}) = \sqrt{\frac{i^p}{\det \mathbb{W}}}\, e^{-i\frac{1}{\pi}\boldsymbol{z}\cdot\mathbb{M}\boldsymbol{z}} \cdot \vartheta(\mathbb{M}\boldsymbol{z}, -\mathbb{M}) \tag{36}$$

which is the multivariable generalization of Jacobi's identity (9).

This is not the place to undertake systematic development of the properties of $\vartheta(\boldsymbol{z},\mathbb{W})$; to those I will return as occasions arise, in response to specific needs.

---

[21] See §**11.12** in H. Cramér, *Mathematical Methods of Statistics* (1946).

[22] I find it convenient at this point to introduce the notation $\mathbb{B} \equiv \mathbb{A}^{-1}$.

[23] I encounter here a small problem: I need a matrix analog of τ, but $\mathbb{T}$ has been preempted. I give the assignment to $\mathbb{W}$ because it lends itself to the easily remembered clutter-reducing usage $\mathbb{M} \equiv \mathbb{W}^{-1}$. In (35) below I will on one occasion draw upon the symmetry of $\mathbb{M}$ to write $\boldsymbol{n}\cdot\mathbb{M}\boldsymbol{z}$ in place of $\boldsymbol{z}\cdot\mathbb{M}\boldsymbol{n}$.

It is sufficient to our immediate needs to observe that we are in position now to write

$$\sum_{\boldsymbol{n}} e^{\beta(\boldsymbol{v}+\boldsymbol{n})\cdot\mathbb{T}(\boldsymbol{v}+\boldsymbol{n})} = e^{\beta\boldsymbol{v}\cdot\mathbb{T}\boldsymbol{v}}\,\vartheta\big(i\beta\mathbb{T}\boldsymbol{v}, -\tfrac{i\beta}{\pi}\mathbb{T}\big) \tag{37.1}$$

$$= \sqrt{\big(-\tfrac{\pi}{\beta}\big)^p \tfrac{1}{\det\mathbb{T}}}\,\vartheta\big(\pi\boldsymbol{v}, \tfrac{\pi}{i\beta}\mathbb{T}^{-1}\big) \tag{37.2}$$

And to notice the factorization (separation of variables) that comes into play when $\mathbb{W}$ is diagonal: if

$$\mathbb{W} = \begin{pmatrix} \omega_1 & 0 & \cdots & 0 \\ 0 & \omega_2 & \cdots & 0 \\ \vdots & \vdots & \ddots & \vdots \\ 0 & 0 & \cdots & \omega_p \end{pmatrix}$$

then

$$\vartheta(\boldsymbol{z}, \mathbb{W}) = \vartheta(z_1, \omega_1)\cdot\vartheta(z_2, \omega_2)\cdot\cdots\cdot\vartheta(z_p, \omega_p) \tag{38}$$

in which connection we are reminded that a similar factorization pertains to—and in fact lies at the heart of the proof of—the Gauss integral formula (33).

5. Application to the rectangular box problem. Taking the Feynman formalism—and more specifically (18)—as our point of departure, and drawing freely upon information developed in §3, we have

$$K(\boldsymbol{x}, t; \boldsymbol{y}, 0) = \sqrt{\big(\tfrac{i}{h}\big)^2 \det\big\|\tfrac{\partial^2 S_0}{\partial x_i \partial y_j}\big\|}\cdot\sum_{\alpha=0}^{3}(-)^\alpha\sum_{\boldsymbol{n}}\exp\big\{\tfrac{i}{\hbar}S_\alpha\big\}$$

$$\tfrac{i}{\hbar}S_\alpha = \beta(\boldsymbol{v}_\alpha+\boldsymbol{n})\cdot\mathbb{T}(\boldsymbol{v}_\alpha+\boldsymbol{n})$$

where $\beta \equiv im/2\hbar t$ and

$$\mathbb{T} = \begin{pmatrix} 4a_1^2 & 0 \\ 0 & 4a_2^2 \end{pmatrix}$$

$$\boldsymbol{v}_0 = \begin{pmatrix} (+x_1 - y_1)/2a_1 \\ (+x_2 - y_2)/2a_2 \end{pmatrix}$$

$$\boldsymbol{v}_1 = \begin{pmatrix} (-x_1 - y_1)/2a_1 \\ (+x_2 - y_2)/2a_2 \end{pmatrix}$$

$$\boldsymbol{v}_2 = \begin{pmatrix} (-x_1 - y_1)/2a_1 \\ (-x_2 - y_2)/2a_2 \end{pmatrix}$$

$$\boldsymbol{v}_3 = \begin{pmatrix} (+x_1 - y_1)/2a_1 \\ (-x_2 - y_2)/2a_2 \end{pmatrix}$$

and where I have—somewhat mysteriously (but see below)—assigned to the prefactor its *direct path* evaluation

$$\sqrt{\big(\tfrac{i}{h}\big)^2 \det\big\|\tfrac{\partial^2 S_0}{\partial x_i \partial y_j}\big\|} = \tfrac{m}{iht}$$

in every case: $\alpha = 0, 1, 2, 3$. With these notations understood, the Feynman formalism has supplied

$$K(\boldsymbol{x}, t; \boldsymbol{y}, 0) = \tfrac{m}{iht} \sum_{\alpha=0}^{3} (-)^{\alpha} e^{\beta \boldsymbol{v}_\alpha \cdot \mathbb{T} \boldsymbol{v}_\alpha} \, \vartheta\big(i\beta \mathbb{T} \boldsymbol{v}_\alpha, -\tfrac{i\beta}{\pi} \mathbb{T}\big)$$

from which we desire to extract eigenvalue and eigenfunction information. To that end, we pass (by means of Jacobi's identity) to the "wave representation" (37.2), writing

$$= \underbrace{\tfrac{m}{iht} \sqrt{\big(-\tfrac{\pi}{\beta}\big)^2 \tfrac{1}{\det \mathbb{T}}}}_{\tfrac{1}{4a_1 a_2} = \tfrac{1}{4 \cdot \text{area}} = \tfrac{1}{\text{area of fundamental unit}}} \sum_{\alpha=0}^{3} (-)^{\alpha} \, \vartheta\big(\pi \boldsymbol{v}_\alpha, \tfrac{\pi}{i\beta} \mathbb{T}^{-1}\big) \tag{39}$$

and observe that $\frac{\pi}{i\beta}\mathbb{T}^{-1}$ is diagonal

$$\tfrac{\pi}{i\beta}\mathbb{T}^{-1} = \begin{pmatrix} \tau_1 & 0 \\ 0 & \tau_2 \end{pmatrix} \quad \text{with} \quad \tau_j = -ht/4ma_j^2$$

so each of the theta functions *factors*: looking first to (38) and then to (7), we have

$$\begin{aligned} \vartheta\big(\pi \boldsymbol{v}_\alpha, \tfrac{\pi}{i\beta}\mathbb{T}^{-1}\big) &= \vartheta(\pi v_{\alpha 1}, \tau_1) \cdot \vartheta(\pi v_{\alpha 2}, \tau_2) \\ &= \Big\{1 + 2\sum_{n_1=1}^{\infty} e^{-i\phi_1 n_1^2} \cos 2\pi n_1 v_{\alpha 1}\Big\}\Big\{1 + 2\sum_{n_2=1}^{\infty} e^{-i\phi_2 n_2^2} \cos 2\pi n_2 v_{\alpha 2}\Big\} \end{aligned}$$

where $\phi_j \equiv -\pi\tau_j = \pi ht/4ma_j^2$ is a convenient abbreviation. Returning with this information to (39), we have

$$\begin{aligned} K(\boldsymbol{x}, t; \boldsymbol{y}, 0) = \tfrac{1}{4a_1 a_2} \Big\{ &\sum_{\alpha=0}^{3} (-)^{\alpha} + 2\sum_{n_1} e^{-i\phi_1 n_1^2} \sum_{\alpha=0}^{3} (-)^{\alpha} \cos 2\pi n_1 v_{\alpha 1} \\ &+ 2\sum_{n_2} e^{-i\phi_2 n_2^2} \sum_{\alpha=0}^{3} (-)^{\alpha} \cos 2\pi n_2 v_{\alpha 2} \\ &+ 4\sum_{n_1}\sum_{n_2} e^{-i(\phi_1 n_1^2 + \phi_2 n_2^2)} \sum_{\alpha=0}^{3} (-)^{\alpha} \cos 2\pi n_1 v_{\alpha 1} \cos 2\pi n_2 v_{\alpha 2} \Big\} \end{aligned}$$

The first term on the right vanishes trivially. Looking to the second term: $\cos 2\pi n_1 v_{01}$ and $\cos 2\pi n_1 v_{31}$ are actually identical (because $v_{01} = v_{31}$), but enter with opposite signs, and the same can be said of $\cos 2\pi n_1 v_{11}$ and $\cos 2\pi n_1 v_{21}$, so the second term vanishes. The third term vanishes by a variant of the same argument. Looking finally to the fourth (and only surviving) term, we once

again appeal to details of the equations that define $\boldsymbol{v}_\alpha$ and obtain[24]

$$\begin{aligned}
&\sum_{\alpha=0}^{3}(-)^\alpha \cos 2\pi n_1 v_{\alpha 1}\cos 2\pi n_2 v_{\alpha 2}\\
&\quad= \cos 2\pi n_1 v_{01}\cos 2\pi n_2 v_{02} - \cos 2\pi n_1 v_{11}\cos 2\pi n_2 v_{\mathbf{02}}\\
&\qquad\qquad + \cos 2\pi n_1 v_{\mathbf{11}}\cos 2\pi n_2 v_{22} - \cos 2\pi n_1 v_{\mathbf{01}}\cos 2\pi n_2 v_{\mathbf{22}}\\
&\quad\equiv \cos\mathcal{X}_{01}\cos\mathcal{X}_{02} - \cos\mathcal{X}_{11}\cos\mathcal{X}_{02} + \cos\mathcal{X}_{11}\cos\mathcal{X}_{22} - \cos\mathcal{X}_{01}\cos\mathcal{X}_{22}\\
&\quad= \big[\cos\mathcal{X}_{01} - \cos\mathcal{X}_{11}\big]\big[\cos\mathcal{X}_{02} - \cos\mathcal{X}_{22}\big] \qquad (40)\\
&\quad= \Big[-2\sin\Big(\frac{\mathcal{X}_{01}+\mathcal{X}_{11}}{2}\Big)\cdot\sin\Big(\frac{\mathcal{X}_{01}-\mathcal{X}_{11}}{2}\Big)\Big]\cdot\\
&\qquad\qquad \Big[-2\sin\Big(\frac{\mathcal{X}_{02}+\mathcal{X}_{22}}{2}\Big)\cdot\sin\Big(\frac{\mathcal{X}_{02}-\mathcal{X}_{22}}{2}\Big)\Big]\\
&\quad= \big[-2\sin\pi n_1(-y_1/a_1)\cdot\sin\pi n_1(+x_1/a_1)\big]\cdot\\
&\qquad\qquad \big[-2\sin\pi n_2(-y_2/a_2)\cdot\sin\pi n_2(+x_2/a_2)\big]\\
&\quad= 4\sin\Big(\frac{n_1\pi}{a_1}x_1\Big)\sin\Big(\frac{n_2\pi}{a_2}x_2\Big)\sin\Big(\frac{n_1\pi}{a_1}y_1\Big)\sin\Big(\frac{n_2\pi}{a_2}y_2\Big) \qquad (41)
\end{aligned}$$

Assembling the results now in hand, we have

$$\begin{aligned}
K(\boldsymbol{x},t;\boldsymbol{y},0) = \tfrac{4}{a_1a_2}\sum_{n_1}\sum_{n_2} e^{-\frac{i}{\hbar}(\mathcal{E}_1 n_1^2+\mathcal{E}_2 n_2^2)\,t}\sin\Big(\frac{n_1\pi}{a_1}x_1\Big)\sin\Big(\frac{n_2\pi}{a_2}x_2\Big)\\
\times\sin\Big(\frac{n_1\pi}{a_1}y_1\Big)\sin\Big(\frac{n_2\pi}{a_2}y_2\Big)
\end{aligned}$$

where the notation $\frac{1}{\hbar}\mathcal{E}_j t \equiv \phi_j = 2\pi h t/8ma_j^2$ conforms to the $\mathcal{E}_j \equiv h^2/8ma_j^2$ of p. 17. Comparison of the result just achieved with (3) gives back precisely the $\{n_1 n_2\}$-indexed eigenfunctions of (22) and eigenvalues of (23).

We have labored hard to recover a result we already possessed. What we have gained is familiarity with a computational technique that retains its utility even in certain cases to which the standard "separation of variables" method is inapplicable. Additionally, we have demonstrated once again the relationship of equivalence between standard formalism and the Feynman formalism, and have seen that it is "Jacobi's identity" that lies at the heart of the interconnection.

We could, in the present instance, have gotten along well enough without any reference to the theory of "theta functions of several variables." I proceeded as I did partly to demonstrate the unifying utility of that theory, and partly to cast new light on the "separation" phenomenon: it was the *diagonality* of the matrix $\mathbb{T}$ that brought (38) into play, and that led ultimately to the key factorization (40).

[24] I write in **boldface** the subscripts I have adjusted; the simple point of the adjustment is that latent simplifications remain invisible so long as a given variable is allowed to wear several names.

The "somewhat mysterious" value assigned to the normalization factor is justified most convincingly by its ultimate success. Had we—as might at first sight have seemed more natural—introduced a *population* of such factors

$$\sqrt{\left(\tfrac{i}{h}\right)^2 \det \left\| \tfrac{\partial^2 S_\alpha}{\partial x_i \partial y_j} \right\|} \quad : \quad \alpha = 0, 1, 2, 3$$

some damaging factors of i would have intruded; those would have put us in violation of the boundary conditions, as they relate to the structure of the propagator, and would also have prevented our achieving

$$\lim_{t \downarrow 0} K(\boldsymbol{x}, t; \boldsymbol{y}, 0) = \delta(\boldsymbol{x} - \boldsymbol{y})$$

I shall not linger to develop details supportive of the preceding remarks.

6. Particle in a right isosceles triangular box. Noting that there do in fact exist (see the following figure) non-rectangular quadrilateral boxes that tesselate the

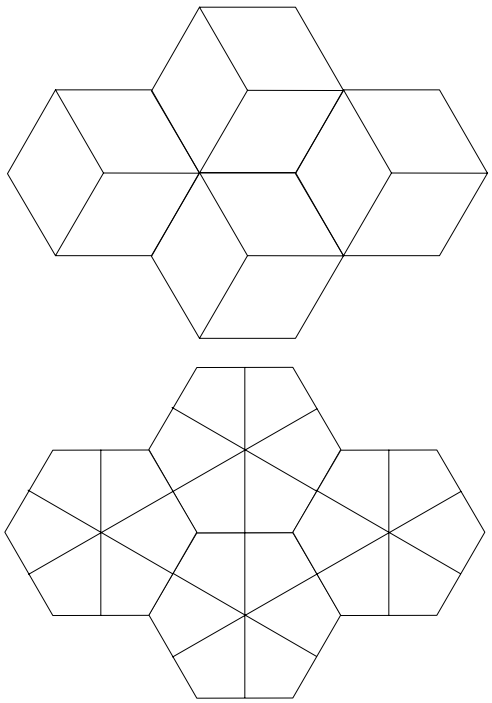

FIGURE 13: *Two examples of non-rectangular quadrilaterals that reflectively tesselate the plane. I know of no other examples. Both designs possess third-order vertices; neither, therefore, can be drawn as a two-color map.*

plane, I turn my attention now to a small population of *triangular* box problems. A little experimental doodling suggests, and Thomas Wieting has managed very

elegantly to prove,[25] that there exist precisely four triangles that reflectively tesselate the plane. They are, in what will emerge to be their order of the ascending computational complexity,

- the 45-45-90 triangle,
- the 60-60-60 triangle,
- the 30-60-90 triangle,
- the 30-30-120 triangle

and give rise to the tesselations shown in Figure 14. We concern ourselves here

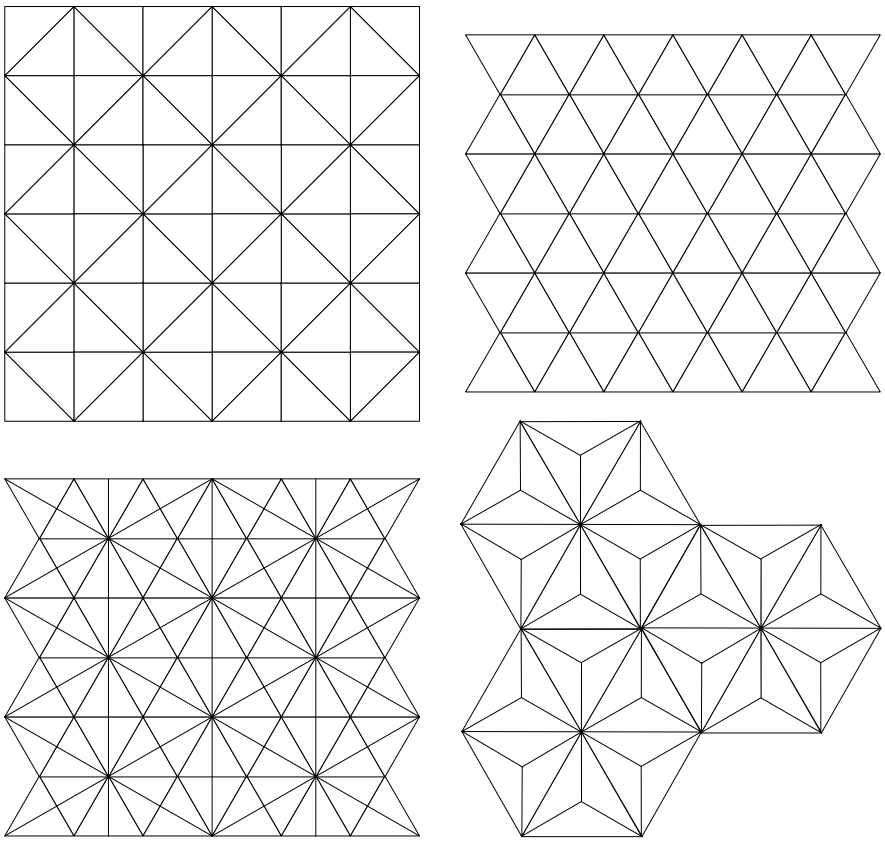

FIGURE 14: *The four possible triangular reflective tesselations of the plane. Vertices of odd order are present only in the final case 30-30-120; unambiguous parity assignments are possible in each of the other cases.*

with the quantum physics of the simplest case.

The fundamental unit in the case 45-45-90 contains a total of eight cells, as illustrated in Figure 15. Elaborating upon notation introduced in Figure 16,

[25] Personal communication, (1980).

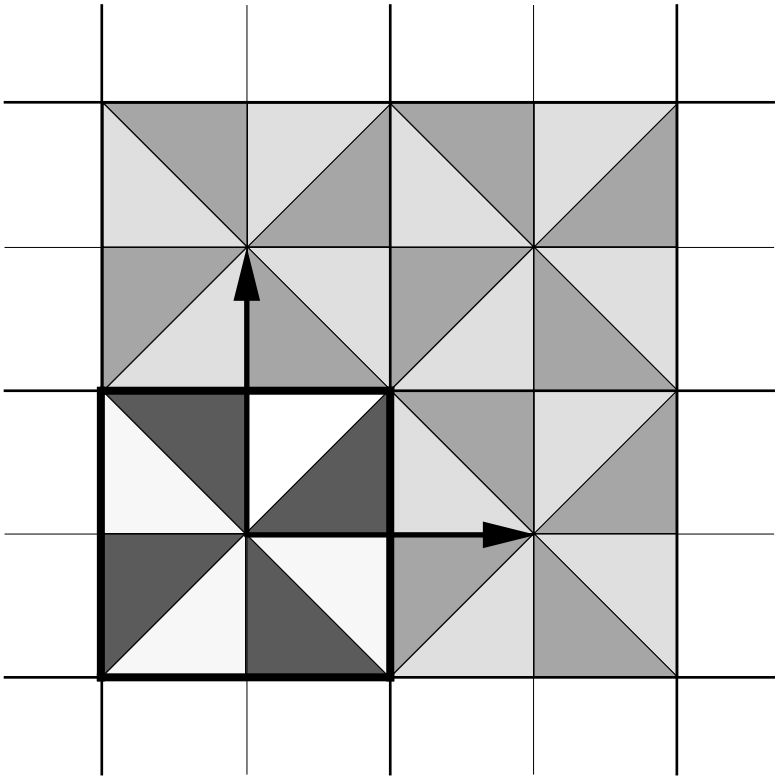

FIGURE 15: *The physical box (white) is joined with seven of its reflective images to form the fundamental unit characteristic of the right isosceles triangular box problem.*

we have the following equations:

$$\boldsymbol{x}_0 = \begin{pmatrix} x_1 \\ x_2 \end{pmatrix} = -\boldsymbol{x}_4 \quad : \quad \text{both even}$$

$$\boldsymbol{x}_1 = \begin{pmatrix} -x_1 \\ +x_2 \end{pmatrix} = -\boldsymbol{x}_5 \quad : \quad \text{both odd}$$

$$\boldsymbol{x}_2 = \begin{pmatrix} -x_2 \\ +x_1 \end{pmatrix} = -\boldsymbol{x}_6 \quad : \quad \text{both even}$$

$$\boldsymbol{x}_3 = \begin{pmatrix} -x_2 \\ -x_1 \end{pmatrix} = -\boldsymbol{x}_7 \quad : \quad \text{both odd}$$

Our simplified Feynman formalism (summation only over the direct/reflected *classical* paths) now supplies

$$K(\boldsymbol{x}, t; \boldsymbol{y}, 0) = \tfrac{m}{iht} \sum_{\alpha=0}^{7} (-)^{\alpha} \sum_{\boldsymbol{n}} \exp\left\{ \tfrac{i}{\hbar} S_{\alpha} \right\}$$

$$\tfrac{i}{\hbar} S_{\alpha} = \beta(\boldsymbol{v}_{\alpha} + \boldsymbol{n}) \cdot \mathbb{T}\,(\boldsymbol{v}_{\alpha} + \boldsymbol{n})$$

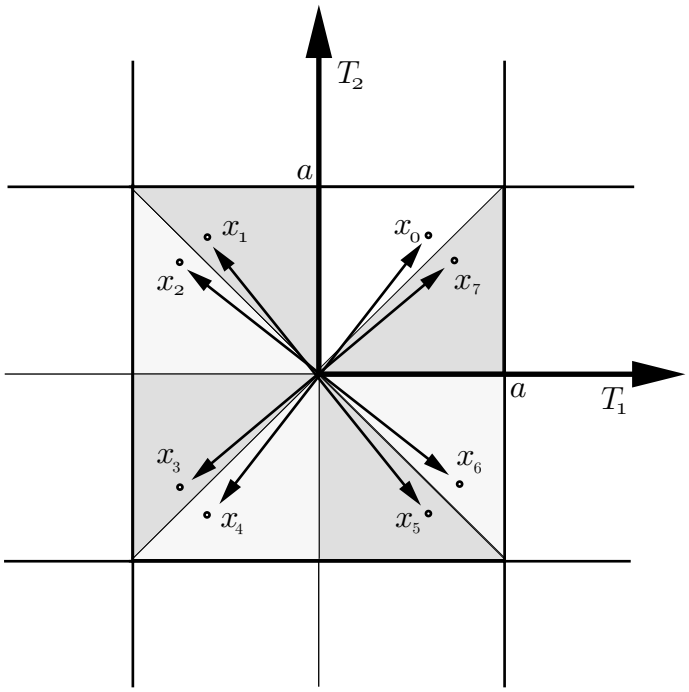

FIGURE 16: *The fundamental unit of the 45-45-90 tesselation, and associated notations. Here again, I have been careful to rig the notation so as to make it possible to write*

$$\text{parity of } \boldsymbol{x}_\alpha = (-)^\alpha$$

The short sides of the box have length a, so the tesselation has period $2a$ in both primary directions (which are in this case orthogonal).

where β retains its previous meaning and where

$$\mathbb{T} = 4a^2 \begin{pmatrix} 1 & 0 \\ 0 & 1 \end{pmatrix} \quad \text{is again diagonal, and} \quad \boldsymbol{v}_\alpha = (\boldsymbol{x}_\alpha - \boldsymbol{y})/2a$$

The argument which (by appeal to Jacobi's identity) gave us (39) now gives

$$K(\boldsymbol{x},t;\boldsymbol{y},0) = \tfrac{1}{4a^2}\sum_{\alpha=0}^{7}(-)^\alpha \vartheta(\pi\boldsymbol{v}_\alpha, \tfrac{\pi}{i\beta}\mathbb{T}^{-1})$$

$$\tfrac{\pi}{i\beta}\mathbb{T}^{-1} = \tau\begin{pmatrix} 1 & 0 \\ 0 & 1 \end{pmatrix} \quad \text{with} \quad \tau = -\tfrac{ht}{4ma^2}$$

$$= \tfrac{1}{4a^2}\sum_{\alpha=0}^{7}(-)^\alpha \vartheta(\pi v_{\alpha 1},\tau)\cdot\vartheta(\pi v_{\alpha 2},\tau)$$

$$= \tfrac{1}{4a^2}\sum_{\alpha=0}^{7}(-)^\alpha \big\{1 + 2\sum_{n_1=1}^{\infty} e^{-i\phi n_1^2} C_{\alpha 1}\big\}\big\{1 + 2\sum_{n_2=1}^{\infty} e^{-i\phi n_2^2} C_{\alpha 2}\big\}$$

where $\phi = -\pi\tau = \pi ht/4ma^2$ and where I have found it convenient to adopt the abbreviations

$$C_{\alpha 1} \equiv \cos \mathcal{X}_{\alpha 1} \equiv \cos 2\pi n_1 v_{\alpha 1}$$
$$C_{\alpha 2} \equiv \cos \mathcal{X}_{\alpha 2} \equiv \cos 2\pi n_2 v_{\alpha 2}$$

Trivially

$$\sum_{\alpha=0}^{7} (-)^\alpha = 0$$

while

$$\sum_{\alpha=0}^{7} (-)^\alpha C_{\alpha 1} = (C_{01} - C_{51}) + (C_{21} - C_{31}) + (C_{41} - C_{11}) + (C_{61} - C_{71}) = 0$$
$$\sum_{\alpha=0}^{7} (-)^\alpha C_{\alpha 2} = (C_{02} - C_{12}) + (C_{22} - C_{72}) + (C_{42} - C_{52}) + (C_{62} - C_{32}) = 0$$

because the bracketed terms cancel pairwise. So we have

$$K(\boldsymbol{x}, t; \boldsymbol{y}, 0) = \tfrac{1}{a^2} \sum_{n_1=1}^{\infty} \sum_{n_2=1}^{\infty} e^{-\frac{i}{\hbar}\mathcal{E}(n_1^2+n_2^2)} \sum_{\alpha=0}^{7} (-)^\alpha C_{\alpha 1} C_{\alpha 2} \tag{42}$$

To understand the surviving $\sum_\alpha$ we as a first step adopt the "principle of disallowed aliases," writing

$$\begin{aligned}
\sum_{\alpha=0}^{7} (-)^\alpha C_{\alpha 1} C_{\alpha 2} = \;& C_{01}C_{02} - C_{11}C_{12} + C_{21}C_{22} - C_{31}C_{32} \\
& + C_{41}C_{42} - C_{51}C_{52} + C_{61}C_{62} - C_{71}C_{72} \\
= \;& C_{01}C_{02} - C_{41}C_{02} + C_{21}C_{22} - C_{21}C_{62} \\
& + C_{41}C_{42} - C_{01}C_{42} + C_{61}C_{62} - C_{61}C_{22} \\
= \;& \big[C_{01}C_{02} - C_{41}C_{02} + C_{41}C_{42} - C_{01}C_{42}\big] \\
& + \big[C_{21}C_{22} - C_{21}C_{62} + C_{61}C_{62} - C_{61}C_{22}\big] \\
= \;& \big[C_{01} - C_{41}\big]\big[C_{02} - C_{42}\big] + \big[C_{21} - C_{61}\big]\big[C_{22} - C_{62}\big] \\
= \;& \big[\cos \mathcal{X}_{01} - \cos \mathcal{X}_{41}\big]\big[\cos \mathcal{X}_{02} - \cos \mathcal{X}_{42}\big] \\
& + \big[\cos \mathcal{X}_{21} - \cos \mathcal{X}_{61}\big]\big[\cos \mathcal{X}_{22} - \cos \mathcal{X}_{62}\big] \\
= \;& 4\Big\{ \sin\Big(\frac{\mathcal{X}_{01} + \mathcal{X}_{41}}{2}\Big) \cdot \sin\Big(\frac{\mathcal{X}_{01} - \mathcal{X}_{41}}{2}\Big) \\
& \qquad \times \sin\Big(\frac{\mathcal{X}_{02} + \mathcal{X}_{42}}{2}\Big) \cdot \sin\Big(\frac{\mathcal{X}_{02} - \mathcal{X}_{42}}{2}\Big) \\
& + \sin\Big(\frac{\mathcal{X}_{21} + \mathcal{X}_{61}}{2}\Big) \cdot \sin\Big(\frac{\mathcal{X}_{21} - \mathcal{X}_{61}}{2}\Big) \\
& \qquad \times \sin\Big(\frac{\mathcal{X}_{22} + \mathcal{X}_{62}}{2}\Big) \cdot \sin\Big(\frac{\mathcal{X}_{22} - \mathcal{X}_{62}}{2}\Big) \Big\}
\end{aligned}$$

Recalling now the definitions of $\mathcal{X}_{\alpha 1}$ and $\mathcal{X}_{\alpha 2}$, we have

$$\sum_{\alpha=0}^{7}(-)^{\alpha}C_{\alpha 1}C_{\alpha 2} = 4\Big\{ \sin\Big(\frac{n_1\pi}{a}x_1\Big)\sin\Big(\frac{n_2\pi}{a}x_2\Big)\sin\Big(\frac{n_1\pi}{a}y_1\Big)\sin\Big(\frac{n_2\pi}{a}y_2\Big) - \sin\Big(\frac{n_1\pi}{a}x_2\Big)\sin\Big(\frac{n_2\pi}{a}x_1\Big)\sin\Big(\frac{n_1\pi}{a}y_1\Big)\sin\Big(\frac{n_2\pi}{a}y_2\Big)\Big\}$$

Returning with this information to (42), and borrowing some notation from (22) (i.e., from the rectangular box problem, made square by setting $a_1 = a_2 = a$) we have

$$K(\boldsymbol{x},t;\boldsymbol{y},0) = \sum_{n_1=1}^{\infty}\sum_{n_2=1}^{\infty} e^{-\frac{i}{\hbar}\mathcal{E}(n_1^2+n_2^2)}[\psi_{n_1n_2}(x_1,x_2) - \psi_{n_1n_2}(x_2,x_1)]\psi_{n_1n_2}(y_1,y_2)$$

The bracketed function—which can be described

$$[\text{etc}] = \begin{vmatrix} \sqrt{\frac{2}{a}}\sin(\frac{\pi}{a}n_1x_1) & \sqrt{\frac{2}{a}}\sin(\frac{\pi}{a}n_1x_2) \\ \sqrt{\frac{2}{a}}\sin(\frac{\pi}{a}n_2x_1) & \sqrt{\frac{2}{a}}\sin(\frac{\pi}{a}n_2x_2) \end{vmatrix} \equiv \Psi_{n_1n_2}(x_1,x_2)$$

—is antisymmetric in $\{n_1, n_2\}$,[26] so only

$$\begin{aligned} \tfrac{1}{2}[\psi_{n_1n_2}(y_1,y_2) - \psi_{n_2n_1}(y_1,y_2)] &= \text{antisymmetric component of } \psi_{n_1n_2}(y_1,y_2) \\ &= \tfrac{1}{2}\Psi_{n_1n_2}(y_1,y_2) \end{aligned}$$

contributes effectively to the summation process. We can therefore write

$$K(\boldsymbol{x},t;\boldsymbol{y},0) = \tfrac{1}{2}\sum_{n_1=1}^{\infty}\sum_{n_2=1}^{\infty} e^{-\frac{i}{\hbar}\mathcal{E}(n_1^2+n_2^2)}\Psi_{n_1n_2}(x_1,x_2)\Psi_{n_1n_2}(y_1,y_2)$$

But every term in the sum is now counted *twice*; we are led therefore to impose the constraint $n_2 > n_1$, writing

$$\sum_{n_1=1}^{\infty}\sum_{n_2=1}^{\infty} = 2\sum_{\boldsymbol{n}} \quad : \quad \boldsymbol{n} \text{ takes values indicated in Figure 17}$$

We come thus to the conclusion that the right isosceles box problem gives rise to energy eigenvalues that can be described determinentally

$$\Psi_{n_1n_2}(x_1,x_2) = \frac{2}{a}\begin{vmatrix} \sin(\frac{\pi}{a}n_1x_1) & \sin(\frac{\pi}{a}n_1x_2) \\ \sin(\frac{\pi}{a}n_2x_1) & \sin(\frac{\pi}{a}n_2x_2) \end{vmatrix} \tag{43}$$

and to the energy spectrum

$$E_{n_1n_2} = \mathcal{E}(n_1^2+n_2^2) \quad \text{with} \quad \mathcal{E} \equiv \frac{h^2}{8ma^2} \tag{44}$$

[26] It is antisymmetric also in $\{x_1, x_2\}$, but physically $0 \le x_1 \le x_2 \le a$; the point with coordinates $\{x_2, x_1\}$ lies in an *image* of the physical box.

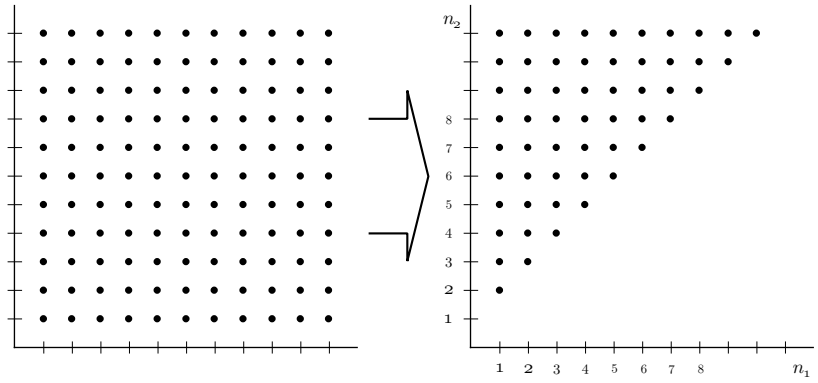

FIGURE 17: *The quantum numbers of the square box problem (on the left) compared with those of the 45-45-90 box (on the right). The eigenstates are antisymmetrized square box states, so a kind of "exclusion principle" is in effect. The eigenvalues are identical, except that those associated with the triangular box have reduced degeneracy (evident as "erased lattice points" in the figure), and those with $n_1 = n_2$ are excluded altogether.*

In (43) we have recovered precisely the eigenstates that Morse & Feshbach[27] obtain by antisymmetrization of the square box states.

Morse & Feshbach (see their Figure 6.10) attempt to provide graphical representation of some properties of the eigenfunctions $\Psi_{n_1 n_2}(x_1, x_2)$, but with the assistance of a modern resource such as *Mathematica* one can do much better than was possible in 1953, and learn correspondingly sharper things. I describe *how* I generated the following figures, in the hope that my reader will be thus encouraged to undertake some hands-on exploration. One begins by describing (and giving names to) the eigenfunctions in which one has interest:

```
F12[x_,y_]:=Sin[Pi*1*x]Sin[Pi*2*y]-Sin[Pi*2*x]Sin[Pi*1*y]
F23[x_,y_]:=Sin[Pi*2*x]Sin[Pi*3*y]-Sin[Pi*3*x]Sin[Pi*2*y]
F49[x_,y_]:=Sin[Pi*4*x]Sin[Pi*9*y]-Sin[Pi*9*x]Sin[Pi*4*y]
```

[27] *Methods of Theoretical Physics I*, p. 756. They remark that "the analysis [of eigenfunctions in several dimensions] is rather more involved when the equation is not separable in coordinates suitable for the boundary. Unfortunately only two nonseparable cases have been solved in detail, one for a boundary which is an isosceles right triangle. This is probably too simple to bring out all the complexities; nevertheless it is worth some discussion." They make the ensuing discussion more complicated than it need be by placing the right angle at the origin. And unaccountably, they neglect to identify the "other case."

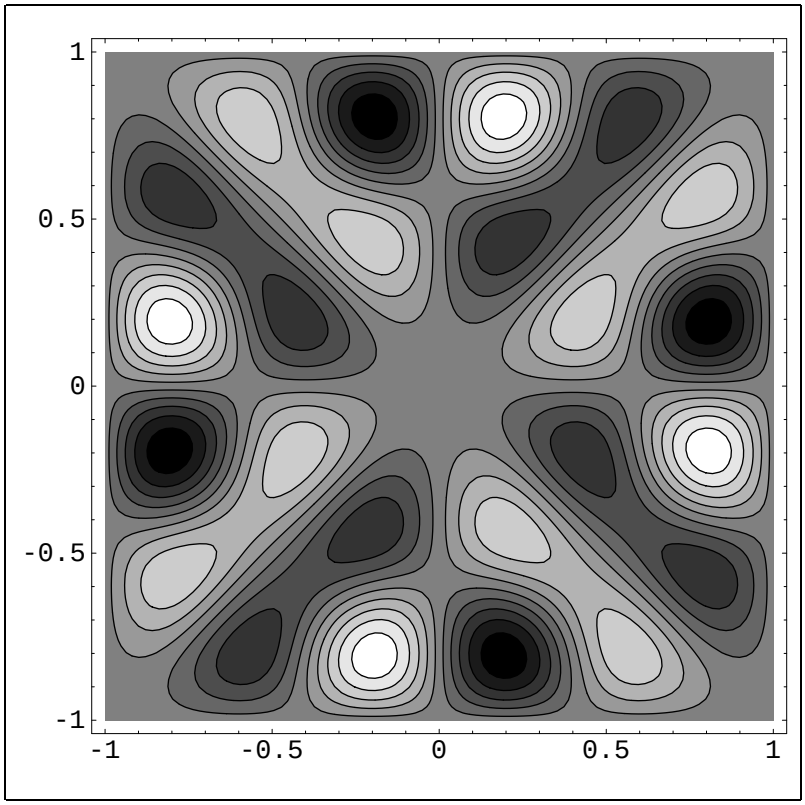

FIGURE 18: *Contour plot of the state* $\Psi_{23}(x_1, x_2)$.

Commands of the form

```
G23=ContourPlot[F23[x,y],{x,-1,1},{y,-1,1},PlotPoints->100]
```

then produce graphics of which Figure 18 is representative. Clarity is sometimes served by eliminating the shading, which is accomplished by

```
H23=ContourPlot[F23[x,y],{x,-1,1},{y,-1,1},PlotPoints->100,
ContourShading->False]
```

with results such as are evident in Figure 19. To plot nodal lines one calls up a standard package

```
<<Graphics‘ImplicitPlot‘
```

and enters the command

```
Nodes23=ImplicitPlot[F23[x,y]==0,{x,-1,1},{y,-1,1},
PlotPoints->150]
```

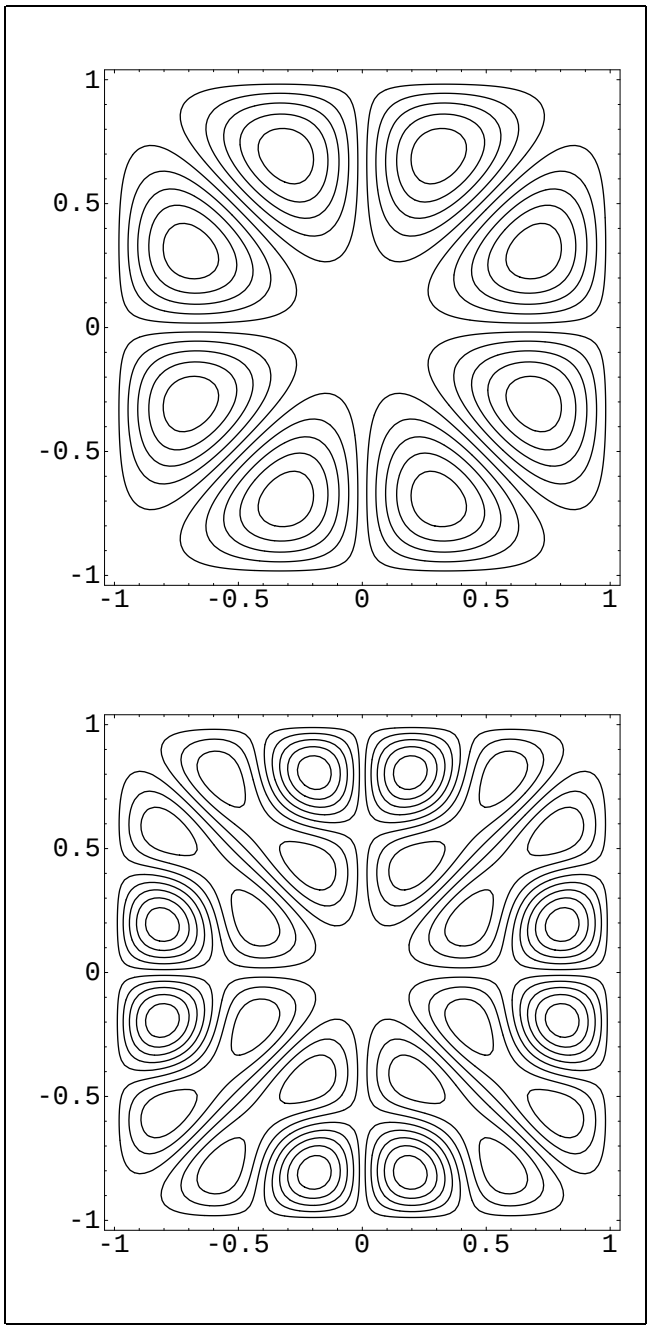

FIGURE 19: *Unshaded contour plots of the ground state* $\Psi_{12}(x_1, x_2)$ *and—compare the preceding figure—of* $\Psi_{23}(x_1, x_2)$.

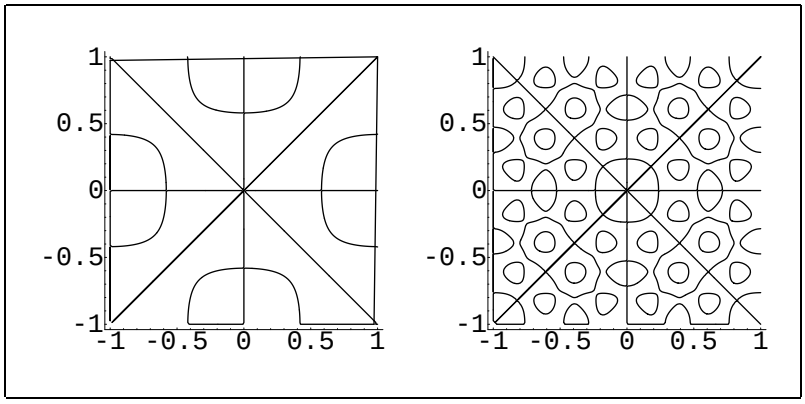

FIGURE 20: *Nodal lines of the states* $\Psi_{23}(x_1, x_2)$ *and* $\Psi_{49}(x_1, x_2)$. *Here as in both of the two preceding figures, the point* $\{x_1, x_2\}$ *ranges over the entire fundamental unit (physical box plus seven images) and the scale parameter* a *has been set equal to unity.*

A pair of such designs is shown in Figure 20.

Examination of such figures shows them to be most complex when n_1 and n_2 share few common factors, and to exhibit a kind of scaling property when $n_1 : n_2 = 1 : 2$. It is in all cases evident also that, as Morse & Feshbach observe, the nodal lines "do not fall into two mutually orthogonal families" as is the pattern in all separable cases.

7. Particle in an equilateral triangular box. The fundamental unit contains in this case (see Figure 21) a total of six cells, which reproduce the tesselated plane by non-orthogonal translation. It is from that non-orthogonality that the following argument acquires its novelty, and its relative complexity.[28] Elaborating upon the notation introduced in Figure 23, we note that the sequences

$$\boldsymbol{x}_0 \longrightarrow \boldsymbol{x}_2 \longrightarrow \boldsymbol{x}_4 \quad \text{and} \quad \boldsymbol{x}_5 \longrightarrow \boldsymbol{x}_1 \longrightarrow \boldsymbol{x}_3$$

are achieved by action of the 120° rotation matrix

$$\mathbb{R} = \tfrac{1}{2}\begin{pmatrix} -1 & -\sqrt{3} \\ \sqrt{3} & -1 \end{pmatrix}$$

[28] It is interesting to note that (see Figure 22) orthogonality can be purchased by *doubling the size of the fundamental unit*: complexity excluded at the front door thus gains entry by a sidedoor. These two modes of approach—which amount simply to distinct methods of partitioning the same sum-over-paths—give rise to arguments the details of which look initially quite different, but which ultimately converge. What we have encountered is the first vivid evidence of a circumstance that in fact pertains quite generally: *the definition of the fundamental unit is always, to some degree, conventional*.

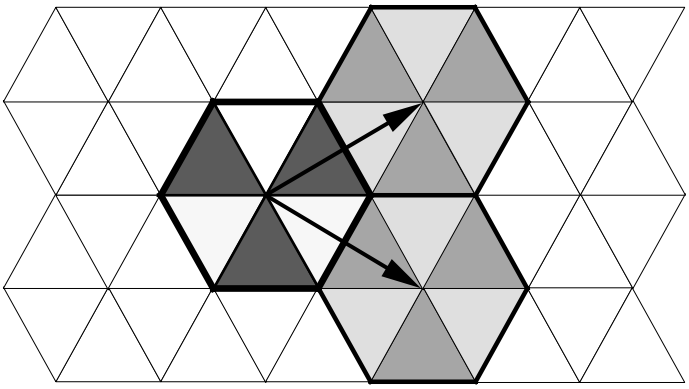

FIGURE 21: *The 6-element fundamental unit of the equilateral triangular box problem. Note the non-orthogonality of the associated translation vectors.*

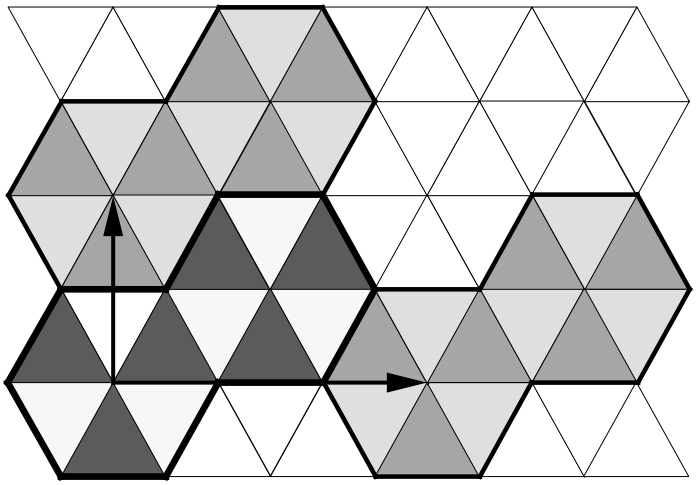

FIGURE 22: *An alternative 12-element fundamental unit that reproduces the tesselated plane by* orthogonal *translation.*

while $\boldsymbol{x}_0 \longrightarrow \boldsymbol{x}_5$ is achieved by reflection in the line defined by the 60° unit vector

$$\boldsymbol{e} = \tfrac{1}{2}\begin{pmatrix} 1 \\ \sqrt{3} \end{pmatrix}$$

To accomplish the latter objective we form the matrix

$$\mathbb{P} = \begin{pmatrix} e_1 e_1 & e_1 e_2 \\ e_2 e_1 & e_2 e_2 \end{pmatrix} = \tfrac{1}{4}\begin{pmatrix} 1 & \sqrt{3} \\ \sqrt{3} & 3 \end{pmatrix}$$

that projects onto $\boldsymbol{e}$; we note that every $\boldsymbol{x}$ can be resolved

$$\boldsymbol{x} = \mathbb{P}\boldsymbol{x} + (\mathbb{I} - \mathbb{P}\boldsymbol{x}) = \boldsymbol{x}_{\text{para}} + \boldsymbol{x}_{\perp}$$

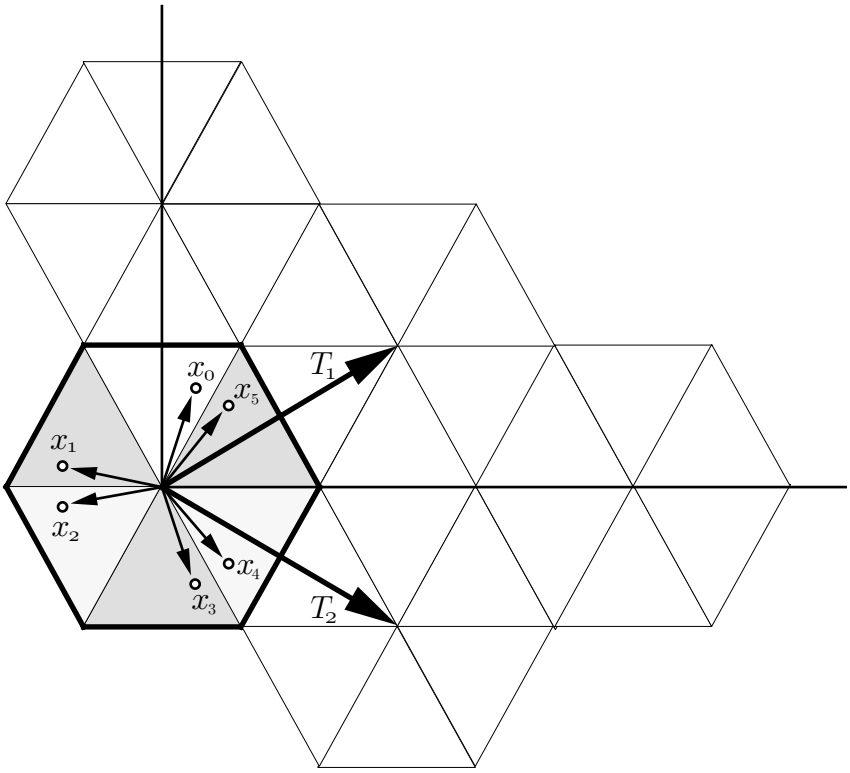

FIGURE 23: *The 6-element fundamental unit of the equilateral box problem, and associated notations. Again things have been rigged so as to achieve*

$$\text{parity of } \boldsymbol{x}_\alpha = (-)^\alpha$$

Scale is set by

$$a \equiv \text{length of each side}$$

and the box therefore has

$$\text{area} = \tfrac{1}{4}\sqrt{3}a^2$$

and that reflection in the $\boldsymbol{e}$-line produces

$$\boldsymbol{x}_{\text{reflected}} = \boldsymbol{x}_{\text{para}} - \boldsymbol{x}_\perp = \underbrace{(2\mathbb{P} - \mathbb{I})}\boldsymbol{x}$$

$$\equiv \mathbb{Q} \quad \text{is an improper rotation matrix}$$

In the present instance

$$\mathbb{Q} = \tfrac{1}{2}\begin{pmatrix} -1 & \sqrt{3} \\ \sqrt{3} & 1 \end{pmatrix}$$

From the preceding remarks we are led to the following equations:

$$\begin{aligned}
\boldsymbol{x}_0 &= \begin{pmatrix} +1 & 0 \\ 0 & +1 \end{pmatrix} \boldsymbol{x} \quad \text{with} \quad \boldsymbol{x} \equiv \begin{pmatrix} x_1 \\ x_2 \end{pmatrix} \\
\boldsymbol{x}_1 &= \tfrac{1}{2} \begin{pmatrix} -1 & -\sqrt{3} \\ -\sqrt{3} & +1 \end{pmatrix} \boldsymbol{x}_0 \\
\boldsymbol{x}_2 &= \tfrac{1}{2} \begin{pmatrix} -1 & -\sqrt{3} \\ +\sqrt{3} & -1 \end{pmatrix} \boldsymbol{x}_0 \\
\boldsymbol{x}_3 &= \begin{pmatrix} +1 & 0 \\ 0 & -1 \end{pmatrix} \boldsymbol{x}_0 \\
\boldsymbol{x}_4 &= \tfrac{1}{2} \begin{pmatrix} -1 & +\sqrt{3} \\ -\sqrt{3} & -1 \end{pmatrix} \boldsymbol{x}_0 \\
\boldsymbol{x}_5 &= \tfrac{1}{2} \begin{pmatrix} -1 & +\sqrt{3} \\ +\sqrt{3} & +1 \end{pmatrix} \boldsymbol{x}_0
\end{aligned}$$

The non-orthogonal translation vectors are (reading from the figure) given by

$$\boldsymbol{T}_1 = \tfrac{a}{2} \begin{pmatrix} 3 \\ +\sqrt{3} \end{pmatrix} \quad \text{and} \quad \boldsymbol{T}_2 = \tfrac{a}{2} \begin{pmatrix} 3 \\ -\sqrt{3} \end{pmatrix}$$

and have lengths

$$T_1 = T_2 = \sqrt{3}a$$

Moreover

$$\boldsymbol{T}_1 \cdot \boldsymbol{T}_2 = \tfrac{3}{2}a^2 = T_1 T_2 \cos 60^\circ$$

so we have

$$\mathbb{T} = \tfrac{3}{2}a^2 \begin{pmatrix} 2 & 1 \\ 1 & 2 \end{pmatrix}$$

$$\det \mathbb{T} = 3 \cdot \left(\tfrac{3}{2}a^2\right)^2$$

$$\mathbb{T}^{-1} = \left(\tfrac{3}{2}a^2\right)^{-1} \begin{pmatrix} \frac{2}{3} & -\frac{1}{3} \\ -\frac{1}{3} & \frac{2}{3} \end{pmatrix}$$

Our simplified Feynman formalism now supplies

$$K(\boldsymbol{x}, t; \boldsymbol{y}, 0) = \tfrac{m}{iht} \sum_{\alpha=0}^{5} (-)^\alpha \sum_{\boldsymbol{n}} \exp\left\{ \tfrac{i}{\hbar} S_\alpha \right\}$$

$$\tfrac{i}{\hbar} S_\alpha = \beta(\boldsymbol{v}_\alpha + \boldsymbol{n}) \cdot \mathbb{T}\,(\boldsymbol{v}_\alpha + \boldsymbol{n})$$

where the vectors $\boldsymbol{v}_\alpha$ were defined at (27); it proves convenient to postpone for a moment their actual evaluation. The argument which (by appeal to Jacobi's identity) gave us (39) now gives us

$$= \underbrace{\tfrac{m}{iht} \sqrt{\left(-\tfrac{\pi}{\beta}\right)^2 \tfrac{1}{\det \mathbb{T}}}} \sum_{\alpha=0}^{5} (-)^\alpha \, \vartheta\left(\pi \boldsymbol{v}_\alpha, \tfrac{\pi}{i\beta} \mathbb{T}^{-1}\right) \tag{45}$$

$$= \tfrac{1}{\sqrt{3}(\frac{3}{2}a^2)} = \tfrac{1}{6 \cdot \text{area}} = \frac{1}{\text{area of fundamental unit}}$$

Because $\mathbb{T}$ in non-diagonal we cannot (as in previous cases) immediately invoke the factorization principle (38) but must work a bit before we can extract useful information from (45). Recalling from (35) the definition

$$\vartheta(\boldsymbol{z},\mathbb{W}) \equiv \sum_{\boldsymbol{n}} e^{i\pi\,\boldsymbol{n}\cdot\mathbb{W}\boldsymbol{n}} e^{-2i\,\boldsymbol{n}\cdot\boldsymbol{z}}$$

of $\vartheta(\boldsymbol{z},\mathbb{W})$, we observe that only the even part of the second factor contributes to the extended sum,[29] so we have (compare (7))

$$\vartheta(\boldsymbol{z},\mathbb{W}) = \sum_{\boldsymbol{n}} e^{i\pi\,\boldsymbol{n}\cdot\mathbb{W}\boldsymbol{n}} \cos 2\boldsymbol{n}\cdot\boldsymbol{z} \tag{46}$$

Returning with (46) to (45), we have

$$K(\boldsymbol{x},t;\boldsymbol{y},0) = \tfrac{1}{6\cdot\text{area}} \sum_{\alpha=0}^{5} (-)^{\alpha} \sum_{\boldsymbol{n}} e^{i\pi\,\boldsymbol{n}\cdot\mathbb{W}\boldsymbol{n}} \cos 2\pi\,\boldsymbol{n}\cdot\boldsymbol{v}_{\alpha}$$

where

$$\mathbb{W} = \tfrac{\pi}{i\beta}\mathbb{T}^{-1} = \tau \begin{pmatrix} 2 & -1 \\ -1 & 2 \end{pmatrix} \quad \text{with} \quad \tau = -\tfrac{1}{3}\tfrac{ht}{\frac{3}{2}ma^2}$$

entails

$$i\pi\mathbb{W} = -\tfrac{i}{\hbar}\mathbb{E}t \quad \text{with} \quad \mathbb{E} \equiv \tfrac{1}{2}\mathcal{E} \begin{pmatrix} 2 & -1 \\ -1 & 2 \end{pmatrix} \quad \text{and} \quad \mathcal{E} \equiv \tfrac{1}{3}\tfrac{h^2}{\frac{3}{2}ma^2}$$

It now follows (use $\boldsymbol{n}\cdot\mathbb{E}\boldsymbol{n} = \mathcal{E}(n_1^2 - n_1n_2 + n_2^2)$ and interchange the order of summation) that

$$K(\boldsymbol{x},t;\boldsymbol{y},0) = \tfrac{1}{6\cdot\text{area}} \sum_{\boldsymbol{n}} e^{-\frac{i}{\hbar}\mathcal{E}(n_1^2 - n_1n_2 + n_2^2)\,t} \sum_{\alpha=0}^{5} (-)^{\alpha} \cos 2\pi\,\boldsymbol{n}\cdot\boldsymbol{v}_{\alpha} \tag{47}$$

Turning our attention now to evaluation of the $\sum_{\alpha}$, we first construct (with major assistance from *Mathematica*) the vectors $\boldsymbol{v}_{\alpha}$ and obtain results which make natural the introduction of the following dimensionless variables:

$$\begin{aligned} X_0 &\equiv \tfrac{\pi}{3a}(\,2x_1) & Y_0 &\equiv \tfrac{\pi}{3a}(\,2y_1) \\ X_1 &\equiv \tfrac{\pi}{3a}(-x_1 + \sqrt{3}x_2) & Y_1 &\equiv \tfrac{\pi}{3a}(-y_1 + \sqrt{3}y_2) \\ X_2 &\equiv \tfrac{\pi}{3a}(-x_1 - \sqrt{3}x_2) & Y_2 &\equiv \tfrac{\pi}{3a}(-y_1 - \sqrt{3}y_2) \end{aligned}$$

These definitions are, by the way, reminiscent of the equations that describe the cube roots of unity, and entail

$$\begin{aligned} X_0 + X_1 + X_2 &= 0 \\ X_0^2 + X_1^2 + X_2^2 &= 6(\tfrac{\pi}{3a})^2(x_1^2 + x_2^2) \end{aligned}$$

[29] I allude with this phrase to the fact that the points $\{\pm\boldsymbol{n}\}$ lie at the vertices of a hypercube in $\boldsymbol{n}$-space; diametrically opposite points cancel pairwise in consequence of the oddness of the sine function.

The results reported by *Mathematica* can in this notation be described

$$\begin{aligned}
-\pi\,\boldsymbol{v}_0 &= \begin{pmatrix} X_2-Y_2 \\ X_1-Y_1 \end{pmatrix} \\
-\pi\,\boldsymbol{v}_1 &= \begin{pmatrix} X_0-Y_2 \\ X_1-Y_1 \end{pmatrix} \\
-\pi\,\boldsymbol{v}_2 &= \begin{pmatrix} X_1-Y_2 \\ X_0-Y_1 \end{pmatrix} \\
-\pi\,\boldsymbol{v}_3 &= \begin{pmatrix} X_1-Y_2 \\ X_2-Y_1 \end{pmatrix} \\
-\pi\,\boldsymbol{v}_4 &= \begin{pmatrix} X_0-Y_2 \\ X_2-Y_1 \end{pmatrix} \\
-\pi\,\boldsymbol{v}_5 &= \begin{pmatrix} X_2-Y_2 \\ X_0-Y_1 \end{pmatrix}
\end{aligned}$$

From these highly patterned[30] equations it follows that

$$\begin{aligned}
\sum_{\alpha=0}^{5}(-)^\alpha \cos 2\pi\,\boldsymbol{n}\cdot\boldsymbol{v}_\alpha = &+\cos 2[n_1(X_2-Y_2)+n_2(X_1-Y_1)] \\
&-\cos 2[n_1(X_0-Y_2)+n_2(X_1-Y_1)] \\
&+\cos 2[n_1(X_1-Y_2)+n_2(X_0-Y_1)] \\
&-\cos 2[n_1(X_1-Y_2)+n_2(X_2-Y_1)] \\
&+\cos 2[n_1(X_0-Y_2)+n_2(X_2-Y_1)] \\
&-\cos 2[n_1(X_2-Y_2)+n_2(X_0-Y_1)] \\
\\
= &+\cos 2[(n_1X_2+n_2X_1)-(n_1Y_2+n_2Y_1)] \\
&-\cos 2[(n_2X_2+n_1X_1)-(\quad\text{ditto}\quad)] \\
&+\cos 2[(n_1X_1+n_2X_0)-(\quad\text{ditto}\quad)] \\
&-\cos 2[(n_2X_1+n_1X_0)-(\quad\text{ditto}\quad)] \\
&+\cos 2[(n_1X_0+n_2X_2)-(\quad\text{ditto}\quad)] \\
&-\cos 2[(n_2X_0+n_1X_2)-(\quad\text{ditto}\quad)]
\end{aligned}$$

It is elementary that

$$\begin{aligned}
\cos 2(A-C)-\cos 2(B-C) &= (\cos 2A-\cos 2B)\cos 2C+(\sin 2A-\sin 2B)\sin 2C \\
&= -2\sin(A+B)\sin(A-B)\cos 2C+2\cos(A+B)\sin(A-B)\sin 2C
\end{aligned}$$

so after some slight rearrangement we have

[30] Look, in reference to Figure 23, to the relation of $\boldsymbol{v}_0$ to $\boldsymbol{v}_3$, of $\boldsymbol{v}_2$ to $\boldsymbol{v}_1$, of $\boldsymbol{v}_4$ to $\boldsymbol{v}_5$. And to the sequences $\boldsymbol{v}_0\to\boldsymbol{v}_2\to\boldsymbol{v}_4$, $\boldsymbol{v}_1\to\boldsymbol{v}_3\to\boldsymbol{v}_5$. One gains the impression that the equations could almost have been written directly—without calculation.

$$\sum_{\alpha=0}^{5}(-)^{\alpha}\cos 2\pi\boldsymbol{n}\cdot\boldsymbol{v}_{\alpha} = -2F\cdot\cos 2[n_1Y_2+n_2Y_1] - 2G\cdot\sin 2[n_1Y_2+n_2Y_1] \quad (48)$$

where the abbreviations F and G are defined

$$\begin{aligned} F \equiv\ & \sin[(n_1+n_2)(X_2+X_1)]\sin[(n_1-n_2)(X_2-X_1)] \\ & +\ \sin[(n_1+n_2)(X_0+X_2)]\sin[(n_1-n_2)(X_0-X_2)] \\ & +\ \sin[(n_1+n_2)(X_1+X_0)]\sin[(n_1-n_2)(X_1-X_0)] \end{aligned}$$

$$\begin{aligned} G \equiv & -\cos[(n_1+n_2)(X_2+X_1)]\sin[(n_1-n_2)(X_2-X_1)] \\ & -\cos[(n_1+n_2)(X_0+X_2)]\sin[(n_1-n_2)(X_0-X_2)] \\ & -\cos[(n_1+n_2)(X_1+X_0)]\sin[(n_1-n_2)(X_1-X_0)] \end{aligned}$$

Returning with (48) to (47), we obtain a description of $K(\boldsymbol{x},t;\boldsymbol{y},0)$ which still only faintly resembles the (3) from which it is our objective to read off the eigenvalues and eigenfunctions of an equilaterally confined quantum particle. It is in an effort to enhance the resemblance that we undertake the following manipulations.

Let dimensionless vectors $\boldsymbol{\xi}$ and $\boldsymbol{\zeta}$ be defined

$$\begin{aligned} \xi_1 &\equiv \tfrac{\pi}{3a}x_1 & \zeta_1 &\equiv \tfrac{\pi}{3a}y_1 \\ \xi_2 &\equiv \tfrac{\pi}{3a}\sqrt{3}x_2 & \zeta_2 &\equiv \tfrac{\pi}{3a}\sqrt{3}y_2 \end{aligned}$$

in which notation

$$\begin{aligned} X_0 &= 2\xi_1 & Y_0 &= 2\zeta_1 \\ X_1 &= -\xi_1+\xi_2 & Y_1 &= -\zeta_1+\zeta_2 \\ X_2 &= -\xi_1-\xi_2 & Y_2 &= -\zeta_1-\zeta_2 \end{aligned}$$

permit us to write

$$\begin{aligned} F = F_{\boldsymbol{n}}(\xi_1,\xi_2) \equiv\ & \sin[(n_1+n_2)(2\xi_1)]\sin[(n_1-n_2)(2\xi_2)] \\ & -\ \sin[(n_1+n_2)(\xi_1+\xi_2)]\sin[(n_1-n_2)(3\xi_1-\xi_2)] \\ & +\ \sin[(n_1+n_2)(\xi_1-\xi_2)]\sin[(n_1-n_2)(3\xi_1+\xi_2)] \quad (49.1) \end{aligned}$$

$$\begin{aligned} G = G_{\boldsymbol{n}}(\xi_1,\xi_2) \equiv\ & \cos[(n_1+n_2)(2\xi_1)]\sin[(n_1-n_2)(2\xi_2)] \\ & +\cos[(n_1+n_2)(\xi_1+\xi_2)]\sin[(n_1-n_2)(3\xi_1-\xi_2)] \\ & -\cos[(n_1+n_2)(\xi_1-\xi_2)]\sin[(n_1-n_2)(3\xi_1+\xi_2)] \quad (49.2) \end{aligned}$$

When (47) is written

$$\begin{aligned} K(\boldsymbol{x},t;\boldsymbol{y},0) = & -\tfrac{2}{6\cdot\text{area}}\sum_{\boldsymbol{n}}\left\{e^{-\frac{i}{\hbar}\mathcal{E}(n_1^2-n_1n_2+n_2^2)t}F_{\boldsymbol{n}}(\xi_1,\xi_2)\right\}\cos 2[n_1Y_2+n_2Y_1] \\ & -\tfrac{2}{6\cdot\text{area}}\sum_{\boldsymbol{n}}\left\{e^{-\frac{i}{\hbar}\mathcal{E}(n_1^2-n_1n_2+n_2^2)t}G_{\boldsymbol{n}}(\xi_1,\xi_2)\right\}\sin 2[n_1Y_2+n_2Y_1] \end{aligned}$$

it becomes evident that, since the expressions within braces are both $\{n_1 n_2\}$-antisymmetric, only the antisymmetric parts of $\cos 2[\text{etc.}]$ and $\sin 2[\text{etc.}]$ actually contribute to the $\sum_{\boldsymbol{n}}$, and those are given by

$$\begin{aligned}
&\tfrac{1}{2}\big\{\cos 2[n_1 Y_2 + n_2 Y_1] - \cos 2[n_2 Y_2 + n_1 Y_1]\big\} \\
&\qquad = -\sin[(n_1+n_2)(Y_2+Y_1)]\sin[(n_1-n_2)(Y_2-Y_1)] \\
&\qquad = -\sin[(n_1+n_2)(2\zeta_1)]\sin[(n_1-n_2)(2\zeta_2)] \\
&\tfrac{1}{2}\big\{\sin 2[n_1 Y_2 + n_2 Y_1] - \sin 2[n_2 Y_2 + n_1 Y_1]\big\} \\
&\qquad = +\cos[(n_1+n_2)(Y_2+Y_1)]\sin[(n_1-n_2)(Y_2-Y_1)] \\
&\qquad = -\cos[(n_1+n_2)(2\zeta_1)]\sin[(n_1-n_2)(2\zeta_2)]
\end{aligned}$$

We are in position therefore to write

$$\begin{aligned}
K(\boldsymbol{x},t;\boldsymbol{y},0) = \tfrac{2}{6\cdot\text{area}}\sum_{\boldsymbol{n}} e^{-\frac{i}{\hbar}\mathcal{E}(n_1^2 - n_1 n_2 + n_2^2)t} \qquad (50)\\
\times\Big\{\ F_{\boldsymbol{n}}(\xi_1,\xi_2)\cdot\sin[(n_1+n_2)(2\zeta_1)]\sin[(n_1-n_2)(2\zeta_2)] \\
+ G_{\boldsymbol{n}}(\xi_1,\xi_2)\cdot\cos[(n_1+n_2)(2\zeta_1)]\sin[(n_1-n_2)(2\zeta_2)]\Big\}
\end{aligned}$$

and to notice that the factor that multiplies $F_{\boldsymbol{n}}(\xi_1,\xi_2)$ is the exact ζ-analog of one of the three terms that enters into the definition (49.1) of $F_{\boldsymbol{n}}(\xi_1,\xi_2)$, and that a similar remark pertains to the factor that multiplies $G_{\boldsymbol{n}}(\xi_1,\xi_2)$. We have therefore moved closer to our goal—which is to achieve structural imitation of (3)—but to realize that goal we must introduce one fundamentally new idea:

8. Sum over spectral symmetries. Look to the exponent in (50), where we encounter

$$n_1^2 - n_n n_2 + n_2^2 = \tfrac{1}{2}\boldsymbol{n}^{\intercal}\begin{pmatrix} 2 & -1 \\ -1 & 2\end{pmatrix}\boldsymbol{n}$$

The following equations

$$\begin{pmatrix} 2 & -1 \\ -1 & 2\end{pmatrix}\begin{pmatrix} 1 \\ 1\end{pmatrix} = 1\cdot\begin{pmatrix} 1 \\ 1\end{pmatrix} \quad\text{and}\quad \begin{pmatrix} 2 & -1 \\ -1 & 2\end{pmatrix}\begin{pmatrix} 1 \\ -1\end{pmatrix} = 3\cdot\begin{pmatrix} 1 \\ -1\end{pmatrix}$$

summarize the spectral properties of the symmetric matrix, and put us in position to write

$$\begin{pmatrix} 2 & -1 \\ -1 & 2\end{pmatrix} = \tfrac{1}{2}\cdot\begin{pmatrix} 1 & 1 \\ 1 & -1\end{pmatrix}^{\intercal}\begin{pmatrix} 1 & 0 \\ 0 & 3\end{pmatrix}\begin{pmatrix} 1 & 1 \\ 1 & -1\end{pmatrix}$$

The immediate implication is that

$$\begin{aligned}
n_1^2 - n_n n_2 + n_2^2 &= \tfrac{1}{4}\hat{\boldsymbol{n}}^{\intercal}\begin{pmatrix} 1 & 0 \\ 0 & 3\end{pmatrix}\hat{\boldsymbol{n}} \quad\text{with}\quad \hat{\boldsymbol{n}} \equiv \begin{pmatrix} 1 & 1 \\ 1 & -1\end{pmatrix}\boldsymbol{n} \\
&= \tfrac{1}{4}\big[(n_1+n_2)^2 + 3(n_1-n_2)^2\big] \qquad (51)\\
&= \tfrac{1}{4}\underbrace{\big[\hat{n}_1^2 + 3\hat{n}_2^2\big]}_{\equiv N(\hat{\boldsymbol{n}})} = \tfrac{1}{4}(\hat{n}_1 + i\sqrt{3}\hat{n}_2)(\hat{n}_1 - i\sqrt{3}\hat{n}_2)
\end{aligned}$$

I interrupt the argument to comment that the matrix

$$\mathbb{Z} \equiv \begin{pmatrix} 1 & 1 \\ 1 & -1 \end{pmatrix} = \sqrt{2} \cdot \{\text{improper } 45^\circ \text{ rotation matrix}\}$$

possesses the property that (since it has integral elements) it maps

$$\text{lattice vectors} \longmapsto \text{lattice vectors}$$

Its specific action is illustrated in Figure 24, and it arises also in the connection described in Figure 25. Orthogonality is such a natural idea that it can be

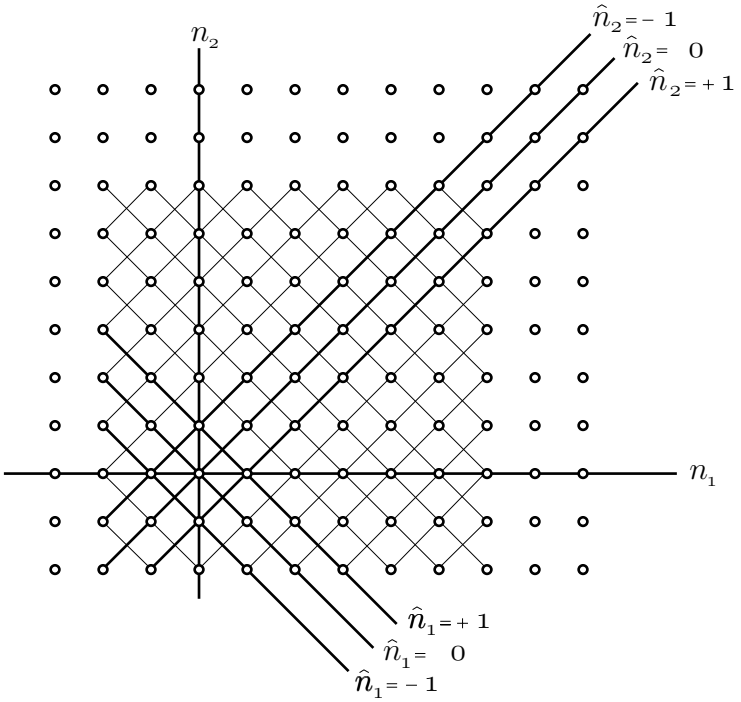

FIGURE 24: *The integers $\hat{n}_1 = n_1 + n_2$ and $\hat{n}_2 = n_1 - n_2$ describe points of the $\mathbf{n}$-lattice if and only if they are either both even or both odd; when of opposite parity they refer to the “interstitial lattice.”*

expected to enter spontaneously into the discussion—as, indeed, it has; it was not introduced “by hand” (as would have been the case had we opted to take the 12-element fundamental unit as our starting point), hinges upon no explicit appeal to the factorization principle (38), and the occurance of $\mathbb{Z}$—the “orthogonalizer”—is simply its defining symptom.

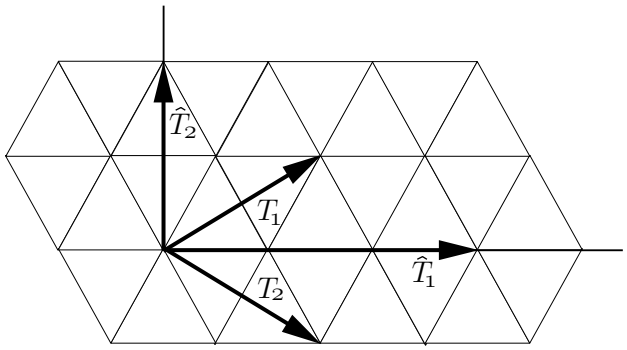

FIGURE 25: *The orthogonal translation vectors* $\{\hat{\boldsymbol{T}}_1, \hat{\boldsymbol{T}}_2\}$ *associated with the 12-element fundamental unit (Figure 22) stand evidently in this relation to the non-orthogonal translation vectors* $\{\boldsymbol{T}_1, \boldsymbol{T}_2\}$ *associated with the 6-element fundamental unit (Figure 21):*

$$\begin{aligned} \hat{\boldsymbol{T}}_1 &= \boldsymbol{T}_1 + \boldsymbol{T}_2 \\ \hat{\boldsymbol{T}}_2 &= \boldsymbol{T}_1 - \boldsymbol{T}_2 \end{aligned} \quad \textit{; i.e.,} \quad \begin{pmatrix} \hat{\boldsymbol{T}}_1 \\ \hat{\boldsymbol{T}}_2 \end{pmatrix} = \mathbb{Z} \begin{pmatrix} \boldsymbol{T}_1 \\ \boldsymbol{T}_2 \end{pmatrix}$$

The entry of $\mathbb{Z}$ *into our argument represents a kind of "spontaneous crosstalk" between the 6-element and 12-element formulations of the theory.*

Equation (51) clinches what has recently become increasingly evident: the indices $\{\hat{n}_1, \hat{n}_2\}$ are—it is now clear—more neatly adapted to our problem than are the "natural" indices $\{n_1, n_2\}$. Their introduction permits the following notational simplifications of (50) and (49):

$$K(\boldsymbol{x}, t; \boldsymbol{y}, 0) = \tfrac{1}{3\cdot\text{area}} {\sum_{\hat{\boldsymbol{n}}}}' e^{-\frac{i}{\hbar}\mathcal{E}\frac{1}{4}(\hat{n}_1^2 + 3\hat{n}_2^2)t} \Big\{ \begin{array}{r} \hat{F}_{\hat{\boldsymbol{n}}}(\xi_1, \xi_2) \cdot \sin[2\hat{n}_1\zeta_1] \sin[2\hat{n}_2\zeta_2] \\ + \hat{G}_{\hat{\boldsymbol{n}}}(\xi_1, \xi_2) \cdot \cos[2\hat{n}_1\zeta_1] \sin[2\hat{n}_2\zeta_2] \end{array} \Big\} \quad (52)$$

where

$$\begin{aligned} \hat{F}_{\hat{\boldsymbol{n}}}(\xi_1, \xi_2) \equiv \sin[2\hat{n}_1\xi_1] \sin[2\hat{n}_2\xi_2] &- \sin[\hat{n}_1(\xi_1 + \xi_2)] \sin[\hat{n}_2(3\xi_1 - \xi_2)] \\ &+ \sin[\hat{n}_1(\xi_1 - \xi_2)] \sin[\hat{n}_2(3\xi_1 + \xi_2)] \end{aligned} \quad (53.1)$$

$$\begin{aligned} \hat{G}_{\hat{\boldsymbol{n}}}(\xi_1, \xi_2) \equiv \cos[2\hat{n}_1\xi_1] \sin[2\hat{n}_2\xi_2] &+ \cos[\hat{n}_1(\xi_1 + \xi_2)] \sin[\hat{n}_2(3\xi_1 - \xi_2)] \\ &- \cos[\hat{n}_1(\xi_1 - \xi_2)] \sin[\hat{n}_2(3\xi_1 + \xi_2)] \end{aligned} \quad (53.2)$$

and where the $\sum$ wears a prime to signal that (see again Figure 24) *only points* $\hat{\boldsymbol{n}}$ *for which* $\hat{n}_1$ *and* $\hat{n}_2$ *have the same parity* participate in the summation process.

To tabulate the function $N(\hat{n}_1, \hat{n}_2) \equiv \hat{n}_1^2 + 3\hat{n}_2^2$ is to be struck by the fact that N assumes identical values at patterned arrays of distinct points on the $\hat{\boldsymbol{n}}$-lattice. My immediate objective will be to identify/describe those patterns.

We will then be in position to regroup the terms that contribute to the sum (52), and to achieve our desired result. To that end I observe that the following equations

$$\begin{aligned}
&\sin(a_1z_1+a_2z_2)\sin(b_1z_1+b_2z_2)-\sin(a_1z_1-a_2z_2)\sin(b_1z_1-b_2z_2)\\
&\qquad=\sin(a_1+b_1)z_1\sin(a_2+b_2)z_2-\sin(a_1-b_1)z_1\sin(a_2-b_2)z_2\\
&\cos(a_1z_1+a_2z_2)\sin(b_1z_1+b_2z_2)-\cos(a_1z_1-a_2z_2)\sin(b_1z_1-b_2z_2)\\
&\qquad=\cos(a_1+b_1)z_1\sin(a_2+b_2)z_2-\cos(a_1-b_1)z_1\sin(a_2-b_2)z_2
\end{aligned}\tag{54}$$

have the status of *identities*, which (once stated) are very easy to prove.[31] Using the first of these identities to manipulate the last two terms on the right side of (53.1), and the second to manipulate the last two terms on the right side of (53.2), we obtain (after some slight adjustment)

$$\begin{aligned}
\hat{F}_{\hat{\boldsymbol{n}}}(\xi_1,\xi_2)&=\sin[2\hat{n}_1\xi_1]\sin[2\hat{n}_2\xi_2]+\sin[2\tfrac{-\hat{n}_1+3\hat{n}_2}{2}\xi_1]\sin[2\tfrac{-\hat{n}_1-\hat{n}_2}{2}\xi_2]\\
&\qquad+\sin[2\tfrac{-\hat{n}_1-3\hat{n}_2}{2}\xi_1]\sin[2\tfrac{+\hat{n}_1-\hat{n}_2}{2}\xi_2]\\
\hat{G}_{\hat{\boldsymbol{n}}}(\xi_1,\xi_2)&=\cos[2\hat{n}_1\xi_1]\sin[2\hat{n}_2\xi_2]+\cos[2\tfrac{-\hat{n}_1+3\hat{n}_2}{2}\xi_1]\sin[2\tfrac{-\hat{n}_1-\hat{n}_2}{2}\xi_2]\\
&\qquad+\cos[2\tfrac{-\hat{n}_1-3\hat{n}_2}{2}\xi_1]\sin[2\tfrac{+\hat{n}_1-\hat{n}_2}{2}\xi_2]
\end{aligned}$$

and are motivated by the structure of these results to write

$$\left.\begin{aligned}
\tfrac{1}{2}\begin{pmatrix}(-\hat{n}_1+3\hat{n}_2)\\(-\hat{n}_1-\hat{n}_2)\end{pmatrix}&=\mathbb{A}\begin{pmatrix}n_1\\n_2\end{pmatrix}\quad\text{with}\quad\mathbb{A}\equiv\tfrac{1}{2}\begin{pmatrix}-1&+3\\-1&-1\end{pmatrix}\\
\tfrac{1}{2}\begin{pmatrix}(-\hat{n}_1-3\hat{n}_2)\\(+\hat{n}_1-\hat{n}_2)\end{pmatrix}&=\mathbb{B}\begin{pmatrix}n_1\\n_2\end{pmatrix}\quad\text{with}\quad\mathbb{B}\equiv\tfrac{1}{2}\begin{pmatrix}-1&-3\\+1&-1\end{pmatrix}
\end{aligned}\right\}\tag{55}$$

The matrices $\mathbb{A}$ and $\mathbb{B}$ are unimodular

$$\det\mathbb{A}=\det\mathbb{B}=1$$

and their shared characteristic polynomial

$$\det(\mathbb{A}-\lambda\mathbb{I})=\det(\mathbb{B}-\lambda\mathbb{I})=\lambda^2+\lambda+1\equiv\varphi(\lambda)$$

is "cyclotomic."[32] The roots of $\varphi(\lambda)$ are the complex cube roots of unity:

$$\varphi(\lambda)=0\quad\Longrightarrow\quad\lambda=\frac{-1\pm\sqrt{-3}}{2}=e^{\pm i\frac{2}{3}\pi}$$

[31] I omit the proofs, but see pp. 104, 175 & 213 of the research notes cited in Footnote 18.

[32] Which is to say: it has the form $\lambda^{p-1}+\lambda^{p-2}+\cdots+1$ with p an odd prime; see p. 55 of H. Pollard, *The Theory of Algebraic Numbers* (1950).

By the Cayley-Hamilton theorem

$$\mathbb{A}^2 + \mathbb{A} + \mathbb{I} = \mathbb{O}$$

From this it follows that

$$\begin{aligned} \mathbb{A}^2 &= -\mathbb{A} - \mathbb{I} \\ &= \mathbb{B} \quad \text{by inspection} \end{aligned}$$

and that

$$\begin{aligned} \mathbb{A}^3 &= -\mathbb{A}^2 - \mathbb{A} \\ &= \mathbb{I} \end{aligned}$$

Evidently $\mathbb{A}^{-1} = \mathbb{B}$. More immediately to the point, we by quick calculation have

$$\mathbb{A}^{\mathsf{T}}\mathbb{G}\mathbb{A} = \mathbb{G} \quad \text{with} \quad \mathbb{G} \equiv \begin{pmatrix} 1 & 0 \\ 0 & 3 \end{pmatrix}$$

from which it follows that $N(\hat{\boldsymbol{n}}) = \hat{\boldsymbol{n}}^{\mathsf{T}}\mathbb{G}\,\hat{\boldsymbol{n}}$ is invariant under the action of $\mathbb{A}$:[33]

$$N(\hat{\boldsymbol{n}}) = N(\mathbb{A}\hat{\boldsymbol{n}}) = N(\mathbb{A}^2\hat{\boldsymbol{n}}) \tag{56}$$

The same (to return to our starting point) can be said of the functions $\hat{F}_{\hat{\boldsymbol{n}}}(\xi_1, \xi_2)$ and $\hat{G}_{\hat{\boldsymbol{n}}}(\xi_1, \xi_2)$, and is made manifest if we introduce

$$\left.\begin{aligned} f_{\hat{\boldsymbol{n}}}(\xi_1, \xi_2) &\equiv \sin[2\hat{n}_1\xi_1]\sin[2\hat{n}_2\xi_2] \\ g_{\hat{\boldsymbol{n}}}(\xi_1, \xi_2) &\equiv \cos[2\hat{n}_1\xi_1]\sin[2\hat{n}_2\xi_2] \end{aligned}\right\} \tag{57}$$

and write

$$\left.\begin{aligned} \hat{F}_{\hat{\boldsymbol{n}}}(\xi_1, \xi_2) &= f_{\hat{\boldsymbol{n}}}(\xi_1, \xi_2) + f_{\mathbb{A}\hat{\boldsymbol{n}}}(\xi_1, \xi_2) + f_{\mathbb{A}^2\hat{\boldsymbol{n}}}(\xi_1, \xi_2) \\ \hat{G}_{\hat{\boldsymbol{n}}}(\xi_1, \xi_2) &= g_{\hat{\boldsymbol{n}}}(\xi_1, \xi_2) + g_{\mathbb{A}\hat{\boldsymbol{n}}}(\xi_1, \xi_2) + g_{\mathbb{A}^2\hat{\boldsymbol{n}}}(\xi_1, \xi_2) \end{aligned}\right\} \tag{58}$$

The meaning of my section title (see the top of the page) begins at this point to become clear.

Equation (56) to exhaust the invariance structure of $N(\hat{\boldsymbol{n}})$; trivially, one has invariance also under the reflective transformations

$$\begin{pmatrix} \hat{n}_1 \\ \hat{n}_2 \end{pmatrix} \longmapsto \begin{pmatrix} -\hat{n}_1 \\ +\hat{n}_2 \end{pmatrix}, \text{ else } \begin{pmatrix} +\hat{n}_1 \\ -\hat{n}_2 \end{pmatrix}, \text{ else } \begin{pmatrix} -\hat{n}_1 \\ -\hat{n}_2 \end{pmatrix}$$

[33] Check it out; we find that indeed

$$\begin{aligned} \hat{n}_1^2 + 3\hat{n}_2^2 &= \Big(\frac{-\hat{n}_1 + 3\hat{n}_2}{2}\Big)^2 + 3\Big(\frac{-\hat{n}_1 - \hat{n}_2}{2}\Big)^2 \\ &= \Big(\frac{-\hat{n}_1 - 3\hat{n}_2}{2}\Big)^2 + 3\Big(\frac{+\hat{n}_1 - \hat{n}_2}{2}\Big)^2 \end{aligned}$$

Each of the points $\hat{\boldsymbol{n}}$, $\mathbb{A}\hat{\boldsymbol{n}}$ and $\mathbb{B}\hat{\boldsymbol{n}}$ is a member, therefore, of a *quartet*. The simplest way to generate/organize this 12-fold population of lattice points is to introduce this "*sixth* root of unity"[34]

$$\mathbb{U} \equiv -\mathbb{B} = \tfrac{1}{2}\begin{pmatrix} +1 & +3 \\ -1 & +1 \end{pmatrix}$$

and with its aid to form two interdigitated sextets, as follows:

$$\left.\begin{array}{l} \hat{\boldsymbol{n}} \longrightarrow \mathbb{U}\hat{\boldsymbol{n}} \longrightarrow \mathbb{U}^2\hat{\boldsymbol{n}} \longrightarrow \mathbb{U}^3\hat{\boldsymbol{n}} \longrightarrow \mathbb{U}^4\hat{\boldsymbol{n}} \longrightarrow \mathbb{U}^5\hat{\boldsymbol{n}} \longrightarrow \text{ back to } \hat{\boldsymbol{n}} \\ \hat{\boldsymbol{m}} \longrightarrow \mathbb{U}\hat{\boldsymbol{m}} \longrightarrow \mathbb{U}^2\hat{\boldsymbol{m}} \longrightarrow \mathbb{U}^3\hat{\boldsymbol{m}} \longrightarrow \mathbb{U}^4\hat{\boldsymbol{m}} \longrightarrow \mathbb{U}^5\hat{\boldsymbol{m}} \longrightarrow \text{ back to } \hat{\boldsymbol{m}} \end{array}\right\} \quad (59)$$

$$\hat{\boldsymbol{m}} \equiv \begin{pmatrix} 1 & 0 \\ 0 & -1 \end{pmatrix}\hat{\boldsymbol{n}}$$

To explore the meaning of (59) we ask *Mathematica* to compute

```
Table[MatrixForm[MatrixPower[{{1/2,3/2},{-1/2,1/2}},p]
.{{a},{b}}],{p,0,5}]
```

and examine the output for various assignments of $\{\mathtt{a} = \hat{n}_1, \mathtt{b} = \hat{n}_2\}$. A pattern quickly emerges. Suppose in the first place that the "seed" $\hat{\boldsymbol{n}}$ lies on the $\hat{n}_1$-axis; (59) gives rise then to a population

$$\begin{pmatrix} 2n \\ 0 \end{pmatrix} \to \begin{pmatrix} n \\ -n \end{pmatrix} \to \begin{pmatrix} -n \\ -n \end{pmatrix} \to \begin{pmatrix} -2n \\ 0 \end{pmatrix} \to \begin{pmatrix} -n \\ n \end{pmatrix} \to \begin{pmatrix} n \\ n \end{pmatrix} \to \begin{pmatrix} 2n \\ 0 \end{pmatrix}$$

which contains only six members (each occurs twice). Associated with this "nuclear population" of lattice points are the associated 12-element populations

$$\begin{pmatrix} 2n+3k \\ k \end{pmatrix}, \begin{pmatrix} n+3k \\ n+k \end{pmatrix}, \begin{pmatrix} n \\ n+2k \end{pmatrix} \text{ plus } 3+3+3=9 \text{ reflective companions}$$

If, on the other hand, the "seed" $\hat{\boldsymbol{n}}$ lies on the $\hat{n}_2$-axis, then (58) gives rise then to the nuclear sextet

$$\begin{pmatrix} 0 \\ 2n \end{pmatrix} \to \begin{pmatrix} 3n \\ n \end{pmatrix} \to \begin{pmatrix} 3n \\ -n \end{pmatrix} \to \begin{pmatrix} 0 \\ -2n \end{pmatrix} \to \begin{pmatrix} -3n \\ -n \end{pmatrix} \to \begin{pmatrix} -3n \\ n \end{pmatrix} \to \begin{pmatrix} 0 \\ 2n \end{pmatrix}$$

in association with which we have the 12-element populations

$$\begin{pmatrix} k \\ 2n+k \end{pmatrix}, \begin{pmatrix} 3n+k \\ n+k \end{pmatrix}, \begin{pmatrix} 3n+2k \\ n \end{pmatrix} \text{ plus } 3+3+3=9 \text{ reflective companions}$$

Here the parameters n and k range on the non-negative integers; we note that the substitutional interchange $n \leftrightarrow k$ sends the first 12-element population into the second, and *vice versa*. Figures 26–29 are intended to make vivid (which is to say, intelligible) the patterns brought thus to light.

---

[34] The idea here is elementary: if $\alpha \equiv e^{i\frac{1}{3}2\pi}$ and $\beta \equiv e^{i\frac{2}{3}2\pi}$ are complex cube roots of unity, then (as a simple figure makes clear) $\gamma \equiv -\beta = e^{i\frac{1}{6}2\pi}$ is the leading sixth root of unity. From $\mathbb{U}^3 = (-\mathbb{B})^3 = -\mathbb{I}$ it follows, of course, that

$$\mathbb{U}^6 = \mathbb{I}$$

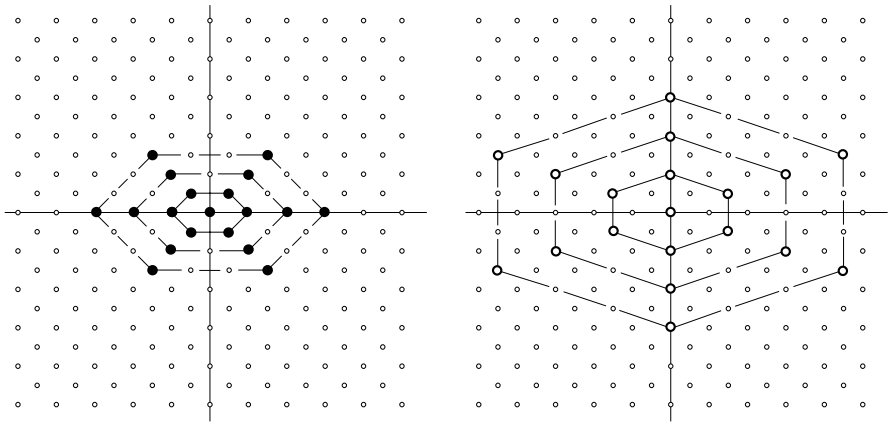

FIGURE 26: *The figure on the left shows several 6-element "nuclear populations" that sprout from "seeds" planted on the $\hat{n}_1$-axis; on the right the seeds are planted on the $\hat{n}_2$-axis. Only same-parity elements of the $\hat{\boldsymbol{n}}$-lattice are shown, since only those correspond to points of the $\boldsymbol{n}$-lattice.*

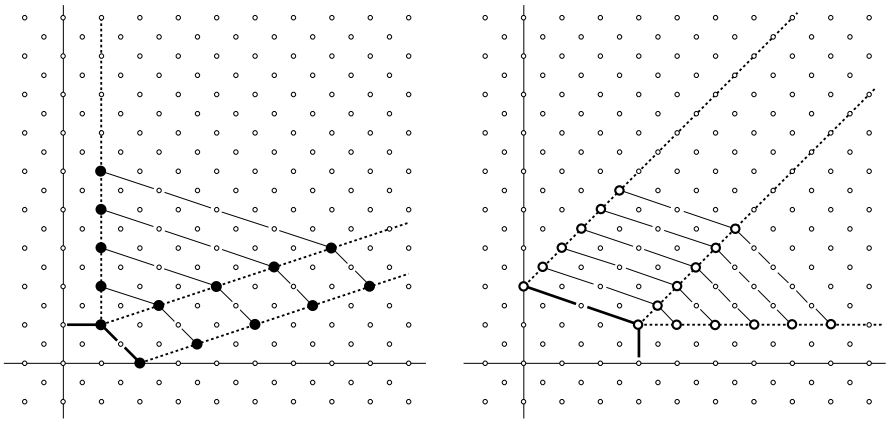

FIGURE 27: *The populations that radiate ($k = 1, 2, 3, \ldots$) from the nuclear populations shown in the preceding figure. Only the positive quadrant is shown; the patterns continue reflectively into other quadrants.*

The emergent picture is summarized in Figure 28, and explained in the caption.

Looking again to the description (52) of $K(\boldsymbol{x}, t; \boldsymbol{y}, 0)$, the idea now is to write

$$\sum_{\hat{\boldsymbol{n}}}{}' = \sum{}'_{\text{wedge points}} \underbrace{\Big\{\sum\nolimits_{\text{orbit identified by a wedge point}}\Big\}}_{\text{“sum over spectral symmetries”}}$$

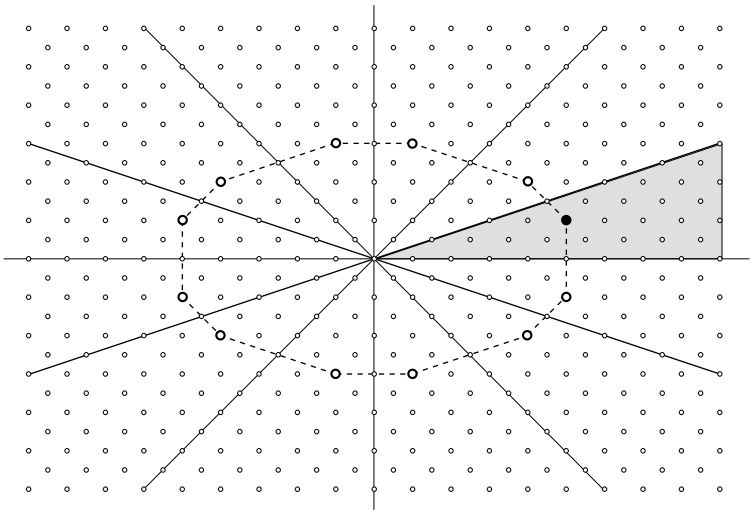

FIGURE 28: *The same-parity sublattice of the $\hat{\boldsymbol{n}}$-lattice is divided into twelve sectors. An arbitrarily selected sector (shaded) will be called the "fundamental sector" or* "wedge." *To each of the points in the interior of the wedge corresponds one point in each of the other eleven sectors; collectively, those comprise the elements of a 12-point* "orbit." *To points on the "edge of the wedge" correspond a quintet of points on alternating sector boundaries, as illustrated in Figure 26; collectively, those comprise the elements of a 6-point orbit. Orbits are inscribed within ellipses of the form $\hat{n}_1^2+3\hat{n}_2^2 = N$. The algebraic meaning of an "orbital tour" is provided by (59).*

The idea is elementary—it is the lattice analog of the introduction of polar coordinates to perform $\iint dxdy$ in the presence of rotational symmetry—but its success hinges on the details; we can (since $N(\hat{\boldsymbol{n}}) \equiv \hat{n}_1^2 + 3\hat{n}_2^2$ is constant on each orbit) write

$$K(\boldsymbol{x},t;\boldsymbol{y},0) = \tfrac{1}{3\cdot\text{area}}{\sum_{\text{wedge}}}' e^{-\frac{i}{\hbar}\mathcal{E}\frac{1}{4}N(\hat{\boldsymbol{n}})t} \sum_{\text{orbit}} \left\{ \hat{F}_{\hat{\boldsymbol{n}}}(\boldsymbol{\xi}) f_{\hat{\boldsymbol{n}}}(\boldsymbol{\zeta}) + \hat{G}_{\hat{\boldsymbol{n}}}(\boldsymbol{\xi}) g_{\hat{\boldsymbol{n}}}(\boldsymbol{\zeta}) \right\}$$

It follows, moreover, from the established principles of orbital design that

$$\sum_{\text{orbit}} \hat{F}_{\hat{\boldsymbol{n}}}(\boldsymbol{\xi}) f_{\hat{\boldsymbol{n}}}(\boldsymbol{\zeta}) = \hat{F}_{\hat{\boldsymbol{n}}}(\boldsymbol{\xi}) \underbrace{\left[f_{\hat{\boldsymbol{n}}}(\boldsymbol{\zeta}) + f_{\mathbb{A}\hat{\boldsymbol{n}}}(\boldsymbol{\zeta}) + f_{\mathbb{A}^2\hat{\boldsymbol{n}}}(\boldsymbol{\zeta}) \right]}_{= \hat{F}_{\hat{\boldsymbol{n}}}(\boldsymbol{\zeta})} + \text{reflective variants}$$

$$\sum_{\text{orbit}} \hat{G}_{\hat{\boldsymbol{n}}}(\boldsymbol{\xi}) g_{\hat{\boldsymbol{n}}}(\boldsymbol{\zeta}) = \hat{G}_{\hat{\boldsymbol{n}}}(\boldsymbol{\xi}) \hat{G}_{\hat{\boldsymbol{n}}}(\boldsymbol{\zeta}) + \text{reflective variants}$$

Concerning those "reflective variants:" it is an implication of the descriptions

of $\hat{F}_{\hat{\boldsymbol{n}}}(\boldsymbol{\xi})$ and $\hat{G}_{\hat{\boldsymbol{n}}}(\boldsymbol{\xi})$ which appear on p. 46 that

$$\left.\begin{array}{lll} \hat{\boldsymbol{n}} \longmapsto \hat{\boldsymbol{m}} \equiv \begin{pmatrix} -\hat{n}_1 \\ \hat{n}_2 \end{pmatrix} & \text{induces} & \left\{ \begin{array}{l} \hat{F}_{\hat{\boldsymbol{n}}}(\boldsymbol{\xi}) \longmapsto \hat{F}_{\hat{\boldsymbol{m}}}(\boldsymbol{\xi}) = -\hat{F}_{\hat{\boldsymbol{n}}}(\boldsymbol{\xi}) \\ \hat{G}_{\hat{\boldsymbol{n}}}(\boldsymbol{\xi}) \longmapsto \hat{G}_{\hat{\boldsymbol{m}}}(\boldsymbol{\xi}) = +\hat{G}_{\hat{\boldsymbol{n}}}(\boldsymbol{\xi}) \end{array} \right. \\ \hat{\boldsymbol{n}} \longmapsto \hat{\boldsymbol{m}} \equiv \begin{pmatrix} \hat{n}_1 \\ -\hat{n}_2 \end{pmatrix} & \text{induces} & \left\{ \begin{array}{l} \hat{F}_{\hat{\boldsymbol{n}}}(\boldsymbol{\xi}) \longmapsto \hat{F}_{\hat{\boldsymbol{m}}}(\boldsymbol{\xi}) = -\hat{F}_{\hat{\boldsymbol{n}}}(\boldsymbol{\xi}) \\ \hat{G}_{\hat{\boldsymbol{n}}}(\boldsymbol{\xi}) \longmapsto \hat{G}_{\hat{\boldsymbol{m}}}(\boldsymbol{\xi}) = -\hat{G}_{\hat{\boldsymbol{n}}}(\boldsymbol{\xi}) \end{array} \right. \end{array}\right\} \tag{60}$$

If $\hat{\boldsymbol{n}}$ lies *interior* to the wedge then it follows from (60) that

$$\begin{aligned} \hat{F}_{\hat{\boldsymbol{n}}}(\boldsymbol{\xi})\hat{F}_{\hat{\boldsymbol{n}}}(\boldsymbol{\zeta}) + \text{reflective variants} &= \big\{1 + (-)^2 + (-)^2 + (-)^2(-)^2\big\}\hat{F}_{\hat{\boldsymbol{n}}}(\boldsymbol{\xi})\hat{F}_{\hat{\boldsymbol{n}}}(\boldsymbol{\zeta}) \\ &= 4\,\hat{F}_{\hat{\boldsymbol{n}}}(\boldsymbol{\xi})\,\hat{F}_{\hat{\boldsymbol{n}}}(\boldsymbol{\zeta}) \\ \hat{G}_{\hat{\boldsymbol{n}}}(\boldsymbol{\xi})\hat{G}_{\hat{\boldsymbol{n}}}(\boldsymbol{\zeta}) + \text{reflective variants} &= \big\{1 + (-)^2 + (+)^2 + (-)^2(+)^2\big\}\hat{G}_{\hat{\boldsymbol{n}}}(\boldsymbol{\xi})\hat{G}_{\hat{\boldsymbol{n}}}(\boldsymbol{\zeta}) \\ &= 4\hat{G}_{\hat{\boldsymbol{n}}}(\boldsymbol{\xi})\hat{G}_{\hat{\boldsymbol{n}}}(\boldsymbol{\zeta}) \end{aligned}$$

If, on the other hand, $\hat{\boldsymbol{n}}$ lies on the *either edge of the wedge* then there are, in either case, only five "reflective variants" to be considered; explicit summation over the points indicated in Figure 26 and described on p. 49 (from which task *Mathematica* removes all the tedium and risk of error) establishes that

$$\left.\begin{array}{l} \hat{F}_{\hat{\boldsymbol{n}}}(\boldsymbol{\xi})\,\hat{F}_{\hat{\boldsymbol{n}}}(\boldsymbol{\zeta}) + \text{reflective variants} \\ \hat{G}_{\hat{\boldsymbol{n}}}(\boldsymbol{\xi})\hat{G}_{\hat{\boldsymbol{n}}}(\boldsymbol{\zeta}) + \text{reflective variants} \end{array}\right\} = 0 \quad : \quad \hat{\boldsymbol{n}} \text{ on edge of wedge}$$

We therefore have

$$K(\boldsymbol{x},t;\boldsymbol{y},0) = \sum_{\text{wedge}}{}'' e^{-\frac{i}{\hbar}\mathcal{E}\frac{1}{4}N(\hat{\boldsymbol{n}})\,t}\,\tfrac{4}{3\cdot\text{area}}\Big\{\hat{F}_{\hat{\boldsymbol{n}}}(\boldsymbol{\xi})\,\hat{F}_{\hat{\boldsymbol{n}}}(\boldsymbol{\zeta}) + \hat{G}_{\hat{\boldsymbol{n}}}(\boldsymbol{\xi})\,\hat{G}_{\hat{\boldsymbol{n}}}(\boldsymbol{\zeta})\Big\}$$

where $\frac{4}{3\cdot\text{area}} = \frac{16}{3\sqrt{3}a^2}$ and where the double prime signals that $\sum$ ranges on same-parity lattice points $\hat{\boldsymbol{n}}$ confined to the *interior* of the wedge. We have at this point achieved our ultimate objective, for we have only to write

$$E(\hat{\boldsymbol{n}}) \equiv \tfrac{h^2}{18ma^2}\big(\hat{n}_1^2 + 3\hat{n}_2^2\big) \quad \text{and} \quad \Psi_{\hat{\boldsymbol{n}}}(\boldsymbol{x}) \equiv \sqrt{\tfrac{16}{3\sqrt{3}a^2}}\Big\{\hat{G}_{\hat{\boldsymbol{n}}}(\boldsymbol{\xi}) + i\hat{F}_{\hat{\boldsymbol{n}}}(\boldsymbol{\xi})\Big\} \tag{61}$$

to obtain

$$K(\boldsymbol{x},t;\boldsymbol{y},0) = \sum_{\text{wedge}}{}'' e^{-\frac{i}{\hbar}E(\hat{\boldsymbol{n}})\,t}\Psi_{\hat{\boldsymbol{n}}}(\boldsymbol{x})\Psi^*_{\hat{\boldsymbol{n}}}(\boldsymbol{y}) \tag{62}$$

—which is an instance of (3).

9. Properties of the spectrum & eigenfunctions. The real and imaginary parts of the eigenfunction $\Psi_{\hat{\boldsymbol{n}}}(\boldsymbol{x})$—heretofore known (apart from a normalization factor) as $\hat{G}_{\hat{\boldsymbol{n}}}(\boldsymbol{\xi})$ and $\hat{F}_{\hat{\boldsymbol{n}}}(\boldsymbol{\xi})$ respectively—are, for the most elementary of general reasons, individually eigenfunctions of the Schrödinger equation. It follows that each of the eigenvalues $E(\hat{\boldsymbol{n}})$ is (in the absence of accidental degeneracy) *doubly degenerate*.

The linear boundaries of the equilateral box in physical $\boldsymbol{x}$-space can, in terms of the dimensionless variables $\boldsymbol{\xi}$ introduced on p. 42, be described

$$\xi_2 = +3\xi_1, \quad \xi_2 = -3\xi_2 \quad \text{and} \quad \xi_2 = \tfrac{1}{2}\pi$$

It follows readily from (53) that $\hat{G}_{\hat{\boldsymbol{n}}}(\boldsymbol{\xi})$ and $\hat{F}_{\hat{\boldsymbol{n}}}(\boldsymbol{\xi})$ both vanish on each of those lines, provided $\hat{n}_1$ and $\hat{n}_2$ are either both even or both odd.

It follows also immediately from the unnumbered equations displayed in the middle of p. 46 that (compare (60))

$$\left.\begin{array}{l} \hat{G}_{\hat{\boldsymbol{n}}}(\boldsymbol{\xi}) \text{ is an even function of } \xi_1, \text{ while } \hat{F}_{\hat{\boldsymbol{n}}}(\boldsymbol{\xi}) \text{ is odd;} \\ \hat{G}_{\hat{\boldsymbol{n}}}(\boldsymbol{\xi}) \text{ and } \hat{F}_{\hat{\boldsymbol{n}}}(\boldsymbol{\xi}) \text{ are both odd functions of } \xi_2 \end{array}\right\} \tag{63}$$

These facts are vividly evident in Figure 30,[35] of which the following figure provides a kind of abstracted cartoon:

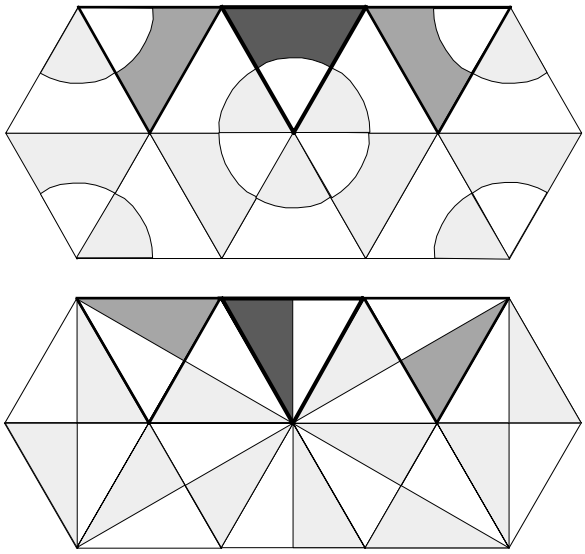

FIGURE 29: *Abstract of the figure pairs of which Figure 30 provides a particular (ground states) instance. Note that the triangles in upper left and upper right can, in each instance, be obtained by rotation of the central (physical) triangle.*

I invite my reader to use techniques previously described, and results now in hand, to construct (for various values of $\hat{\boldsymbol{n}}$) analogs of Figure 20; i.e., to construct maps of the nodal lines characteristic of $\Psi_{\hat{\boldsymbol{n}}}(\boldsymbol{x})$.

[35] To produce the figure I used the just-mentioned unnumbered equations to define `G[m_,n_,x_,y_]` and `F[m_,n_,x_,y_]`, and into the command that produced Figure 18 introduced the option `AspectRatio->1/Sqrt[3]]` so as to achieve a result scaled as it would appear if drawn in physical $\boldsymbol{x}$-space.

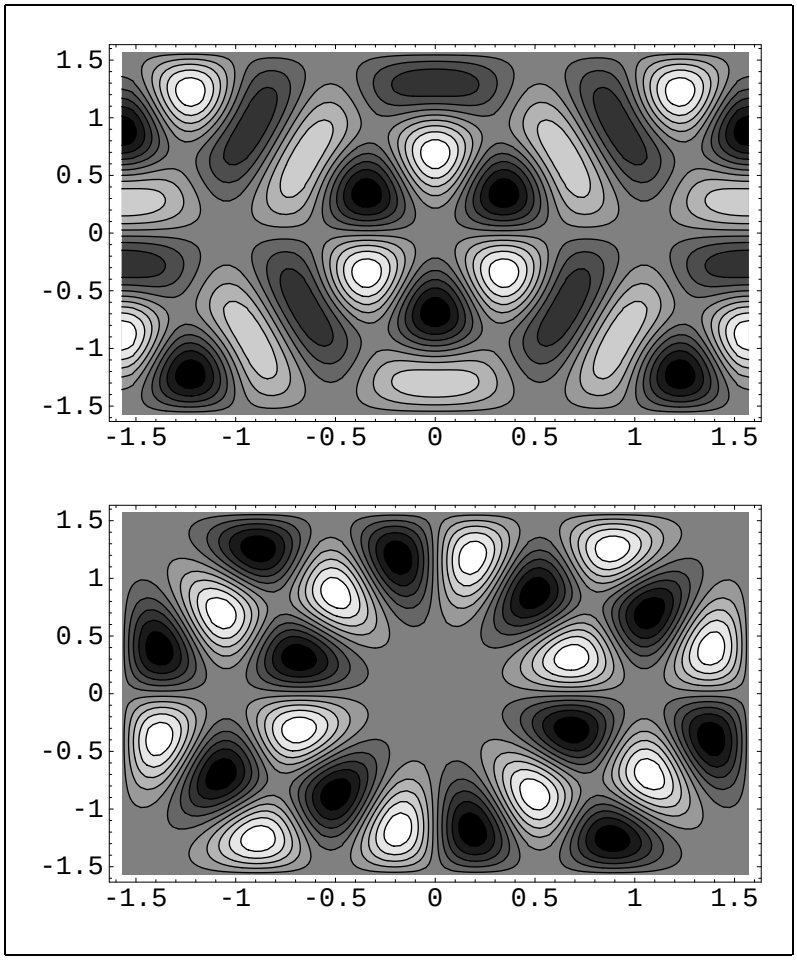

FIGURE 30: *Contour plots of the real and imaginary parts of the ground state* $\Psi_{51}(\boldsymbol{x})$*—contour plots, that is to say, of the even and odd ground states—of a quantum particle in an equilateral box. The identity*

$$\hat{\boldsymbol{n}} = \begin{pmatrix} 5 \\ 1 \end{pmatrix}$$

of the ground state was read from Figure 28, and corresponds (see Figure 24) to the point

$$\boldsymbol{n} = \tfrac{1}{2} \begin{pmatrix} 1 & 1 \\ 1 & -1 \end{pmatrix} \hat{\boldsymbol{n}} = \begin{pmatrix} 3 \\ 2 \end{pmatrix}$$

on our original $\boldsymbol{n}$*-lattice. In both figures the physical box lies top center, with vertices at 11 o-clock, 1 o-clock and the origin.*

It is intuitively evident that if the second of the following figures describes an eigenfunction, then so also do the first and third, and it is curious on its face that $\hat{F}_{\hat{\boldsymbol{n}}}(\boldsymbol{\xi})$ speaks directly of the former but appears to discriminate against the latter two possibilities. Resolution of this little paradox puts us in touch

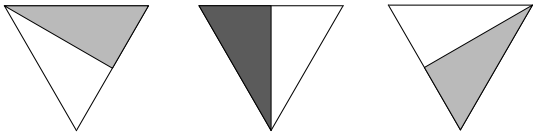

FIGURE 31: *Rotated companions of the central odd eigenstate, who live next door on the tesselated plane.*

with the *representation theory of the symmetry group* of the equilateral box. It has been remarked already (see again the caption to Figure 29) that rotation within the physical box is equivalent to translation on the tesselated plane. Noting that

$$\boldsymbol{x} \longmapsto \boldsymbol{x} \pm \begin{pmatrix} a \\ 0 \end{pmatrix} \quad \Longleftrightarrow \quad \boldsymbol{\xi} \longmapsto \boldsymbol{\xi} \pm \begin{pmatrix} \frac{1}{3}\pi \\ 0 \end{pmatrix}$$

we by elementary calculation obtain

$$\begin{aligned} \hat{F}_{\hat{\boldsymbol{n}}}(\xi_1 \pm \tfrac{1}{3}\pi, \xi_2) = \quad & \cos\theta \cdot \hat{F}_{\hat{\boldsymbol{n}}}(\xi_1, \xi_2) \pm \sin\theta \cdot \hat{G}_{\hat{\boldsymbol{n}}}(\xi_1, \xi_2) \\ \hat{G}_{\hat{\boldsymbol{n}}}(\xi_1 \pm \tfrac{1}{3}\pi, \xi_2) = \mp & \sin\theta \cdot \hat{F}_{\hat{\boldsymbol{n}}}(\xi_1, \xi_2) + \cos\theta \cdot \hat{G}_{\hat{\boldsymbol{n}}}(\xi_1, \xi_2) \end{aligned}$$

$$\theta \equiv \tfrac{2\pi}{3}\hat{n}_1 = 120^\circ \hat{n}_1$$

provided $\hat{n}_1$ and $\hat{n}_2$ are (as their hats indicate them to be) either both even or both odd. In short, the functions $\hat{F}_{\hat{\boldsymbol{n}}}(\boldsymbol{\xi})$ and $\hat{G}_{\hat{\boldsymbol{n}}}(\boldsymbol{\xi})$ fold among themselves in such a way as to achieve—for each given/fixed value of $\hat{\boldsymbol{n}}$—a representation

$$\begin{pmatrix} \hat{F}_{\hat{\boldsymbol{n}}}(\boldsymbol{\xi}_{\text{rotated}}) \\ \hat{G}_{\hat{\boldsymbol{n}}}(\boldsymbol{\xi}_{\text{rotated}}) \end{pmatrix} = \text{rotation matrix} \cdot \begin{pmatrix} \hat{F}_{\hat{\boldsymbol{n}}}(\boldsymbol{\xi}) \\ \hat{G}_{\hat{\boldsymbol{n}}}(\boldsymbol{\xi}) \end{pmatrix}$$

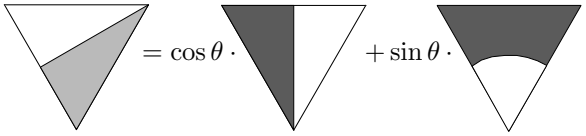

of the group of equilateral symmetries (which is, by the way, clearly isomorphic to the group of permutations on three objects). I suspect that the established principles of group representation theory are in themselves sufficient to yield many of our results, but have elected not to pursue this line of inquiry.

The eigenfunctions discussed above derive both their distinctive functional structure and the pattern of their interrelationships from a "sum over spectral symmetries." I turn now to discussion to two relatively covert properties of the equilateral box spectrum. The first has to do with the number-theoretic mechanism that underlies "accidental degeneracy." The second—which is more geometrical in flavor—has as its objective the (approximate) description of the "density of states." Looking first to the former...

We have (see again (61)) $E(\hat{\boldsymbol{n}}) = \frac{h^2}{18ma^2}N(\hat{\boldsymbol{n}})$ and look therefore to the properties of

$$N(\hat{\boldsymbol{n}}) = N(\hat{n}_1, \hat{n}_2) = \hat{n}_1^2 + 3\hat{n}_2^2$$

with $\hat{\boldsymbol{n}}$ an equi-parity point interior to the wedge (see again Figure 28). Values assumed by the function $N(\hat{\boldsymbol{n}})$ near the vertex of the wedge are displayed in Table 1. To allude (in illustrative connection with the ground state) to the pretty fact that

$$28 = 5^2 + 3 \cdot 1^2 = 4^2 + 3 \cdot 2^2 = 1^2 + 3 \cdot 3^2$$

is to allude to a symmetry (see again Figure 27) which pertains *universally* to the physical system here under discussion. What I have now in mind are the *exceptional* cases of which

$$\begin{aligned} 364 &= 17^2 + 3 \cdot 5^2 = 16^2 + 3 \cdot 6^2 = 1^2 + 3 \cdot 11^2 \\ &= 19^2 + 3 \cdot 1^2 = 11^2 + 3 \cdot 9^2 = 8^2 + 3 \cdot 10^2 \end{aligned}$$

provides the leading example. In the previous example, only $\binom{5}{1}$ lay interior to the wedge; $\binom{4}{2}$, $\binom{1}{3}$ and all their reflective companions lay in other sectors, external to the wedge. But in the example of immediate interest $\binom{17}{5}$ and $\binom{19}{1}$ *both* lie internal to the wedge. How is this phenomenon to be accounted for? Following the lead of Ray Mayer (who solved the problem literally overnight, and rendered instantly obsolete the fragmentary insights I had gained by a lot of "experimental numerology"), we begin by noting it to be an implication of

$$\begin{aligned} N(2m, 2n) &= 4(m^2 + 3n^2) \\ N(2m+1, 2n+1) &= 4(m^2 + 3n^2) + 4(m + 3n) + 4 \\ N(2m+1, 2n) &= 4(m^2 + 3n^2) + 4m + 1 \\ N(2m, 2n+1) &= 4(m^2 + 3n^2) + 4(3n) + 3 \end{aligned}$$

that

$$N(\hat{n}_1, \hat{n}_2) \equiv \begin{cases} 0 \pmod 4 & \text{if } \hat{n}_1 \text{ and } \hat{n}_2 \text{ have the same parity} \\ \pm 1 \pmod 4 & \text{otherwise} \end{cases}$$

Therefore

$$N(\hat{\mathbf{n}}) = 4^\alpha \cdot \text{product of odd primes}$$

$*\,*\,*$		912		948		1008		1092		$*\,*\,*$
	844		**868**		916		988		1084	
$*\,*\,*$		796		832		892		976		
	732		756		804		876		$*\,*\,*$	
$*\,*\,*$		688		724		784		**868**		
	628		652		700		772			
$*\,*\,*$		588		624		684		$*\,*\,*$		
	532		556		604		676			
$*\,*\,*$		496		**532**		592				
	444		468		516		$*\,*\,*$			
$*\,*\,*$		412		448		508				
	364		388		436					
$*\,*\,*$		336		372		$*\,*\,*$				
	292		316		**364**					
$*\,*\,*$		268		304						
	228		252		$*\,*\,*$					
$*\,*\,*$		208		244						
	172		196							
$*\,*\,*$		156		$*\,*\,*$						
	124		148							
$*\,*\,*$		112								
	84		$*\,*\,*$							
$*\,*\,*$		76								
	52									
$*\,*\,*$		$*\,*\,*$								
	28									
$*\,*\,*$										
	$*\,*\,*$									
$*\,*\,*$										
$*\,*\,*$										

TABLE 1: *Values assumed by $N(\hat{n}_1, \hat{n}_2) = \hat{n}_1^2 + 3\hat{n}_2^2$ on the interior of the wedge. $\hat{n}_1$ ranges $\uparrow$ and $\hat{n}_2$ ranges $\rightarrow$ on $\{0, 1, 2, \ldots\}$.* ***Repeated entries*** *are in boldface, and are the entries of special interest.*

when $\hat{\mathbf{n}}$ is an equi-parity lattice point (which is to say: a lattice point of physical relevance). Next we marshal some classical facts of a sort more likely to be familiar to mathematicians than to physicists:[36]

- If P is a prime > 3, then $P \equiv \pm 1 \ (\text{mod} 6)$.[37] In the former case I will say "P is a prime of type p," and in the latter case "... a prime of type q."

- Every p-prime (but no q-prime) can be written

$$p = m^2 + 3n^2$$

and is therefore "composite" in the sense

$$\begin{aligned} p &= (m + jn)(m - jn) \\ &\qquad j \equiv \sqrt{-3} \text{ by extension of the notation } i \equiv \sqrt{-1} \\ &= \text{"norm" } \omega\bar{\omega} \text{ of the algebraic number } \omega \equiv m + jn \end{aligned}$$

Because p is odd, m and n have necessarily opposite parity. And necessarily $mn \neq 0$, which is to say: the lattice point $\binom{m}{n}$ cannot sit "on axis," for statements of the form

$$\text{prime} = \text{square} \qquad \text{or} \qquad \text{prime} = 3 \cdot \text{square}$$

are patently absurd.

The preceding ideas are displayed concretely in Table 2.

- The numbers 3 and 4 are exceptional in the sense that—though neither is a p-prime—both admit of algebraic factorization in the matter characteristic of p-primes:

$$\begin{aligned} 3 &= (0 + j)(0 - j) \\ 4 &= (2 + j0)(2 - j0) = (1 + j)(1 - j) \end{aligned}$$

The striking non-unique factorization of 4 has an origin worthy of comment: the algebraic number (*not* an algebraic integer)

$$U \equiv \tfrac{1}{2}(1 - j)$$

---

[36] See, however, the proceedings (*From Number Theory to Physics*, edited by P. Cartier *et al*) of the Les Houches Conference "Number Theory and Physics" which took place in March, 1989.

[37] See G. H. Hardy & E. M. Wright, *An Introduction to the Theory of Numbers* (4^{th} edition, 1960), p. 13.

Primes $p \equiv +1 \bmod 6$	Primes $q \equiv -1 \bmod 6$
$7 = 2^2 + 3 \cdot 1^2$	5
$13 = 1^2 + 3 \cdot 2^2$	17
$19 = 4^2 + 3 \cdot 1^2$	23
$31 = 2^2 + 3 \cdot 3^2$	29
$37 = 5^2 + 3 \cdot 2^2$	41
$43 = 4^2 + 3 \cdot 3^2$	47
$61 = 7^2 + 3 \cdot 2^2$	53
$67 = 8^2 + 3 \cdot 1^2$	59
$73 = 5^2 + 3 \cdot 4^2$	71
$79 = 2^2 + 3 \cdot 5^2$	83
$97 = 7^2 + 3 \cdot 4^2$	89
$109 = 1^2 + 3 \cdot 6^2$	101
$127 = 10^2 + 3 \cdot 3^2$	107
$139 = 8^2 + 3 \cdot 5^2$	113
$151 = 2^2 + 3 \cdot 7^2$	131
$157 = 7^2 + 3 \cdot 6^2$	137
$163 = 4^2 + 3 \cdot 7^2$	149
$181 = 13^2 + 3 \cdot 2^2$	167
$193 = 1^2 + 3 \cdot 8^2$	173
$199 = 14^2 + 3 \cdot 1^2$	179
$211 = 8^2 + 3 \cdot 7^2$	191
$223 = 14^2 + 3 \cdot 3^2$	197
$229 = 11^2 + 3 \cdot 6^2$	227
$241 = 7^2 + 3 \cdot 8^2$	233
	239

TABLE 2: *If $P > 3$ is prime then $P \equiv \pm 1 \pmod 6$. Here that fact has been used to resolve the primes $3 < P < 250$ into two categories, which I call “primes of type p” and “primes of type q” respectively. The representations $p = m^2 + 3n^2$ were supplied by Mathematica:*

```
<<NumberTheory‘NumberTheoryFunctions‘
QuadraticRepresentation[3,p]
```

See page 306 of Standard Add-on Packages 3.0 for useful references. No q-prime admits of such representation, while the examples

$$4 = 1^2 + 3 \cdot 1^2 = (1 + j1)(1 - j1)$$
$$7 = 1^2 + 3 \cdot 4^2 = (1 + j4)(1 - j4)$$

demonstrate that not every (even/odd) number that does admit of such representation is a p-prime.

has the property that it sends

$$(m+jn) \to U\cdot(m+jn) = (\tfrac{m+3n}{2}) + j(\tfrac{-m+n}{2})$$
$$= \begin{cases} \text{algebraic integer if } m \text{ and } n \text{ have same parity} \\ \text{but not otherwise, and not in particular when} \\ \omega = m+jn \text{ is a factor of 3 or any } p\text{-prime} \end{cases}$$

and thus reproduces the action of the matrix $\mathbb{U}$ encountered previously. We are not surprised to discover that

$$U^3 = -1 \quad (\text{therefore } U^6 = 1) \quad \text{and } U \text{ has unit norm}$$

Repeated application of U to the factor $(2+j0)$ of 4 yields (compare (59)) a hexagonal loop of algebraic integers

$$(2+j0) \to (1-j) \to (-1-j) \to (-2-j0) \to (-1+j) \to (1+j) \to (2+j0)$$

but

$$U\cdot(\text{factor of 3 or a } p\text{-prime}) = \text{not an algebraic integer}$$

- $(m_1+jn_1)(m_2+jn_2) = (m_1m_2-3n_1n_2)+j(m_1n_2+m_2n_1)$ has norm $(m_1m_2-3n_1n_2)^2+3(m_1n_2+m_2n_1)^2 = (m_1^2+3n_1^2)(m_2^2+3n_2^2)$, so quite generally

$$\text{norm of product} = \text{product of norms}$$

It follows from results now in hand that every (necessarily even) number of the form

$$N = 4^\alpha 3^\beta p_1^{\mu_1}\cdots p_k^{\mu_k} \quad : \quad \alpha = 1,2,3,\ldots$$

can be written

$$= m^2+3n^2 \quad \text{with } m \text{ and } n \text{ either both even or both odd}$$

And it is almost obvious[38] that if q is a q-prime then

$$(m^2+3n^2)\cdot q^\lambda \text{ is expressible } (\tilde{m}^2+3\tilde{n}^2) \text{ if an only if } \lambda \text{ is even}$$

We arrive thus at this REPRESENTATION THEOREM:

$$\begin{aligned} N(\hat{\boldsymbol{n}}) &= \hat{n}_1^2+3\hat{n}_2^2 \quad : \quad \hat{\boldsymbol{n}} \text{ interior to the wedge (Figure 28)} \\ &= 4^\alpha 3^\beta p_1^{\mu_1}\cdots p_k^{\mu_k}\cdot Q^2 \qquad (64) \\ &\qquad\qquad Q \equiv q_1^{\nu_1}\cdots q_\ell^{\nu_\ell} \end{aligned}$$

Table 3 illustrates the concrete meaning of (64).

[38] So nearly obvious that I omit the tediously number-theoretic proof; for related discussion (in connection actually with the m^2+n^2 problem) see for example §11.1 in G. E. Andrews, *Number Theory* (1971).

Prime factors of $N(\hat{\boldsymbol{n}})$	Continuation
$28 = 4 \cdot 7$	$\mathbf{532} = 4 \cdot 7 \cdot 19$
$52 = 4 \cdot 13$	$556 = 4 \cdot 139$
$76 = 4 \cdot 19$	$588 = 4 \cdot 3 \cdot 7^2$
$84 = 4 \cdot 3 \cdot 7$	$592 = 4^2 \cdot 37$
$112 = 4^2 \cdot 7$	$604 = 4 \cdot 151$
$124 = 4 \cdot 31$	$624 = 4^2 \cdot 3 \cdot 13$
$148 = 4 \cdot 37$	$628 = 4 \cdot 157$
$156 = 4 \cdot 3 \cdot 13$	$652 = 4 \cdot 163$
$172 = 4 \cdot 43$	$676 = 4 \cdot 13^2$
$196 = 4 \cdot 7^2$	$684 = 4 \cdot 3^2 \cdot 19$
$208 = 4^2 \cdot 13$	$688 = 4^2 \cdot 43$
$228 = 4 \cdot 3 \cdot 19$	$700 = 4 \cdot 7 \cdot \langle 5 \rangle^2$
$244 = 4 \cdot 61$	$724 = 4 \cdot 181$
$252 = 4 \cdot 3^2 \cdot 7$	$732 = 4 \cdot 3 \cdot 61$
$268 = 4 \cdot 67$	$756 = 4 \cdot 3^3 \cdot 7$
$292 = 4 \cdot 73$	$772 = 4 \cdot 193$
$304 = 4^2 \cdot 19$	$784 = 4^2 \cdot 7^2$
$316 = 4 \cdot 79$	$796 = 4 \cdot 199$
$336 = 4^2 \cdot 3 \cdot 7$	$804 = 4 \cdot 3 \cdot 67$
$\mathbf{364} = 4 \cdot 7 \cdot 13$	$832 = 4^3 \cdot 13$
$372 = 4 \cdot 3 \cdot 31$	$844 = 4 \cdot 211$
$388 = 4 \cdot 97$	$\mathbf{868} = 4 \cdot 7 \cdot 31$
$412 = 4 \cdot 103$	$876 = 4 \cdot 3 \cdot 73$
$436 = 4 \cdot 109$	$892 = 4 \cdot 223$
$444 = 4 \cdot 3 \cdot 37$	$912 = 4^2 \cdot 3 \cdot 19$
$448 = 4^3 \cdot 7$	$916 = 4 \cdot 229$
$468 = 4 \cdot 3^2 \cdot 13$	$948 = 4 \cdot 3 \cdot 79$
$496 = 4^2 \cdot 31$	$964 = 4 \cdot 241$
$508 = 4 \cdot 127$	$976 = 4^2 \cdot 61$
$516 = 4 \cdot 3 \cdot 43$	$988 = 4 \cdot 13 \cdot 19$

TABLE 3: *The entries have been taken (in ascending order) from Table 1, and their factors displayed in conformity with (64). Only one instance of a q-factor appears; it is the $\langle 5 \rangle$ at 700, and does enter squared, as (64) stipulates.*

To uncover the mechanism by which spectral degeneracy emerges from (64), let us for the moment suppose that all factors (except Q) enter with unit multiplicity and that (as is the case with most of the entries in Table 3) only a single p-prime is present; we then have

$$\begin{aligned} N(\hat{\boldsymbol{n}}) = \hat{n}_1^2 + 3\hat{n}_2^2 &= 4 \cdot 3 \cdot p \cdot Q^2 \\ &= (\omega_4\bar{\omega}_4)(\omega_3\bar{\omega}_3)(\pi\bar{\pi}) \cdot Q^2 \\ &= (\Omega\bar{\Omega}) \cdot Q^2 \quad \text{with} \quad \Omega \equiv \omega_4\omega_3\pi \\ &\qquad\qquad\qquad\qquad\qquad \equiv m + jn \\ &= (m^2 + 3n^2) \cdot Q^2 \\ &= (Qm)^2 + 3(Qn)^2 \end{aligned} \tag{65}$$

where (see the following figure)

$$\begin{aligned} &\omega_4 \text{ is one of the 6 factors of 4} \\ &\omega_3 \text{ is one of the 2 factors of 3} \\ &\pi \text{ is one of the 4 factors of } p \end{aligned} \tag{66}$$

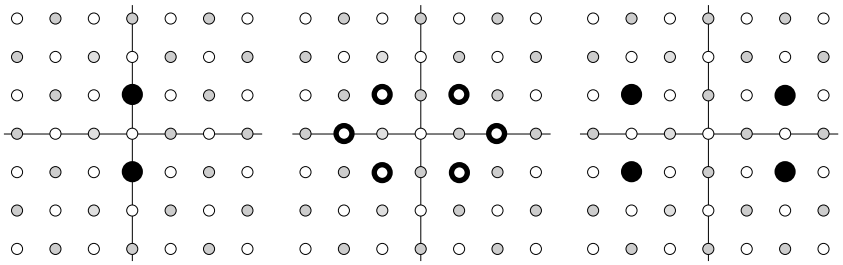

FIGURE 32: *Figures drawn on the (m, n)-lattice used to represent algebraic integers $\omega = m + jn$; open circles identify points where m and n have the same parity, shaded circles identify points where they have opposite parity. The figure on the left describes integers with norm $\omega\bar{\omega} = 3$; the central figure describes integers with $\omega\bar{\omega} = 4$; the figure on the right ($\omega\bar{\omega} = 7$), with its rectangular arrangement of odd-parity points, illustrates the pattern characteristic of all p-primes. Both 3 and 4 are, in this respect and in their separate ways, exceptional.*

It is owing entirely to the universal presence in (64) of at least one 4-factor that the coordinates $\binom{m}{n}$ of Ω—whence also the coordinates $\binom{\hat{n}_1}{\hat{n}_2}$ of $Q\Omega$ —have the *same* parity, and it is (as we have seen) owing to the latter circumstance that the norm-preserving transformations $\Omega \mapsto U^{\text{power}}\Omega$ also preserve "integrality." And, of course, both norm and integrality are preserved by all sign-adjustments:

$$\tbinom{m}{n} \longmapsto \begin{cases} \tbinom{m}{-n} & : \text{ conjugation} \\ \tbinom{-m}{-n} & : \text{ negation} \\ \tbinom{-m}{n} & : \text{ their compose} \end{cases}$$

Thus, from a number-theoretic point of view, does Ω—which is to say $\hat{\boldsymbol{n}}$—acquire its familiar eleven companions, as illustrated in Figure 28; one member of that 12-element set lies invariably in the "physical wedge," and by adroit exercise of the options presented at (66) we can always arrange (as a matter of convention) that it be Ω itself.

Serially relaxing now the restrictions that were written into (65), for ascending powers of 3 we have

$$\begin{aligned}
3^0 = \omega\bar{\omega} \quad &: \quad \omega = \ \ 1 \text{ or negative} \\
3^1 = \omega\bar{\omega} \quad &: \quad \omega = j \ \ \text{or conjugate} \\
3^2 = \omega\bar{\omega} \quad &: \quad \omega = \ \ 3 \text{ or negative} \\
3^3 = \omega\bar{\omega} \quad &: \quad \omega = j3 \text{ or conjugate} \\
&\ \vdots
\end{aligned}$$

Evidently adjustments of the form $3 \mapsto 3^{\text{power}}$ leave the architecture of preceding results unaffected, and therefore cannot be a source of spectal multiplicity. Nor can $4 \mapsto 4^{\text{power}>1}$, if for this somewhat different reason:

$$4^\alpha = \omega\bar{\omega} \quad : \quad \omega = 2^\alpha U^{0,1,2,3,4,5}$$

so the hexagonal structure illustrated in Figure 32 is dilated, but left otherwise intact. The number-theoretic origins of spectral degeneracy come for the first time into clear view when one looks to the effect of $p \mapsto p^{\text{power}}$. To illustrate those, I look to the (in every respect typical) leading case $p = 7$:

$$\begin{aligned}
7^1 = \pi\bar{\pi} \quad &: \quad \pi \equiv (2 + j) \\
7^2 = \omega\bar{\omega} \quad &: \quad \omega = \begin{cases} \pi\pi = (1 + j4) \text{ or conjugate} \ \text{↬} \ (13 + j3) \\ \pi\bar{\pi} = 7 \text{ (self-conjugate)} \end{cases} \\
7^3 = \omega\bar{\omega} \quad &: \quad \omega = \begin{cases} \pi\pi\pi = (-10 + j9) \text{ or conjugate} \ \text{↬} \ (37 + j) \\ \pi\pi\bar{\pi} = 7\pi = (14 + j7) \text{ or conjugate} \ \text{↬} \ (35 + j7) \end{cases} \\
7^4 = \omega\bar{\omega} \quad &: \quad \omega = \begin{cases} \pi\pi\pi\pi = (-47 + j8) \text{ or conjugate} \ \text{↬} \ (47 + j8) \\ \pi\pi\pi\bar{\pi} = 7\pi\pi = (7 + j28) \text{ or conjugate} \ \text{↬} \ (91 + j21) \\ \pi\pi\bar{\pi}\bar{\pi} = 7^2 = 49 \text{ (self-conjugate)} \end{cases} \\
&\ \vdots
\end{aligned}$$

where the meaning of ↬ is explained below.[39] Looking to the list (Table 4) of

[39] Multiplication by ascending powers of U sends 2ω on a hexagonal tour, of which the following is typical:

$$2\omega = 2\pi\pi = 2(1 + j4) \to (-11 + j5) \to (-13 - j3) \to \text{their negatives}$$

I set all signs positive (so as to be in the first quadrant), pick the entry with the largest real component (so as to land in the wedge), and signal what I have done by writing

$$(1 + j4) \ \text{↬} \ (13 + j3)$$

I appropriate $2 = \sqrt{4}$ from the invariable 4-factor to insure that the tour visits only algebraic *integers*.

Surviving Cases
$196 = 4 \cdot 7^2$
$\mathbf{364} = 4 \cdot 7 \cdot 13$
$\mathbf{532} = 4 \cdot 7 \cdot 19$
$588 = 4 \cdot 3 \cdot 7^2$
$676 = 4 \cdot 13^2$
$784 = 4^2 \cdot 7^2$
$\mathbf{868} = 4 \cdot 7 \cdot 31$
$988 = 4 \cdot 13 \cdot 19$

TABLE 4: *Here, extracted from Table 3, are the only cases in which two or more p-primes (the same or different) enter into the prime factorization of* $N(\hat{\boldsymbol{n}})$.

of cases yet unaccounted for, we have

$$196 = 4 \cdot 7^2 = (13 + j3)(13 - j3) = (14 + j0)(14 - j0)$$

and see that 196 is "accidentally not accidentally degenerate" only because one of the associated lattice points happens to lie on the *edge* of the wedge. An identical remark pertains to each of the cases 588, 676 and 784.

We are first presented with a pair of *distinct* p-primes in the case

$$364 = 4 \cdot 7 \cdot 13 = 4 \cdot (2 + j)(2 - j) \cdot (1 + j2)(1 - j2)$$

which acquires its 2-fold accidental degeneracy from the circumstance that Ω can be defined in two distinct ways:

$$364 = \Omega\bar{\Omega} \quad \text{with} \quad \Omega = \begin{cases} 2(2 + j)(1 + j2) & \text{or conjugate} \quad \not\mapsto \quad (19 + j\ \ ) \\ 2(2 + j)(1 - j2) & \text{or conjugate} \quad \not\mapsto \quad (17 + j5) \end{cases}$$

Thus do we comprehend a fact about the number 364—it is the smallest integer that can be expressed

$$\text{integer} = (\text{integer})^2 + 3 \cdot (\text{integer})^2$$

in six different ways—that engaged our attention already on p. 55. Similarly

$$532 = \Omega\bar{\Omega} \quad \text{with} \quad \Omega = \begin{cases} 2(2 + j)(4 + j\ \ ) & \text{or conjugate} \quad \not\mapsto \quad (23 + j\ \ ) \\ 2(2 + j)(4 - j\ \ ) & \text{or conjugate} \quad \not\mapsto \quad (12 + j4) \end{cases}$$

$$868 = \Omega\bar{\Omega} \quad \text{with} \quad \Omega = \begin{cases} 2(2 + j)(2 + j3) & \text{or conjugate} \quad \not\mapsto \quad (29 + j3) \\ 2(2 + j)(2 - j3) & \text{or conjugate} \quad \not\mapsto \quad (26 + j8) \end{cases}$$

$$988 = \Omega\bar{\Omega} \quad \text{with} \quad \Omega = \begin{cases} 2(1 + j2)(4 + j) & \text{or conjugate} \quad \not\mapsto \quad (29 + j7) \\ 2(1 + j2)(4 - j) & \text{or conjugate} \quad \not\mapsto \quad (31 + j3) \end{cases}$$

The final example

$$988 = 29^2 + 3 \cdot 7^2 = 32^2 + 3 \cdot 3^2$$

previously escaped our notice only because the lattice point $\binom{31}{3}$ lies beyond the compass of Table 1.

It is by now clear that to determine the degeneracy $g(\hat{\boldsymbol{n}})$ of an eigenvalue $E(\hat{\boldsymbol{n}})$ of the equilateral triangular box problem, we have in principle "only" to display $N = \hat{n}_1^2 + 3\hat{n}_2^2$ in the factored form (64)

$$N = 4^\alpha 3^\beta p_1^{\mu_1} p_2^{\mu_2} \cdots p_k^{\mu_k} Q^2$$

Q need not itself be factored

Then to write

$$\begin{aligned} p_1 &= \pi_1 \bar{\pi}_1 \quad \text{with} \quad \pi_1 = m_1 + jn_1 \\ p_2 &= \pi_2 \bar{\pi}_2 \quad \text{with} \quad \pi_2 = m_2 + jn_2 \\ &\vdots \\ p_1 &= \pi_k \bar{\pi}_k \quad \text{with} \quad \pi_k = m_k + jn_k \end{aligned}$$

Then to figure out (this being a fairly straightforward combinatorial problem which I am not motivated to pursue in detail) in how many ways one can write

$$N = 4^{\alpha-1} 3^\beta \, \Omega\bar{\Omega} \cdot Q^2$$

$$\Omega = 2 \underbrace{\tbinom{\pi_1}{\bar{\pi}_1} \cdots \tbinom{\pi_1}{\bar{\pi}_1}}_{\mu_1 \text{ factors}} \underbrace{\tbinom{\pi_2}{\bar{\pi}_2} \cdots \tbinom{\pi_2}{\bar{\pi}_2}}_{\mu_2 \text{ factors}} \cdots \underbrace{\tbinom{\pi_k}{\bar{\pi}_k} \cdots \tbinom{\pi_k}{\bar{\pi}_k}}_{\mu_k \text{ factors}}$$

without landing on the edge of the wedge (which happens when Ω is real); within each bracket one is to select either the upper member or the lower. When N is large the initial factorization may, of course, be unfeasible. And the algorithm, since contingent upon that factorization, fails to display $g(\hat{n}_1, \hat{n}_2)$ as an explicit function.

It is because I am a physicist writing for physicists that I have allowed myself to drone on for ten pages about a little problem a number theorist would probably prefer to treat by other means,[40] or perhaps to assign as an exercise.[41] The mathematical literature does supply some pretty formulæ; we can, for example, write[42]

$$\text{degeneracy of } N = \sum_{\text{divisors } d \text{ of } M} (-3|d)$$

where $M \equiv N/4^\alpha$ and $(-3|d)$ is known to *Mathematica* as `JacobiSymbol[-3,d]` By numerical experimentation I have satisfied myself that the preceding formula does indeed work, but that it contributes no actual power that it not already ours.

---

[40] See §16.9 in Hardy & Wright (Footnote 36).

[41] See the reference on p. 122 of E. D. Bolker's *Elementary Number Theory: An Algebraic Approach* (1970) to his "Problem 41.39"!

[42] See P. Bachmann's *Niedere Zahlentheorie*. I am indebted to Joe Roberts for this reference.

Concerning the second of the spectral topics to which I alluded on p. 55 we can be relatively brief. The equation[43]

$$x^2 + 3y^2 = N$$

describes an ellipse on the (x, y)-plane. Drawing inspiration from (61) and Figure 28, we ask "How many lattice points can, in plausible approximation, be expected to lie within the shaded elliptical sector shown in the following figure?" Introducing polar coordinates in the usual way, we have

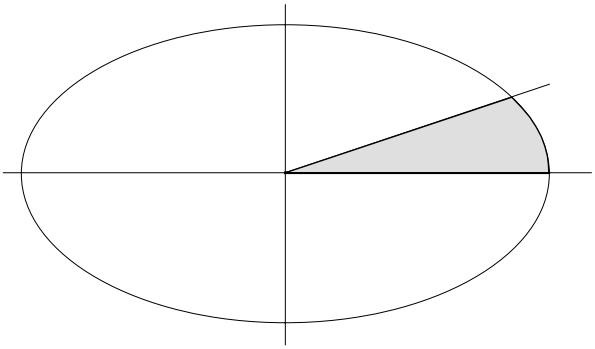

FIGURE 33: *How many equi-parity lattice points are interior to the shaded sector?*

$$\begin{aligned}\text{sector area} &= \int_0^{\theta_{\max}} \tfrac{1}{2} r^2 \, d\theta \\ &= \tfrac{N}{2} \int_0^{\arctan \frac{1}{3}} \frac{1}{\cos^2\theta + 3\sin^2\theta} \, d\theta \\ &= \tfrac{\pi}{12\sqrt{3}} N \quad \text{according to } \textit{Mathematica}\end{aligned}$$

Since each lattice point preempts unit area, and only half the lattice points are equi-parity points, we expect in leading approximation to have

$$\text{number of statepoints } \hat{\boldsymbol{n}} \approx \tfrac{\pi}{24\sqrt{3}} N = 0.075575N$$

This formula systematically over-estimates the number of statepoints (at $N = 900$ it yields the number 68, but according to Table 1 there are in fact only 57 points $\hat{\boldsymbol{n}}$ with $\hat{n}_1^2 + 3\hat{n}_2^2 \leq 900$), but fails to make any provision for the fact that points on the edge of the wedge are excluded. Easily

$$\begin{aligned}\text{lower edge length} &= \sqrt{N} \\ \text{sloping edge length} &= \sqrt{\tfrac{5}{6} N}\end{aligned}$$

[43] For purposes of the present discussion I find it convenient to adopt this simplified notation: $\hat{n}_1 \mapsto x$, $\hat{n}_2 \mapsto y$.

In refined approximation we expect therefore to have

$$\begin{aligned}\text{number of statepoints } \hat{\boldsymbol{n}} &\approx \tfrac{\pi}{24\sqrt{3}}N - \tfrac{1}{4}\Big[1+\sqrt{\tfrac{5}{6}}\,\Big]\sqrt{N} \\ &= 0.075575N - 0.478218\sqrt{N}\end{aligned} \tag{67}$$

—the accuracy of which is suggested by the following table:

N	Estimated	Observed
100	3	4
200	8	10
300	14	16
400	21	23
500	27	29
600	34	36
700	40	43
800	47	50
900	54	57
1000	60	64

TABLE 5: *Numerical evidence bearing on the accuracy of the (67). The $\sqrt{N}$ term appears to over-compensate a bit.*

We conclude—drawing now upon (61); i.e., upon $N = \frac{18ma^2}{h^2}E = (\frac{3ap}{h})^2$—that

$$\begin{aligned}\text{number of energy eigenvalues } &\leq E \equiv \tfrac{1}{2m}p^2 \\ &\approx \tfrac{\pi}{24\sqrt{3}}(\tfrac{3ap}{h})^2 - \tfrac{1}{4}\Big[1+\sqrt{\tfrac{5}{6}}\,\Big](\tfrac{3ap}{h})\end{aligned}$$

But (recalling points remarked already on pp. 38 & 51)

$$\begin{aligned}\text{box area} &= \tfrac{1}{4}\sqrt{3}a^2 \\ \text{box perimeter} &= 3a \\ \text{states/eigenvalue (absent any accidental degeneracy)} &= 2\end{aligned}$$

so (after a little algebraic simplification) we have

$$\begin{aligned}\mathcal{N}(E) &\equiv \textit{number of states} \text{ with energy eigenvalues} \leq E \\ &\approx \tfrac{(\text{box area})\cdot\pi p^2}{h^2} - \underbrace{\tfrac{1}{2}\Big[1+\sqrt{\tfrac{5}{6}}\,\Big]}_{=\,0.956435\,\sim\,1}\tfrac{(\text{box perimeter})\cdot p}{h} \qquad (69.1) \\ &\Big\downarrow \\ &= \tfrac{(\text{box area})\cdot\pi p^2}{h^2} \quad \text{asymptotically} \qquad (69.2)\end{aligned}$$

where "asymptotically" wears any of the meanings (large box, large momentum, small $\hbar$) one might associate with divergence of the dimensionless number $ap/\hbar$. Morse & Feshbach, at p. 761 of their Volume I, play a similar game, as it relates to a rectangular box of arbitrary proportion; they obtain a similar result, and state that the method "presumably holds for boundaries of any shape." The topic has been explored in elaborate detail by R. Balian & C. Block in a series of papers[44] which acquire special interest in relation to the general drift of my own remarks because (particularly in their second paper) the authors draw heavily upon the Feynmanesque ideas.

The classical phase space available to a particle that moves about in the interior of a box (area A) with energy not greater than E has a 4-volume given (since spatial cross sections are box-shaped, while momental cross sections are circles of radius $p = \sqrt{2mE}$) by

$$\mathcal{V}(E) = A \cdot \pi p^2$$

A folk theorem—as old as quantum mechanics itself, but (so far as I am aware) nameless, and not susceptible to general proof—asserts that the number of quantum states available to such a particle is given in leading approximation by

$$\mathcal{N}(E) = \frac{\mathcal{V}(E)}{h^{\text{degrees of freedom}}} = \frac{A \cdot \pi p^2}{h^2}$$

It is interesting—if perhaps not terribly surprising—that this result agrees precisely with (69.2).

By differentiation of $\mathcal{N}(E)$ we obtain the so-called spectral density or

$$\begin{aligned}\text{density of states } \rho(E) &\equiv \frac{d\mathcal{N}(E)}{dE} \\ &= \tfrac{(\text{box area})\cdot 2\pi m}{h^2} - 0.956435\, \tfrac{\text{box perimeter}}{h\cdot\text{speed}}\end{aligned}$$

(here "speed" $\equiv \sqrt{2E/m}$) which is frequently of more immediate physical interest than $\mathcal{N}(E)$ itself; we recall, for example, that in statistical mechanics

[44] "Distribution of eigenfrequencies for the wave equation in a finite domain," Annals of Physics, **60**, 401 (1970) and **69**, 76 (1972). These papers are made valuable not least by their extensive bibliographies; Balian & Block point out that the shape-independence of the leading term—presumed by Morse & Feshbach—was in fact proved in 1911 by H. Weyl. And M. Kac, in §4 of the paper cited in my first footnote, tells the story of how Weyl acquired interest in the problem (which Hilbert thought would not be solved in his lifetime). It seems that one Wolfskehl had endowed a prize to be awarded to the person who first proved Fermat's last theorem, and that proceeds were in the meantime to be used to bring eminent speakers to Göttingen. It was in a series of lectures presented under those auspices in 1910 by H. A. Lorentz, and attended by the young Weyl, that the problem, derived from a question initially posed by James Jeans, was mentioned.

the partition function can be described

$$\begin{aligned} Z(T) &\equiv \sum_{\text{states}} e^{-\frac{1}{kT}E(\text{state})} \\ &= \int_0^\infty e^{-\frac{E}{kT}}\rho(E)\,dE = \text{ Laplace transform of the spectral density} \end{aligned}$$

I mention these familiar facts because they connect up in at least two ways to points central to this essay. We note, in the first place, that

$$\begin{aligned} \rho(E) &= \text{locally averaged "slope of a staircase"} \\ &= \left\langle \frac{\text{rise = normal/accidental degeneracy } g(E)}{\text{run = interval } \Delta E \text{ between consecutive eigenvalues}} \right\rangle \end{aligned}$$

but that to pursue the details of this remark—to undertake to disentangle the respective contributions of numerator and denominator—is to be at risk of learning more of number theory than of physics; I therefore won't.[45] More interesting to me is the second point of contact:

To make a preliminary point in the simplest possible terms, assume the Hamiltonian H of a quantum system to be time-independent. Then

$$|\psi)_t = \mathsf{U}(t)|\psi)_0 \quad \text{with} \quad \mathsf{U}(t) = \exp\{-\tfrac{i}{\hbar}\mathsf{H}t\}$$

In the x-representation we recover precisely (4)

$$(x|\psi)_t = \int (x|\mathsf{U}(t)|y)dy(y|\psi)_0$$

which shows the propagator to have the character of a matrix representation of

[45] For a sense of the opportunities here passed by, see Chapter 15 of the text by G. E. Andrews, cited already in Footnote 37. To illustrate the methods characteristic of the "geometry of numbers" Andrews reviews Gauss' proof that

$$\lim_{N\to\infty} \tfrac{1}{N}\sum_{n=0}^{N} \{\text{number of solutions of } n = p^2 + q^2\} = \pi$$

and Dirichlet's proof that

$$\lim_{N\to\infty} \sum_{n=0}^{N} \{\text{number of divisors of } n\} = N\{\log N + \text{some constant}\}$$

Variants of both formulæ have acquired direct physical relevance in preceding paragraphs.

the operator $\mathsf{U}(t)$:

$$\begin{aligned} K(x,t;y,0) &= (x|\mathsf{U}(t)|y) \equiv \text{element } U_{xy}(t) \text{ of } \mathbb{U}(t) \\ &= \sum\sum (x|m)(m|\mathsf{U}(t)|n)(n|y) \\ &\downarrow \\ &= \sum_n e^{-\frac{i}{\hbar}E_n t}(x|n)(n|y) \quad \text{when} \quad \mathsf{H}|n) = E_n|n) \end{aligned}$$

It becomes natural in this light to speak of the (representation-independent) *trace* of $\mathbb{U}(t)$:

$$\begin{aligned} \mathrm{tr}\,\mathbb{U}(t) &= \int \Big\{ \sum_n e^{-\frac{i}{\hbar}E_n t}(x|\psi)(\psi|x) \Big\}\, dx \\ &= \sum_n e^{-\frac{i}{\hbar}E_n t} \quad \text{by} \quad \int (\psi|x)(x|\psi)\, dx = 1 \end{aligned}$$

Relaxing now our tacit presumption that the spectrum is non-degenerate, and taking certain notational liberties (of the form $\sum \to \int$), we obtain

$$\begin{aligned} \text{trace of the propagator} \equiv \int K(x,t;x,0)\, dx \\ = \int e^{-\frac{i}{\hbar}Et}\rho(E)\, dE \\ = \underbrace{\text{partition function } Z(T)}_{\text{Laplace transform of spectral density}} \text{ with } \tfrac{1}{kT} \to \tfrac{i}{\hbar}t \end{aligned} \tag{70}$$

We stand thus in prospect of a "trace theorem" which serves to establish a direct connection between the spectral density on the one hand and (on the other) a collective property of the classical "orbits" (paths that end where they began).

There is, of course, nothing novel about (70); it is as old as the hills.[46] But those hills yielded gold when prospected by (amongst many others) Balian & Bloch, Michael Berry and—most notably—Martin Gutzwiller in the 1970's. The resulting theory—which has been nicely reviewed in a recent monograph by M. Brack & R. Bhaduri[47] and is notable for its intricacy—has in more recent times become central to one approach to study of the problem of quantum chaos.[48]

---

[46] See, for example, the introductory sections of Chapter 10 in Feynman & Hibbs, who remark that they find (70) "amusing."

[47] *Semiclassical Physics* (1997); the "Gurtzwiller trace formula" and some of its extensions are treated in Chapters 5 & 6.

[48] See the popular review by Gurtzwiller in the January 1992 issue of *Scientific American*.

10. Particle in a bisected equilateral box. The problem now before us stands to the 60-60-60 problem (§§7–9) rather like the 45-45-90 problem (§6) stands to the square-box problem; in each case, it is by "bisection" that the latter problem goes over into the former. "Bisection" amounts to the installation of an adjusted boundary condition, and in each case that is accomplished by (in effect) discarding solutions that do not possess suitably placed nodal lines—solutions which do not possess, that is to say, an appropriate antisymmetry property. This much is intuitively pretty clear; my objective will be to trace the details by which results consistent with that intuition emerge spontaneously from application of the analytical machinery now at our command. Since most of the work (and all of the digressions) lie now behind us, we can be relatively brief, though the 30-60-90 problem is in some respects the most complex we will have occasion to consider. I will be at pains to proceed as though following steps spelled out in our "cookbook," as it has emerged. Our dimensioned box

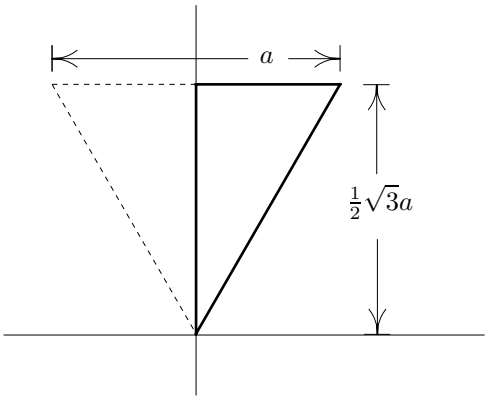

FIGURE 34: *The 30-60-90 box, got by "bisecting" the equilateral box treated earlier.*

is shown in the preceding figure; it has

$$\text{box area} = \tfrac{1}{8}\sqrt{3}a^2$$

$$\text{box perimeter} = \tfrac{1}{2}\big[3+\sqrt{3}\,\big]a$$

STEP ONE: COORDINATIZE THE TESSELATED PLANE. This, in the first instance, entails identification of a "fundamental unit," which can be accomplished in (infinitely) many ways, of which some are more natural than others. All options lead to the same ultimate result, but each lends its distinctive coloration to the intervening computation. Two options natural to the 30-60-90 problem (variants of those encountered already in connection with the 60-60-60 problem: see again Figures 21 & 22) are shown in Figures 35 & 36. We adopt the former (see Figure 37) in order to minimize the amount of fresh computation we have to perform, and to expose most clearly the relationship between physics in an equilateral box and physics in its bisection; for an account of the argument as it proceeds from the 24-element option see the material cited in Footnote 2.

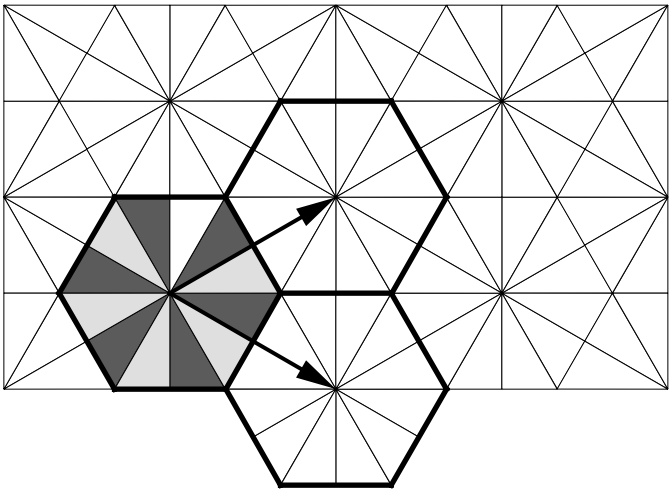

FIGURE 35: *The 12-element fundamental unit upon which the analytical work developed in the text is based; we select this option in order to achieve maximal consonance with the work which in previous sections proceeded from Figure 21.*

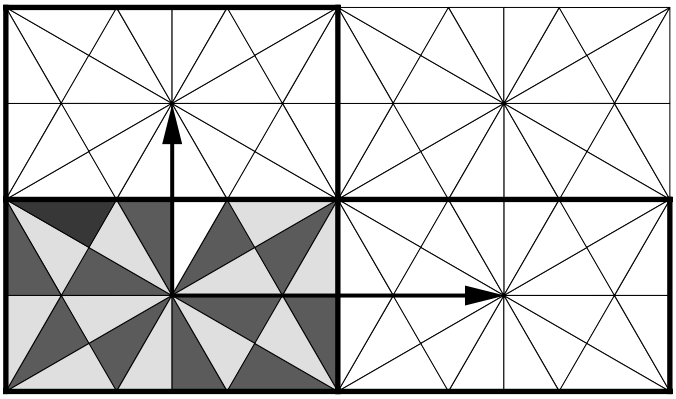

FIGURE 36: *An alternative 24-element fundamental unit that reproduces the tesselated plane by* orthogonal *translation. Note the rectangularity of the unit, which in Figure 22 we were not able to achieve. The inessential analytical simplification purchased by orthogonality is more than paid for by the concomitant obligation to keep track of an increased number of fundamental image points.*

Proceeding now in reference to Figure 37, we note that $\boldsymbol{x}_0, \boldsymbol{x}_1, \boldsymbol{x}_2, \boldsymbol{x}_3, \boldsymbol{x}_4$ and $\boldsymbol{x}_5$ are defined precisely as they were in the equilateral case (Figure 23)—though $\boldsymbol{x}_0$ ranges now on a relatively restricted domain—and that

$$\boldsymbol{x}_{k+6} = -\boldsymbol{x}_k \quad : \quad k = 0, 1, 2, 3, 4, 5$$

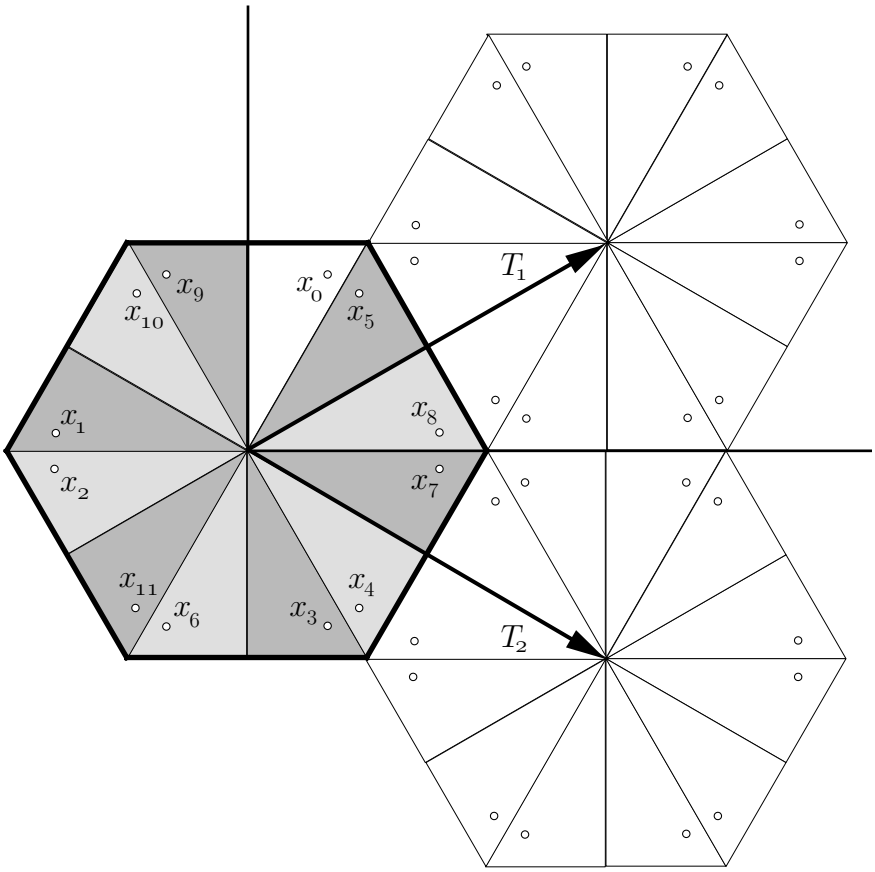

FIGURE 37: *Notated enlargement of Figure 35, which expands upon notations introduced in Figure 23.*

Again things have been rigged so as to achieve (in all cases)

$$\text{parity of } \boldsymbol{x}_\alpha = (-)^\alpha$$

Borrowing from previous work (p. 39) we have without labor the fundamental image coordinates reported at the top of the next page. The translation vectors are given also as before; we have

$$\boldsymbol{T}_1 = \tfrac{a}{2}\begin{pmatrix} 3 \\ +\sqrt{3} \end{pmatrix} \quad \text{and} \quad \boldsymbol{T}_2 = \tfrac{a}{2}\begin{pmatrix} 3 \\ -\sqrt{3} \end{pmatrix}$$

so the matrix $\mathbb{T}$ defined at (27)—of which we will soon have need—can be described

$$\mathbb{T} = \tfrac{3}{2}a^2\begin{pmatrix} 2 & 1 \\ 1 & 2 \end{pmatrix}, \quad \det\mathbb{T} = 3\cdot\left(\tfrac{3}{2}a^2\right)^2 \quad \text{and} \quad \mathbb{T}^{-1} = \left(\tfrac{3}{2}a^2\right)^{-1}\begin{pmatrix} \frac{2}{3} & -\frac{1}{3} \\ -\frac{1}{3} & \frac{2}{3} \end{pmatrix}$$

$$
\begin{aligned}
\boldsymbol{x}_0 &= \begin{pmatrix} +1 & 0 \\ 0 & +1 \end{pmatrix} \boldsymbol{x} \qquad = -\boldsymbol{x}_6 \quad \text{with} \quad \boldsymbol{x} \equiv \begin{pmatrix} x_1 \\ x_2 \end{pmatrix} \\
\boldsymbol{x}_1 &= \tfrac{1}{2} \begin{pmatrix} -1 & -\sqrt{3} \\ -\sqrt{3} & +1 \end{pmatrix} \boldsymbol{x}_0 = -\boldsymbol{x}_7 \\
\boldsymbol{x}_2 &= \tfrac{1}{2} \begin{pmatrix} -1 & -\sqrt{3} \\ +\sqrt{3} & -1 \end{pmatrix} \boldsymbol{x}_0 = -\boldsymbol{x}_8 \\
\boldsymbol{x}_3 &= \begin{pmatrix} +1 & 0 \\ 0 & -1 \end{pmatrix} \boldsymbol{x}_0 \qquad = -\boldsymbol{x}_9 \\
\boldsymbol{x}_4 &= \tfrac{1}{2} \begin{pmatrix} -1 & +\sqrt{3} \\ -\sqrt{3} & -1 \end{pmatrix} \boldsymbol{x}_0 = -\boldsymbol{x}_{10} \\
\boldsymbol{x}_5 &= \tfrac{1}{2} \begin{pmatrix} -1 & +\sqrt{3} \\ +\sqrt{3} & +1 \end{pmatrix} \boldsymbol{x}_0 = -\boldsymbol{x}_{11}
\end{aligned}
$$

STEP TWO: EXPRESS THE SUM-OVER-PATHS AS A SUM OF THETA FUNCTIONS. It is a lesson of experience—not informed by any compelling general argument—that because our particle moves "freely" (meaning subject only to impulsive wall forces) the hypothetical "test paths" contemplated by Hamilton make no net contribution to Feynman's sum-over-paths; that in the class of problems here under review (see again p. 9) we have, in simplified consequence of the Feynman formalism, the statements

$$
\begin{aligned}
K(\boldsymbol{x},t;\boldsymbol{y},0) &= \sum_{\text{all paths}} \left(\tfrac{m}{iht}\right)^{\frac{\text{dimension}}{2}} e^{\frac{i}{\hbar}S[\text{classical reflective path}]} \\
&= \tfrac{m}{iht} \sum_{\alpha=0}^{11} (-)^{\alpha} \sum_{\boldsymbol{n}} \exp\left\{\tfrac{i}{\hbar} S_\alpha\right\} \\
&\qquad\qquad \tfrac{i}{\hbar} S_\alpha = \beta(\boldsymbol{v}_\alpha + \boldsymbol{n}) \cdot \mathbb{T}\,(\boldsymbol{v}_\alpha + \boldsymbol{n})
\end{aligned}
$$

where (as before) $\beta \equiv im/2\hbar t$ and where the vectors $\boldsymbol{v}_\alpha$ were defined at (27); here as before it serves the interests of clarity to postpone for a moment their actual evaluation. Reading again from (37.1), we have

$$
= \tfrac{m}{iht} \sum_{\alpha=0}^{11} (-)^{\alpha} e^{\beta \boldsymbol{v}_\alpha \cdot \mathbb{T} \boldsymbol{v}_\alpha}\, \vartheta\big(i\beta \mathbb{T} \boldsymbol{v}_\alpha, -\tfrac{i\beta}{\pi} \mathbb{T}\big)
$$

STEP THREE: PASS, BY JACOBI'S IDENTITY, TO THE WAVE REPRESENTATION. Reading from (37.2) we have (compare (45))

$$
= \tfrac{1}{\text{area of fundamental unit}} \sum_{\alpha=0}^{11} (-)^{\alpha}\, \vartheta\big(\pi \boldsymbol{v}_\alpha, \tfrac{\pi}{i\beta} \mathbb{T}^{-1}\big) \tag{71}
$$

We note in passing that "area of the fundamental unit" has the same value as in the equilateral case, but stands in a different relation to the area of the box:

$$
\text{area of fundamental unit} = 12 \cdot \text{area of box} = \tfrac{3}{2}\sqrt{3} a^2
$$

STEP FOUR: EXPAND THE THETA FUNCTION. Drawing upon (46) we obtain

$$K(\boldsymbol{x},t;\boldsymbol{y},0) = \tfrac{1}{12\cdot\text{area}} \sum_{\boldsymbol{n}} e^{-\frac{i}{\hbar}\mathcal{E}(n_1^2 - n_1 n_2 + n_2^2)\,t} \sum_{\alpha=0}^{11} (-)^\alpha \cos 2\pi\, \boldsymbol{n}\cdot\boldsymbol{v}_\alpha \tag{72}$$

by the manipulations that gave (47), and in which $\mathcal{E}$ retains its former meaning:

$$\mathcal{E} \equiv \tfrac{2}{9}\tfrac{h^2}{ma^2}$$

Our objective in the next two steps is first to lump together all terms with numerically identical "energy exponentials," and then to "resolve the lumps" so as to achieve

$$(x\text{-dependent factor}) \cdot (y\text{-dependent factor})$$

There are several ways to proceed, depending upon how heavily we are willing to draw upon results obtained already in connection with the equilateral box problem. I have elected to proceed afresh, by slight re-organization of our former line of argument:

STEP FIVE: SUM OVER SPECTRAL SYMMETRIES. Which, if we were working on a truly clean blackboard, we would have first to identify; I will be content simply to summarize what we already know in this regard. We know (see again the beginning of §8) that it is entirely natural to write

$$\begin{aligned} n_1^2 - n_n n_2 + n_2^2 &= \tfrac{1}{4}\left[(n_1+n_2)^2 + 3(n_1-n_2)^2\right] \\ &= \tfrac{1}{4}\hat{\boldsymbol{n}}^{\intercal}\begin{pmatrix} 1 & 0 \\ 0 & 3 \end{pmatrix}\hat{\boldsymbol{n}} \quad \text{with} \quad \hat{\boldsymbol{n}} \equiv \begin{pmatrix} 1 & 1 \\ 1 & -1 \end{pmatrix}\boldsymbol{n} \\ &= \tfrac{1}{4}\underbrace{\left[\hat{n}_1^2 + 3\hat{n}_2^2\right]}_{\equiv N(\hat{\boldsymbol{n}})} = \tfrac{1}{4}(\hat{n}_1 + i\sqrt{3}\hat{n}_2)(\hat{n}_1 - i\sqrt{3}\hat{n}_2) \end{aligned}$$

And we know that $N(\hat{\boldsymbol{n}})$ is invariant under the operations described by (59); each (equi-parity) lattice point $\hat{\boldsymbol{n}}$ therefore has (see again the "orbits" shown in Figures 26 & 28) five or eleven "companions," according as it lives on the upper/lower "edge of the wedge" or in its interior. It becomes in this light natural to reorganize the right side of (72), writing

$$K(\boldsymbol{x},t;\boldsymbol{y},0) = \tfrac{1}{12\cdot\text{area}} \sum_{\text{wedge}} e^{-\frac{i}{\hbar}\mathcal{E}\frac{1}{4}N(\hat{\boldsymbol{n}})\,t} \Big\{ \sum_{\text{orbit}} \sum_{\alpha=0}^{11} (-)^\alpha \cos \pi\, \mathbb{Z}\hat{\boldsymbol{n}}\cdot\boldsymbol{v}_\alpha \Big\} \tag{73}$$

Here $\mathbb{Z}$ is the matrix defined on p. 44; it permits one to write $\hat{\boldsymbol{n}} = \mathbb{Z}\boldsymbol{n}$ and, by inversion, $\boldsymbol{n} = \frac{1}{2}\mathbb{Z}\hat{\boldsymbol{n}}$. Turning our attention now to the expression interior to the braces: the vectors $\hat{\boldsymbol{v}}_\alpha$ were defined at (27)

$$\boldsymbol{v}_\alpha \equiv \mathbb{T}^{-1}\begin{pmatrix} \boldsymbol{S}_\alpha\cdot\boldsymbol{T}_1 \\ \boldsymbol{S}_\alpha\cdot\boldsymbol{T}_2 \end{pmatrix} \quad \text{with} \quad \boldsymbol{S}_\alpha \equiv \boldsymbol{x}_\alpha - \boldsymbol{y}$$

and by extension (use $\boldsymbol{x}_{k+6} = -\boldsymbol{x}_k : k = 0, 1, 2, 3, 4, 5$) of calculations reported on p. 41 we have

$$\begin{aligned}
-\pi\boldsymbol{v}_0 &= \begin{pmatrix} X_2 - Y_2 \\ X_1 - Y_1 \end{pmatrix} & -\pi\boldsymbol{v}_6 &= \begin{pmatrix} -X_2 - Y_2 \\ -X_1 - Y_1 \end{pmatrix} \\
-\pi\boldsymbol{v}_1 &= \begin{pmatrix} X_0 - Y_2 \\ X_1 - Y_1 \end{pmatrix} & -\pi\boldsymbol{v}_7 &= \begin{pmatrix} -X_0 - Y_2 \\ -X_1 - Y_1 \end{pmatrix} \\
-\pi\boldsymbol{v}_2 &= \begin{pmatrix} X_1 - Y_2 \\ X_0 - Y_1 \end{pmatrix} & -\pi\boldsymbol{v}_8 &= \begin{pmatrix} -X_1 - Y_2 \\ -X_0 - Y_1 \end{pmatrix} \\
-\pi\boldsymbol{v}_3 &= \begin{pmatrix} X_1 - Y_2 \\ X_2 - Y_1 \end{pmatrix} & -\pi\boldsymbol{v}_9 &= \begin{pmatrix} -X_1 - Y_2 \\ -X_2 - Y_1 \end{pmatrix} \\
-\pi\boldsymbol{v}_4 &= \begin{pmatrix} X_0 - Y_2 \\ X_2 - Y_1 \end{pmatrix} & -\pi\boldsymbol{v}_{10} &= \begin{pmatrix} -X_0 - Y_2 \\ -X_2 - Y_1 \end{pmatrix} \\
-\pi\boldsymbol{v}_5 &= \begin{pmatrix} X_2 - Y_2 \\ X_0 - Y_1 \end{pmatrix} & -\pi\boldsymbol{v}_{11} &= \begin{pmatrix} -X_2 - Y_2 \\ -X_0 - Y_1 \end{pmatrix}
\end{aligned}$$

Recalling again the definition (and noting the symmetry) of $\mathbb{Z}$, we have

$$-\pi\mathbb{Z}\hat{\boldsymbol{n}}\cdot\boldsymbol{v}_\alpha = \begin{pmatrix} \hat{n}_1 \\ \hat{n}_2 \end{pmatrix}^{\mathsf{T}} \begin{pmatrix} 1 & 1 \\ 1 & -1 \end{pmatrix} (-\pi\boldsymbol{v}_\alpha)$$

giving

$$\begin{aligned}
-\pi\mathbb{Z}\hat{\boldsymbol{n}}\cdot\boldsymbol{v}_0 &= \hat{n}_1[+X_1 + X_2 - Y_1 - Y_2] + \hat{n}_2[-X_1 + X_2 + Y_1 - Y_2] \\
-\pi\mathbb{Z}\hat{\boldsymbol{n}}\cdot\boldsymbol{v}_1 &= \hat{n}_1[+X_1 + X_0 - Y_1 - Y_2] + \hat{n}_2[-X_1 + X_0 + Y_1 - Y_2] \\
-\pi\mathbb{Z}\hat{\boldsymbol{n}}\cdot\boldsymbol{v}_2 &= \hat{n}_1[+X_0 + X_1 - Y_1 - Y_2] + \hat{n}_2[-X_0 + X_1 + Y_1 - Y_2] \\
-\pi\mathbb{Z}\hat{\boldsymbol{n}}\cdot\boldsymbol{v}_3 &= \hat{n}_1[+X_2 + X_1 - Y_1 - Y_2] + \hat{n}_2[-X_2 + X_1 + Y_1 - Y_2] \\
-\pi\mathbb{Z}\hat{\boldsymbol{n}}\cdot\boldsymbol{v}_4 &= \hat{n}_1[+X_2 + X_0 - Y_1 - Y_2] + \hat{n}_2[-X_2 + X_0 + Y_1 - Y_2] \\
-\pi\mathbb{Z}\hat{\boldsymbol{n}}\cdot\boldsymbol{v}_5 &= \hat{n}_1[+X_0 + X_2 - Y_1 - Y_2] + \hat{n}_2[-X_0 + X_2 + Y_1 - Y_2] \\
-\pi\mathbb{Z}\hat{\boldsymbol{n}}\cdot\boldsymbol{v}_6 &= \hat{n}_1[-X_1 - X_2 - Y_1 - Y_2] + \hat{n}_2[+X_1 - X_2 + Y_1 - Y_2] \\
-\pi\mathbb{Z}\hat{\boldsymbol{n}}\cdot\boldsymbol{v}_7 &= \hat{n}_1[-X_1 - X_0 - Y_1 - Y_2] + \hat{n}_2[+X_1 - X_0 + Y_1 - Y_2] \\
-\pi\mathbb{Z}\hat{\boldsymbol{n}}\cdot\boldsymbol{v}_8 &= \hat{n}_1[-X_0 - X_1 - Y_1 - Y_2] + \hat{n}_2[+X_0 - X_1 + Y_1 - Y_2] \\
-\pi\mathbb{Z}\hat{\boldsymbol{n}}\cdot\boldsymbol{v}_9 &= \hat{n}_1[-X_2 - X_1 - Y_1 - Y_2] + \hat{n}_2[+X_2 - X_1 + Y_1 - Y_2] \\
-\pi\mathbb{Z}\hat{\boldsymbol{n}}\cdot\boldsymbol{v}_{10} &= \hat{n}_1[-X_2 - X_0 - Y_1 - Y_2] + \hat{n}_2[+X_2 - X_0 + Y_1 - Y_2] \\
-\pi\mathbb{Z}\hat{\boldsymbol{n}}\cdot\boldsymbol{v}_{11} &= \hat{n}_1[-X_0 - X_2 - Y_1 - Y_2] + \hat{n}_2[+X_0 - X_2 + Y_1 - Y_2]
\end{aligned}$$

which in notations

$$\begin{aligned}
X_0 &= 2\xi_1 & Y_0 &= 2\zeta_1 \\
X_1 &= -\xi_1 + \xi_2 & Y_1 &= -\zeta_1 + \zeta_2 \\
X_2 &= -\xi_1 - \xi_2 & Y_2 &= -\zeta_1 - \zeta_2
\end{aligned}$$

first introduced on p. 42 read

$$
\begin{aligned}
-\pi\mathbb{Z}\hat{\boldsymbol{n}}\cdot\boldsymbol{v}_0 &= \hat{n}_1[-2\xi_1 \quad\quad + 2\zeta_1] + \hat{n}_2[-2\xi_2 \quad\quad + 2\zeta_2] \\
&= [\quad\quad -2\hat{n}_1\xi_1 \quad\quad - 2\hat{n}_2\xi_2] + 2[\hat{n}_1\zeta_1 + \hat{n}_2\zeta_2] \\
-\pi\mathbb{Z}\hat{\boldsymbol{n}}\cdot\boldsymbol{v}_1 &= \hat{n}_1[+\ \xi_1 + \xi_2 + 2\zeta_1] + \hat{n}_2[+3\xi_1 - \xi_2 + 2\zeta_2] \\
&= [+(\hat{n}_1 + 3\hat{n}_2)\xi_1 + (\hat{n}_1 - \hat{n}_2)\xi_2] + 2[\hat{n}_1\zeta_1 + \hat{n}_2\zeta_2] \\
-\pi\mathbb{Z}\hat{\boldsymbol{n}}\cdot\boldsymbol{v}_2 &= \hat{n}_1[+\ \xi_1 + \xi_2 + 2\zeta_1] + \hat{n}_2[-3\xi_1 + \xi_2 + 2\zeta_2] \\
&= [+(\hat{n}_1 - 3\hat{n}_2)\xi_1 + (\hat{n}_1 + \hat{n}_2)\xi_2] + 2[\hat{n}_1\zeta_1 + \hat{n}_2\zeta_2] \\
-\pi\mathbb{Z}\hat{\boldsymbol{n}}\cdot\boldsymbol{v}_3 &= \hat{n}_1[-2\xi_1 \quad\quad + 2\zeta_1] + \hat{n}_2[+2\xi_2 \quad\quad + 2\zeta_2] \\
&= [\quad\quad -2\hat{n}_1\xi_1 \quad\quad + 2\hat{n}_2\xi_2] + 2[\hat{n}_1\zeta_1 + \hat{n}_2\zeta_2] \\
-\pi\mathbb{Z}\hat{\boldsymbol{n}}\cdot\boldsymbol{v}_4 &= \hat{n}_1[+\ \xi_1 - \xi_2 + 2\zeta_1] + \hat{n}_2[+3\xi_1 + \xi_2 + 2\zeta_2] \\
&= [+(\hat{n}_1 + 3\hat{n}_2)\xi_1 - (\hat{n}_1 - \hat{n}_2)\xi_2] + 2[\hat{n}_1\zeta_1 + \hat{n}_2\zeta_2] \\
-\pi\mathbb{Z}\hat{\boldsymbol{n}}\cdot\boldsymbol{v}_5 &= \hat{n}_1[+\ \xi_1 - \xi_2 + 2\zeta_1] + \hat{n}_2[-3\xi_1 - \xi_2 + 2\zeta_2] \\
&= [+(\hat{n}_1 - 3\hat{n}_2)\xi_1 - (\hat{n}_1 + \hat{n}_2)\xi_2] + 2[\hat{n}_1\zeta_1 + \hat{n}_2\zeta_2] \\
-\pi\mathbb{Z}\hat{\boldsymbol{n}}\cdot\boldsymbol{v}_6 &= \hat{n}_1[+2\xi_1 \quad\quad + 2\zeta_1] + \hat{n}_2[+2\xi_2 \quad\quad + 2\zeta_2] \\
&= [\quad\quad +2\hat{n}_1\xi_1 \quad\quad + 2\hat{n}_2\xi_2] + 2[\hat{n}_1\zeta_1 + \hat{n}_2\zeta_2] \\
-\pi\mathbb{Z}\hat{\boldsymbol{n}}\cdot\boldsymbol{v}_7 &= \hat{n}_1[-\ \xi_1 - \xi_2 + 2\zeta_1] + \hat{n}_2[-3\xi_1 + \xi_2 + \zeta_2] \\
&= [-(\hat{n}_1 + 3\hat{n}_2)\xi_1 - (\hat{n}_1 - \hat{n}_2)\xi_2] + 2[\hat{n}_1\zeta_1 + \hat{n}_2\zeta_2] \\
-\pi\mathbb{Z}\hat{\boldsymbol{n}}\cdot\boldsymbol{v}_8 &= \hat{n}_1[-\ \xi_1 - \xi_2 + 2\zeta_1] + \hat{n}_2[+3\xi_1 - \xi_2 + 2\zeta_2] \\
&= [-(\hat{n}_1 - 3\hat{n}_2)\xi_1 - (\hat{n}_1 + \hat{n}_2)\xi_2] + 2[\hat{n}_1\zeta_1 + \hat{n}_2\zeta_2] \\
-\pi\mathbb{Z}\hat{\boldsymbol{n}}\cdot\boldsymbol{v}_9 &= \hat{n}_1[+2\xi_1 \quad\quad + 2\zeta_1] + \hat{n}_2[-2\xi_2 \quad\quad + 2\zeta_2] \\
&= [\quad\quad +2\hat{n}_1\xi_1 \quad\quad - 2\hat{n}_2\xi_2] + 2[\hat{n}_1\zeta_1 + \hat{n}_2\zeta_2] \\
-\pi\mathbb{Z}\hat{\boldsymbol{n}}\cdot\boldsymbol{v}_{10} &= \hat{n}_1[-\ \xi_1 + \xi_2 + 2\zeta_1] + \hat{n}_2[-3\xi_1 - \xi_2 + 2\zeta_2] \\
&= [-(\hat{n}_1 + 3\hat{n}_2)\xi_1 + (\hat{n}_1 - \hat{n}_2)\xi_2] + 2[\hat{n}_1\zeta_1 + \hat{n}_2\zeta_2] \\
-\pi\mathbb{Z}\hat{\boldsymbol{n}}\cdot\boldsymbol{v}_{11} &= \hat{n}_1[-\ \xi_1 + \xi_2 + 2\zeta_1] + \hat{n}_2[+3\xi_1 + \xi_2 + 2\zeta_2] \\
&= [-(\hat{n}_1 - 3\hat{n}_2)\xi_1 + (\hat{n}_1 + \hat{n}_2)\xi_2] + 2[\hat{n}_1\zeta_1 + \hat{n}_2\zeta_2]
\end{aligned}
$$

Writing

$$
\sum_{\alpha=0}^{11}(-)^\alpha \cos\pi\mathbb{Z}\hat{\boldsymbol{n}}\cdot\boldsymbol{v}_\alpha = \Big\{\sum_{\alpha=0}^{5} + \sum_{\alpha=6}^{11}\Big\}(-)^\alpha \cos\pi\mathbb{Z}\hat{\boldsymbol{n}}\cdot\boldsymbol{v}_\alpha
$$

we look specifically to the first sum on the right (which will put us in position to obtain the second by a simple sign adjustment); grouping terms by the scheme $\alpha = \{0,3\},\{1,4\},\{2,5\}$ and making use of the elementary identity

$$
\begin{aligned}
&\cos(A+B+C) - \cos(A-B+C) \\
&\qquad = -2\sin A\cdot\sin B\cdot\cos C - 2\cos A\cdot\sin B\cdot\sin C
\end{aligned}
$$

we obtain

$$\begin{aligned}\sum_{\alpha=0}^{5}(-)^{\alpha}\cos\pi\mathbb{Z}\hat{\boldsymbol{n}}\cdot\boldsymbol{v}_{\alpha}&\\ &= -2\Big\{ + \sin[-2\hat{n}_1\xi_1]\sin[-2\hat{n}_2\xi_2]\\ &\qquad - \sin[(\hat{n}_1+3\hat{n}_2)\xi_1]\sin[(\hat{n}_1-\hat{n}_2)\xi_2]\\ &\qquad + \sin[(\hat{n}_1-3\hat{n}_2)\xi_1]\sin[(\hat{n}_1+\hat{n}_2)\xi_2]\Big\}\cos[2(\hat{n}_1\zeta_1+\hat{n}_2\zeta_2)]\\ &\quad - 2\Big\{ + \cos[-2\hat{n}_1\xi_1]\sin[-2\hat{n}_2\xi_2]\\ &\qquad - \cos[(\hat{n}_1+3\hat{n}_2)\xi_1]\sin[(\hat{n}_1-\hat{n}_2)\xi_2]\\ &\qquad + \cos[(\hat{n}_1-3\hat{n}_2)\xi_1]\sin[(\hat{n}_1+\hat{n}_2)\xi_2]\Big\}\sin[2(\hat{n}_1\zeta_1+\hat{n}_2\zeta_2)]\end{aligned}$$

which in notation introduced on p. 46 reads

$$\sum_{\alpha=0}^{5}(-)^{\alpha}\cos\pi\mathbb{Z}\hat{\boldsymbol{n}}\cdot\boldsymbol{v}_{\alpha} = -2\Big\{\hat{F}_{\hat{\boldsymbol{n}}}(\xi_1,\xi_2)\cos\varphi - \hat{G}_{\hat{\boldsymbol{n}}}(\xi_1,\xi_2)\sin\varphi\Big\} \tag{74.1}$$

with $\varphi \equiv 2(\hat{n}_1\zeta_1+\hat{n}_2\zeta_2)$. Here we have (by slightly different means) reproduced a result encountered already in connection with our analysis of the 60-60-60 box problem; it is the result which led to our first perception of the symmetry structure of $\hat{n}_1^2+3\hat{n}_2^2$—information which in the present discussion we accepted as known in advance—and from which we extracted our description of the equilateral box eigenfunctions. But in the present connection we need also the conjoint statement (got without labor by $\boldsymbol{\xi}\to-\boldsymbol{\xi}$, in which connection recall symmetry conditions (63))

$$\sum_{\alpha=6}^{11}(-)^{\alpha}\cos\pi\mathbb{Z}\hat{\boldsymbol{n}}\cdot\boldsymbol{v}_{\alpha} = -2\Big\{\hat{F}_{\hat{\boldsymbol{n}}}(\xi_1,\xi_2)\cos\varphi + \hat{G}_{\hat{\boldsymbol{n}}}(\xi_1,\xi_2)\sin\varphi\Big\} \tag{74.2}$$

By addition

$$\sum_{\alpha=0}^{11}(-)^{\alpha}\cos\pi\mathbb{Z}\hat{\boldsymbol{n}}\cdot\boldsymbol{v}_{\alpha} = -4\hat{F}_{\hat{\boldsymbol{n}}}(\xi_1,\xi_2)\cos\varphi \tag{75}$$

from which the $\hat{G}$-term has dropped away; it is this cancellation—the effect of which is to eliminate the eigenstates which were invariant with respect to reflection in the ξ_2-axis (i.e., which were even functions of ξ_1)—which principally distinguishes the 30-60-90 box problem from its equilateral companion.

We have thus far summed over the elements of the fundamental unit (and used spectral symmetry information to accomplish that process), but have yet to carry out the

$$\sum_{\text{orbit}} = \text{sum over spectral symmetries}$$

To that end we write

$$\cos\varphi = \cos 2\hat{n}_1\zeta_1 \cos 2\hat{n}_2\zeta_2 - \sin 2\hat{n}_1\zeta_1 \sin 2\hat{n}_2\zeta_2$$

and observe (as we did already at the top of p. 43) that—owing to parity-based cancellations— the first term on the right makes no net contribution to the orbital sum. Arguing now as we did on p. 51, we obtain finally

$$\Big\{ \sum_{\text{orbit}} \sum_{\alpha=0}^{11} (-)^\alpha \cos \pi \mathbb{Z} \hat{\boldsymbol{n}} \cdot \boldsymbol{v}_\alpha \Big\} = 16 \hat{F}_{\hat{\boldsymbol{n}}}(\boldsymbol{\xi}) \hat{F}_{\hat{\boldsymbol{n}}}(\boldsymbol{\zeta}) \tag{76}$$

where the equi-parity point $\hat{\boldsymbol{n}}$ lies necessarily in the interior of the wedge.

STEP SIX: READ OFF EIGENVALUES AND EIGENVECTORS. Returning with (76) to (73), we have

$$K(\boldsymbol{x}, t; \boldsymbol{y}, 0) = \tfrac{4}{3 \cdot \text{area}} \sum_{\text{wedge}}{}'' e^{-\frac{i}{\hbar}\mathcal{E}\frac{1}{4}N(\hat{\boldsymbol{n}})\, t}\ \hat{F}_{\hat{\boldsymbol{n}}}(\boldsymbol{\xi}) \hat{F}_{\hat{\boldsymbol{n}}}(\boldsymbol{\zeta})$$

$$\text{area} = \tfrac{1}{2} \text{ area of equilateral box}$$

We have at this point reached our ultimate objective, for we have only to write

$$E(\hat{\boldsymbol{n}}) \equiv \tfrac{h^2}{18ma^2}\big(\hat{n}_1^2 + 3\hat{n}_2^2\big) \quad \text{and} \quad \Psi_{\hat{\boldsymbol{n}}}(\boldsymbol{x}) \equiv \sqrt{\tfrac{32}{3\sqrt{3}a^2}} e^{i(\text{any phase})} \hat{F}_{\hat{\boldsymbol{n}}}(\boldsymbol{\xi}) \tag{77}$$

to obtain (compare (62))

$$K(\boldsymbol{x}, t; \boldsymbol{y}, 0) = \sum_{\text{wedge}}{}'' e^{-\frac{i}{\hbar}E(\hat{\boldsymbol{n}})\, t} \Psi_{\hat{\boldsymbol{n}}}(\boldsymbol{x}) \Psi^*_{\hat{\boldsymbol{n}}}(\boldsymbol{y}) \tag{78}$$

—which is an instance of (3).

11. Comparative discussion of spectrum & eigenfunctions. The 30-60-90 box, got by bisection of the equilateral box, has (see again Figure 34)

$$\begin{aligned}
\text{area} &= \tfrac{1}{2} \cdot \text{ area of associated equilateral box} \\
&= \tfrac{1}{2} \cdot \tfrac{1}{4}\sqrt{3}a^2 \\
\text{perimeter} &= \tfrac{1}{2} \cdot \text{ perimeter of associated equilateral box} + \tfrac{1}{2}\sqrt{3} \text{ side-length} \\
&= \underbrace{\tfrac{1}{2}\big[1 + \tfrac{1}{\sqrt{3}}\big]}_{} \cdot \text{ perimeter of associated equilateral box} \\
&= 1.577350
\end{aligned}$$

It gives rise to an energy spectrum which is *identical to that of the equilateral box*, and which has the same accidental degeneracy structure (see Table 1). This is somewhat counter-intuitive; we expect the small cymbal to sound higher, but

find in this instance that it supports a fundamental as low as equilateral cymbal from which it was cut. The essential difference (from a spectral point of view) between the two systems resides in the fact that each spectral value is (in the absence of accidental degeneracy) doubly degenerate in the equilateral case, but *singly degenerate* in the bisected case; we have

$$\text{30-60-90 density of states} = \tfrac{1}{2}\cdot \text{ equilateral density of states}$$

with the result that it is not the structure of the spectrum itself but the *location of the* N^{th} *state* ($N = 2, 3, \ldots$) that has been shifted upward by the reduction in box area.

The general drift of the preceding remark is neatly supported by equation (69), which is reproduced below:

$$\begin{aligned}\mathcal{N}(E) &\equiv \textit{number of states} \text{ with energy eigenvalues} \leq E \\ &\approx \tfrac{(\text{box area})\cdot\pi p^2}{h^2} - \underbrace{\tfrac{1}{2}\left[1+\sqrt{\tfrac{5}{6}}\right]}\ \tfrac{(\text{box perimeter})\cdot p}{h} \\ &\qquad\qquad = 0.956435 \sim 1\end{aligned}$$

Evidently

$$\text{box area} \to \tfrac{\text{box area}}{2} \quad \text{serves asymptotically to induce} \quad \mathcal{N}(E) \to \tfrac{1}{2}\mathcal{N}(E)$$

but

$$\text{box perimeter} \to 1.577350\ \tfrac{\text{box perimeter}}{2}$$

causes the leading-order correction term—which (see again Table 5) already over-compensated—to become now even more too large. I hope on another occasion to trace this circumstance to a sense in which the 30-60-90 box is "less nearly round" than the equilateral box.

The 30-60-90 box problem gives rise to a set of eigenfunctions which can be obtained from those of the associated equilateral box problem by a procedure of the design

$$\{\text{60-60-60 eigenfunctions}\} \xrightarrow[\text{renormalization}]{\text{elimination}} \{\text{30-60-90 eigenfunctions}\}$$

The functions that survive the "elimination" process are those that are *antisymmetric* in the variable $\xi_1 \equiv \frac{\pi}{3a}x_1$; in Figure 30, the symmetric function depicted at the top is discarded, while its antisymmetric companion (ground state of the 30-60-90 box) is retained. Renormalization (multiplication by $\sqrt{2}$) is necessary because the bisected box has only half of its former area.

The procedure just described—"opportunistic" in the sense that it involves creation of a new physical system by erection of a barrier on the site of a nodal line of a prior system—is hardly novel; it is used occasionally/casually in a variety of applications (particularly to electrostatics and potential theory), and can be considered basic to the practical application of the "method of images." But some questions relating to the theoretical limits of its utility remain

(so far as I am aware) open. The following remarks are intended to identify a few of the points at issue—points which spring perhaps more naturally from the quantum mechanical than from other more standard manifestations of the method of images.

Comparison of Figure 18 with Figure 30 suggests that we should be able to extract the physics of the 45-45-90 box from that of the square box by precisely the procedure just discussed, and raises this question: Why can't quantum mechanics in a right triangular box of arbitrary proportion be extracted from that of the associated rectangular box? The answer, though elementary, is instructive. Rectangular boxes give rise—whether analysed by separation of

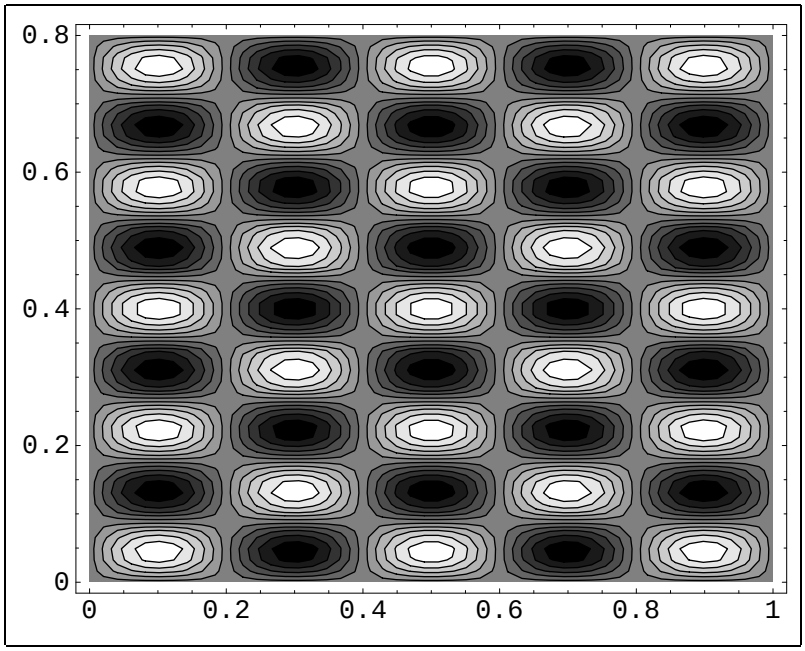

FIGURE 38: *We found at (22), and again (by another method) on p. 26, that the eigenstates of a particle in a rectangular box can be described*

$$\psi_{n_1 n_2}(x_1, x_2) = \sqrt{\tfrac{4}{\text{box area}}}\,\sin\left(\frac{n_1\pi}{a_1}x_1\right)\cdot\sin\left(\frac{n_2\pi}{a_2}x_2\right)$$

In the figure I have set $a_1 = 1$, $a_2 = \frac{4}{5}$, $n_1 = 5$ *and* $n_2 = 9$. *Note that the nodal lines run parallel to the sides of the box.*

variables or by the method of images—to eigenfunctions the nodal lines of which (see the figure) run parallel to the sides of the box; none runs on a diagonal. This remains true when the box becomes square, but then—abruptly—the eigenstates, because of the *enhanced symmetry of the square, become doubly*

degenerate,[49] *and yield diagonal nodal lines when taken in appropriate linear combination*. The situation is illustrated in Figure 39, and amounts, in short, to this: "it takes two to linearly combine," and one does not (in the absence of accidental degeneracy) have two to play with unless the box is square. It is interesting that a situation which from one point of view derives from the delicate circumstances which permit "tesselation of the plane" can, from another point of view, be said to be rooted in a fortuitous spectral degeneracy.

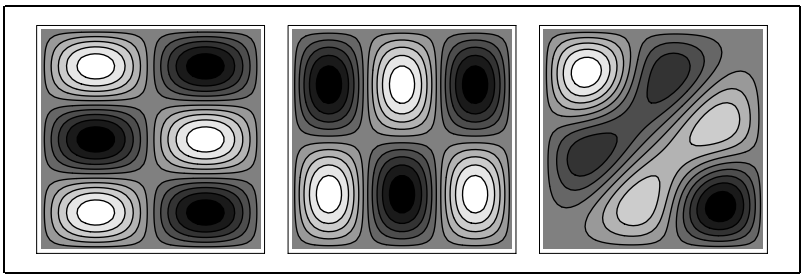

FIGURE 39: *The figure on the left shows the square box state ψ_{23}, at center is the state ψ_{32}, and on the right is their difference, with its diagonal nodal line. The difference state appears in Figure 18 as an eigenstate of the 45-45-90 box problem.*

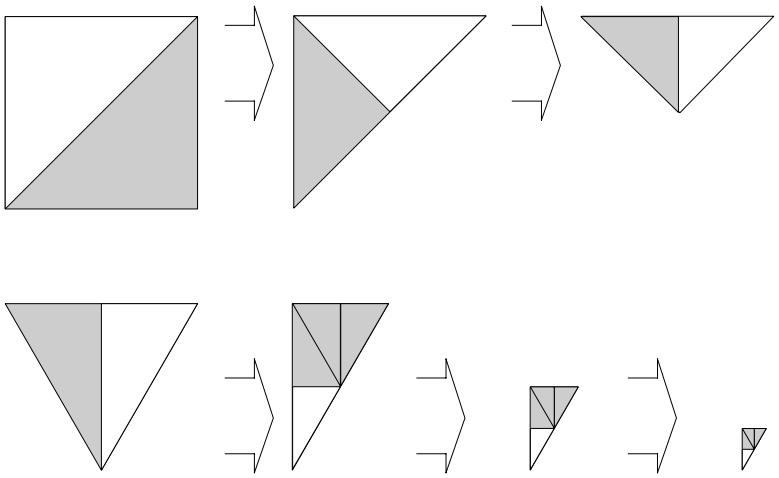

FIGURE 40: *Iterative origin of the self-similarity properties which (presumably) attach to the spectrum and eigenfunctions that arise from the 45-45-90 and 30-60-90 box problems.*

[49] It is amusing to note in this connection that squares are the "roundest" of all rectangles.

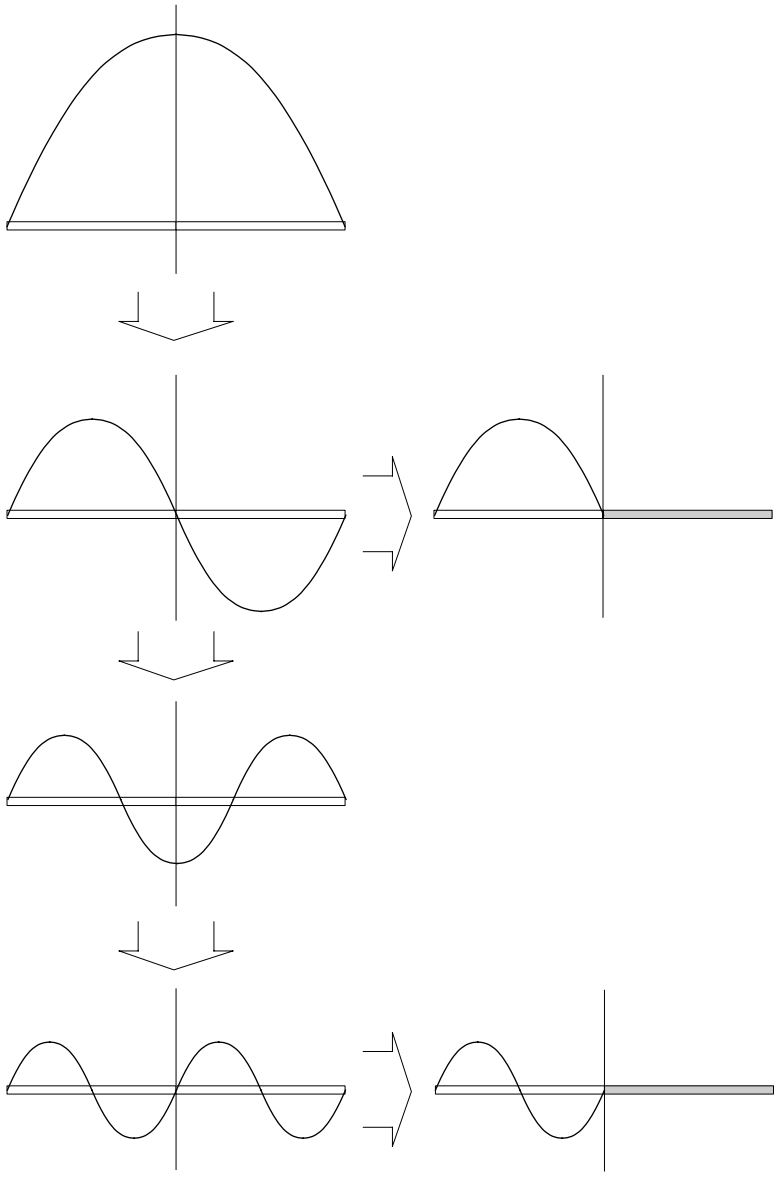

FIGURE 41: *Self-similarity in the one-dimensional box problem; bisection of the box produces eigenstates from which one can, by elementary transformations, recover the parent population. In the figure the amplitudes have been selected arbitrarily. See the text for explanatory remarks.*

The process of opportunistically erecting barriers at nodal lines can, under favorable circumstances, be iterated, as illustrated in Figure 40. The implication —which I will not pursue, but which will already have impressed itself upon any reader who has taken the trouble to do the hands-on exploration advocated on p. 33—is that the eigenfunctions (and also the eigenvalues) encountered in connection with the 45-45-90 and 30-60-90 box problems possess a pretty *scaling property*. A simple precursor of this phenomenon arises from the one-dimensional box problem, and is illustrated in Figure 41; on the left are shown the eigenfunctions of ascending order, on the right are the eigenfunctions of the system which results when a barrier has bisected the box. It is clear both diagramatically and analytically that the latter functions collectively reproduce the parent functions, which could be recovered by elementary deformations. The interesting point is that "reverse iteration" works in this case because all one-dimensional boxes have the same shape.[50] But the boxes produced by diagonal bisection of a square box, or central bisection of an equilateral box, have shapes different from their respective parents. It is evidently *not* possible to recover the anti-nodal eigenfunctions of the square/equilateral parent boxes by reversal of the iterative schemes depicted in Figure 40.

Generalizing... let A be a box of *arbitrary* shape, let ψ_{seed} be selected from the population $\{\psi\}_A$ of eigenfunctions on A, and let B be a selected one of the regions defined by the nodal net of ψ_{seed} (see Figure 42). Erect a barrier on the

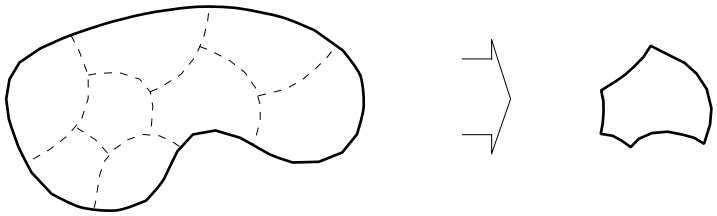

FIGURE 42: *On the left are the box A and the nodal contours of some selected eigenstate ψ_{seed}. On the right is a daughter box B defined by that nodal net.*

boundary ∂B of B and construct the population $\{\psi\}_B$ of eigenfunctions on the daughter box. It becomes, in the light of what's gone before, natural to ask: "What is the relationship of $\{\psi\}_B$ to $\{\psi\}_A$? More particularly, under what conditions does ∂B occur in the nodal nets also of *other* elements of $\{\psi\}_A$? Under what conditions are those ∂B-sharing elements of $\{\psi\}_A$ complete/ orthonormal on B? Tangential evidence[51] leads me to suspect that the answer to all such questions is "Only very exceptionally!" The systems which have been of concern to us are in this light recognized to be *exceptional* systems.

[50] Recall my introductory paragraph.

[51] I am thinking here of, for example, "Bourget's hypotehsis" (see G. Watson's *Theory of Bessel Functions*, §15.28), according to which $J_m(z)$ and $J_n(z)$ (here m and n are positive integers) have no common zeros, apart from the origin.

12. From one in a two-box to two in a one-box. The Feynman formalism, though it purports to be elastic enough to embrace—in principle—the whole of quantum mechanics, permits detailed calculation only in a vaguely-defined population of special cases, and it is to a sharply-defined sub-population that the preceding material specifically refers. The theory in hand brings to mind the trio in a Mozartian opera: three soloists are on stage at the same time—geometry, analysis and number theory—singing finely-balanced harmony in the service of physics. Each, however, is able to perform, whether singly or in concert, only when things are "just so," and too much of "just so" tends to be off-puttingly claustrophobic, to diminish one's interest in the song, to inspire doubt that it pertains usefully to the rude real world.

My objective in what now follows will be to show that results already in hand admit interestingly of a line of physical reinterpretation. And that elaboration of those reinterpretations leads naturally to a modest loosening of the constraints that at present so tightly bind us.

Let *two* particles—m_1 and m_2—inhabit the one-dimensional box of §1. Assume them to move freely except for the impulsive forces of constraint exerted by the walls and the *contact forces which prevent their interpenetation*; we then have

$$0 \leq x_1 \leq x_2 \leq a \quad : \quad \text{all times } t$$

Take the coordinate pair $\{x_1, x_2\}$ to define a point on a plane. The configuration space available to the system has then the triangular form shown in Figure 43. System motion, in such a representation, traces a folded series of line segments, and resembles "billiards on a 45-45-90 triangular table" except in this sole respect: *the "law of reflection" is not (unless $m_1 = m_2$) satisfied on the diagonal.* For the slope of a segment is given by

$$\text{slope} = \frac{\text{instantaneous velocity of } m_2}{\text{instantaneous velocity of } m_1}$$

Clearly

$$\text{slope} \to -\text{slope (law of reflection) when either} \begin{cases} m_1 \text{ bounces elastically of left wall} \\ m_2 \text{ bounces elastically of right wall} \end{cases}$$

but the elementary theory of one-dimensional elastic collisions supplies

$$\text{exit slope} = \frac{2m_1 - (m_1 - m_2)(\text{entry slope})}{(m_1 - m_2) + 2m_2(\text{entry slope})} \tag{79}$$

and by elementary geometrical argument we know that when a ray of slope $\tan\alpha$ is incident upon a mirror of slope $\tan\phi$ the reflected ray has slope $\tan\beta$ with $\beta = 2\phi - \alpha$; moreover

$$\begin{aligned} \tan\beta &= \frac{\tan 2\phi - \tan\alpha}{1 + \tan 2\phi \tan\alpha} \\ &= \frac{2\tan\phi - (1 - \tan^2\phi)\tan\alpha}{(1 - \tan^2\phi) + 2\tan\phi\tan\alpha} \end{aligned} \tag{80}$$

which bears a striking resemblance to (79), from which, however, it differs in one small detail. My immediate objective is to remove that wart. To that end, we notice that that the "energy ellipse" can, by a simple rescaling, be made circular:

$$E = \tfrac{1}{2}(m_1\dot{x}_1^2 + m_2\dot{x}_2^2)$$
$$= \tfrac{1}{2}M(\dot{X}_1^2 + \dot{X}_2^2) \quad \text{with} \quad \begin{cases} X_1 \equiv \sqrt{\frac{m_1}{M}}\, x_1 \\ X_2 \equiv \sqrt{\frac{m_2}{M}}\, x_2 \end{cases}$$

(Here a mass M, of arbitrary value, has been introduced for dimensional reasons; it will be assigned its "natural value" in a moment.) The transformation $\boldsymbol{x} \to \boldsymbol{X}$, since linear, sends lines into lines, but adjusts their slopes:

$$\text{slope} = \sqrt{\tfrac{m_1}{m_2}}\ \text{Slope}$$

In the latter notation (79) can be written

$$\text{exit Slope} = \frac{2\tan\phi - (1-\tan^2\phi)(\text{entry Slope})}{(1-\tan^2\phi) + 2\tan\phi(\text{entry Slope})}$$

with

$$\tan\phi \equiv \sqrt{\tfrac{m_2}{m_1}} = \text{slope of diagonal side of transformed triangle}$$

Comparison with (80) shows that we have, by simple deformation $\boldsymbol{x} \to \boldsymbol{X}$, achieved collisional compliance with the law of reflection. The deformation has

$$\text{Jacobian} = \sqrt{\tfrac{m_1 m_2}{M}}$$
$$= 1 \quad \text{provided we set } M = \sqrt{m_1 m_2} = \text{harmonic mean}$$

which (as a matter simply of convenience) we do so the triangle and its transform will have the same area; the transformation then reads

$$\left.\begin{aligned} x_1 \to X_1 &= \left(\tfrac{m_1}{m_2}\right)^{\frac{1}{4}} x_1 \\ x_2 \to X_2 &= \left(\tfrac{m_2}{m_1}\right)^{\frac{1}{4}} x_2 \end{aligned}\right\} \tag{81}$$

It is "hyperbolic" in the sense that $X_1X_2 = x_1x_2$, and reduces to the identity when $m_1 = m_2$. The point (see again Figure 43) of the preceding remarks is this:

> The $\boldsymbol{X}$-representation of the motion of our 2-particle system is *formally indistinguishable from that of a single billiard ball on a triangular table* of specific design.

Prescribed initial data $\{\boldsymbol{x}, \dot{\boldsymbol{x}}\}_0$ serves, in effect, to inscribe a line in $\boldsymbol{X}$-space. From the unique "reflective covering" of such a line (see Figure 44) one can read

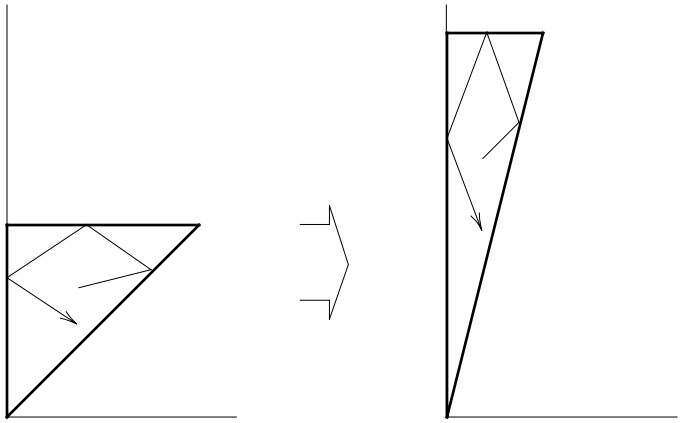

FIGURE 43: *The figure on the left describes—in natural coordinates x_1 and x_2—the adventures of two particles in a one-dimensional box: on the left m_1 has bounced off the left end of the box; at top m_2 has bounced off the right end of the box; on the diagonal the particles have collided. The “law of reflection” does not hold on the diagonal. The figure on the right displays the same information in the coordinates defined by (81), which have been designed to bring collisions into conformity with the law of reflections.*

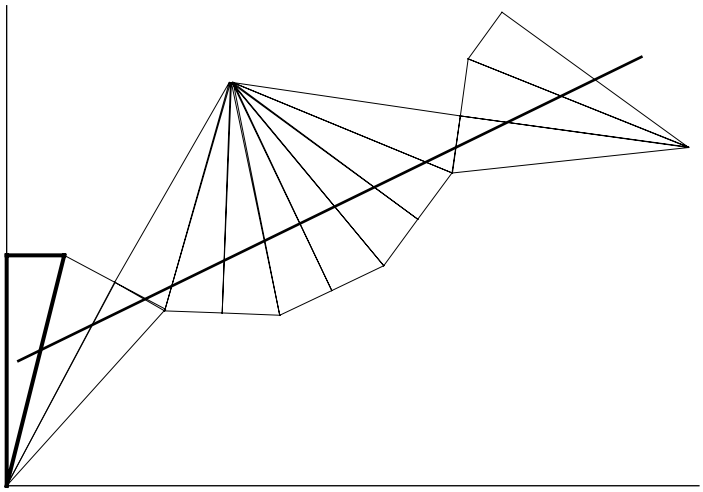

FIGURE 44: *“Reflective covering of a line,” which permits one to read off the collisional implications of prescribed initial data, as explained in the text. The figure is drawn in $\boldsymbol{X}$-space. It was such a figure (see Figure 2 in A. Hobson, “Ergodic properties of a particle moving elastically inside a polygon,”J. Math. Phys.* **16**, *2210 (1975)) that initially inspired my interest in this entire subject.*

off the collisional experiences—past and future—of the particle pair, experiences which (reading from the figure, which has been drawn in the presumption that $(m_2/m_1)^{\frac{1}{4}} = 2$) might be encoded

$$CLRCLCLCLCRLCL\ldots$$

It is because m_1 is here so much less massive than $m_2 = 16m_1$ that we witness so many more L(eft) than R(ight) wall-reflections; poor m_1 really gets pounded.

In three cases and three only—namely the cases $m_1 = m_2$ (when the collisional side of the triangle in $\boldsymbol{X}$-space has slope $= \tan 45°$), $m_2 = 3m_1$ (when slope $= \tan 60°$) and $m_2 = \frac{1}{3}m_1$ (when slope $= \tan 30°$)—do the triangles that cover the population of all possible lines fit together so neatly as to achieve tesselation of the plane. In those cases and those only is it feasible to speak usefully of the *population* of classical trajectories that link a specified initial configuration to a specified terminal configuration (as the Feynman formalism requires). In those cases and those only can we use the results already in hand to obtain an *exact quantum mechanical description of the dynamics of two particles in a one-dimensional box*... but in those cases we *can* do so, which is fairly remarkable. The results in hand are, moreover, nicely pre-adapted to the "indistinguishability physics" which might be imposed in the case $m_1 = m_2$.

One-dimensional two-particle systems of the type considered above were recommended to our attention on grounds of their formal equivalence to certain two-dimensional single-particle systems. But if one has two particles to play with it is easy to devise systems which, while formally detached from billiard physics, are of some independent interest. Suppose, for example, that m_1 and m_2 are constrained not by the walls of a "one-dimensional box" but by the "inextensible string" (of length a) that binds them. The intuitively-evident motion of such a "string molecule" (which, like a turtle, "carries its box on its back") is illustrated in Figure 45. Analytically, one writes

$$x_1 = X + r_1$$
$$x_2 = X + r_2$$

and imposes the side condition

$$m_1 r_1 + m_2 r_2 = 0$$

Then

$$E = \tfrac{1}{2}\big(m_1\dot{x}_1^2 + m_2\dot{x}_2^2\big) = \tfrac{1}{2}M\dot{X}^2 + \tfrac{1}{2}\big(m_1\dot{r}_1^2 + m_2\dot{r}_2^2\big) \quad \text{with } M \equiv m_1 + m_2$$
$$= \tfrac{1}{2}M\big(\dot{X}^2 + \dot{R}^2\big) \quad \text{with } R \equiv +\sqrt{\tfrac{m_2}{m_1}}\,r_2 = -\sqrt{\tfrac{m_1}{m_2}}\,r_1$$

The maximial excursion of the relative coordinate is set by the length of the string; easily

$$0 \leq R \leq R_{\max} = \tfrac{\sqrt{m_1 m_2}}{M}a$$

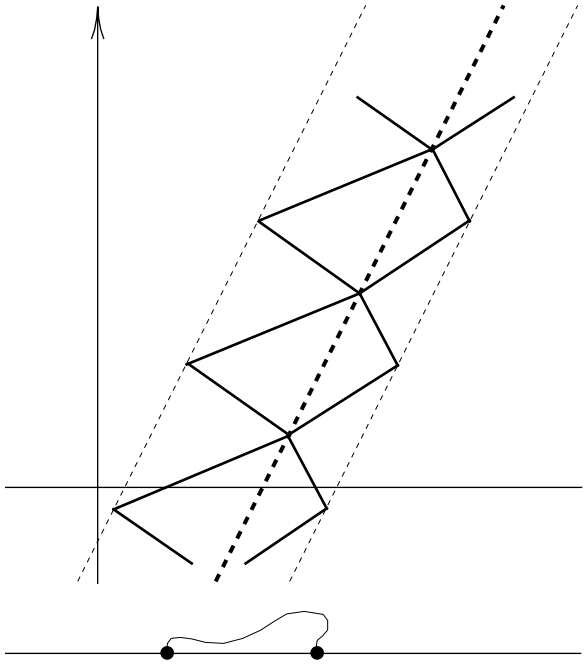

FIGURE 45: *Spacetime diagram of the one-dimensional motion of the “string molecule” shown at bottom. The central dashed line represents the unaccelerated drift of the center of mass. Many related figures can be found in Chapter II of Baylor Fox’s Reed College thesis (May 1996).*

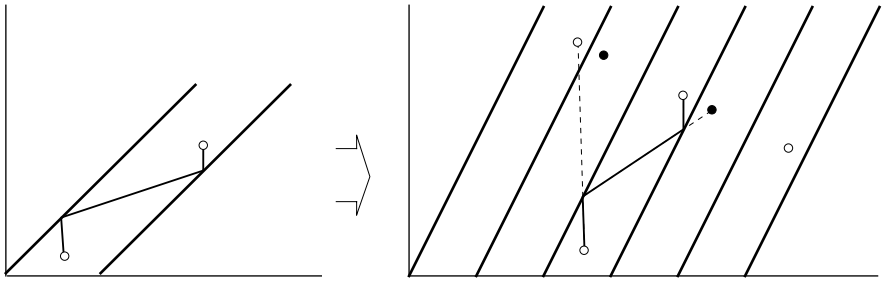

FIGURE 46: *Application of the method of images to the “diatomic string molecule problem” requires an initial deformation (81) so as to acquire the “law of reflection,” but is thereafter straightforward. The molecular problem is evidently equivalent to the problem of “billiards on a table without ends.”*

It is by this point clear that, whether one proceeds directly or (see Figure 46) *via* the method of images,[52] one will be led to separated eigenfunctions of the form

$$\psi(x_1, x_2) = \psi_{\text{unaccelerated drift}}(X) \cdot \psi_{\text{box}}(R)$$

where the latter factor describes the "vibrational" state of the molecule.

13. The one-dimensional triatomic string molecule. Adding one particle and two strings to the system discussed in the preceding paragraph, one obtains the system shown in Figure 47. To avoid complications that are extraneous to the

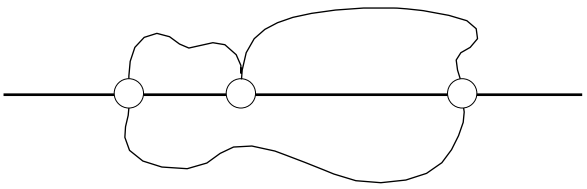

FIGURE 47: *Generic "triatomic string molecule." The constituent "atoms"—reading from left to right—have coordinates x_1, x_2, x_3 and masses m_1, m_2, m_3. They are bound by inextensible massless strings of lengths s_{12}, s_{23} and s_{13}. Without loss of generality we assume $s_{12} \leq s_{23}$; it becomes then fairly natural to assume that*

$$s_{12} \leq s_{23} \leq s_{13} \quad \textit{and} \quad s_{13} \leq s_{12} + s_{23}$$

since in all other cases one or another of the strings would have nothing to do, and could be eliminated.

business now at hand, I will set $m_1 = m_2 = m_3 \equiv m$ and $s_{12} = s_{23} \equiv s$. The center of mass of the 3-body system lives then at

$$X = \tfrac{1}{3}(x_1 + x_2 + x_3)$$

and drifts along uniformly. We agree to concentrate on (vibrational) motion *relative* to the center of mass; writing

$$x_1 = X + r_1$$
$$x_2 = X + r_2$$
$$x_3 = X + r_3$$

[52] For the details—which hold no surprises—see pp. 233–237 of the research notes (1971–1976) cited in Footnote 2. Also treated there is the (formally more interesting) case in which the molecule moves on the surface of a disk.

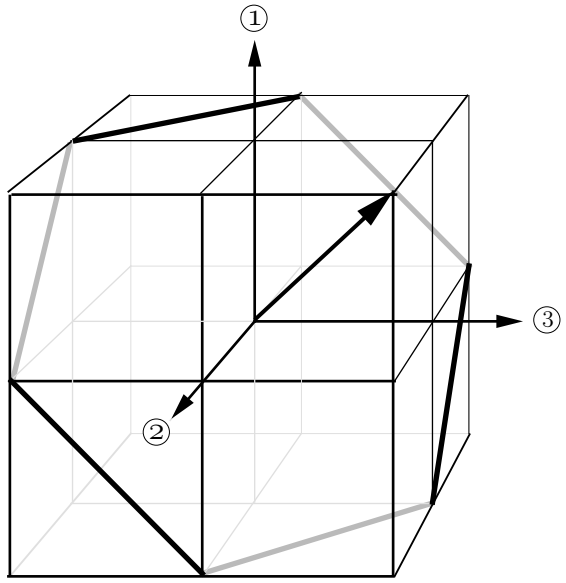

FIGURE 48: *Orientation of the “internal configration plane” in relation to a cube centered at the origin of 3-dimensional r-space. The configuration plane is always normal to the “mass vector” $\boldsymbol{m} \equiv (m_1, m_2, m_3)$; here we have assumed all masses equal.*

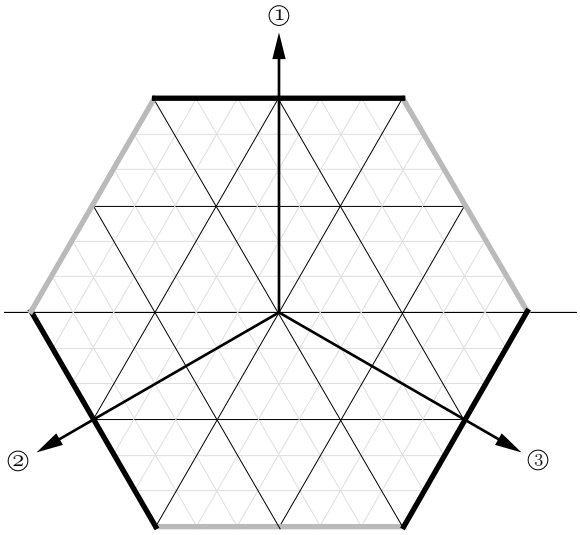

FIGURE 49: *The configuration plane seen face-on. The symmetry inherent in the equation $r_1 + r_2 + r_3 = 0$ is manifest. The lines normal to the n-axis $(n = 1, 2, 3)$ were scribed by stacked planes of constant r_n.*

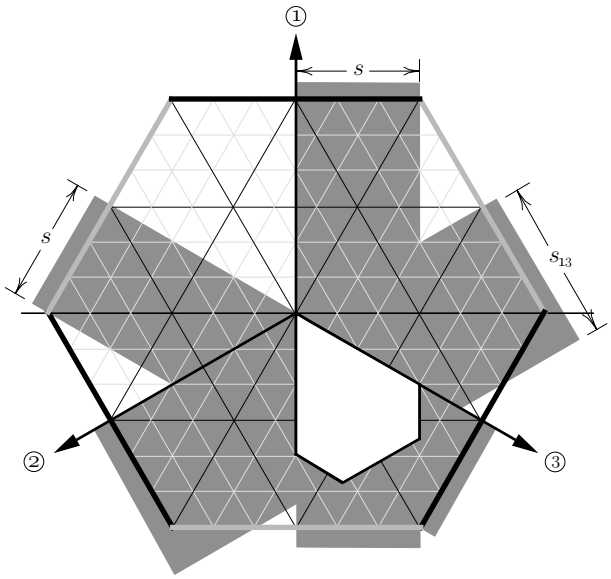

FIGURE 50: *Construction, on the internal configuration plane, of the polygonal domain accessible to the string molecule. It has been assumed that* $s_{12} = s_{23} = s$ *and* $s < s_{13} < 2s$*. Within the polygon, all* r_1*-values are negative and all* r_3*-values are positive, but the coordinate* r_2 *of the interior atom is as often positive as negative.*

the relative coordinates[53] are subject to the linear constraint

$$r_1 + r_2 + r_3 = 0$$

and reside therefore on a 2-dimensional "internal configuration plane" in 3-dimensional r-space. Figure 48 shows the relation of the configuration plane to the coordinate planes. Planes parallel to the latter intersect the internal configuration plane in such a way as to set up the triangular grid shown in Figure 49. Working in reference to that gird, I construct in Figure 50 the polygonal domain accessible to the molecule. The motion of the point representive of the instantaneous internal configuration of the molecule is shown in Figure 51. Two-body collisions—else string-mediated "anticollisions"—occur when the configuration point "bounces off a wall," as spelled out below:

[53] Concerning which (we note it passing) it is intuitively evident that

r_1 is always negative (or zero)
r_3 is always positive (or zero), but
r_2 can have either sign

At wall A: ① & ② collide, ③ is a spectator;

At wall E: ② & ③ collide, ① is a spectator;

At wall D: ① & ② anticollide, ③ is a spectator;

At wall B: ② & ③ anticollide, ① is a spectator;

At wall C: ① & ③ anticollide, ② is a spectator;

Sides A and E intersect at a vertex V_{AE} which refers to the classic three-body collsion which takes place when ①, ② and ③ arrive simultaneously at the origin. Other vertices refer to simultaneous collision-anticollisions: at the vertex V_{AB} ① & ② collide as ② and ③ anticollide. That situation is reversed at V_{DE}. At V_{BC} ③ anticollides simultaneously with ① and ② (the string S_{12} is slack), while at V_{CD} ① anticollides simultaneously with ② and ③ (the string S_{23} is slack).

The construction shown in Figure 44 can be used to develop the trajectory latent in prescribed initial data, but does not tesselate the plane except in the two cases shown in Figure 52. And only the first of those cases yields (for reasons stated in the caption) to analysis by the method of images. That analysis has, in fact, already been accomplished, in §§7–9. To establish explicit contact with that earlier work, we introduce new coordinates which (since x_1 and x_2 were preempted when we assigned coordinates $\{x_1, x_2, x_3\}$ to the "atoms") we call z_1 and z_2; working from the preceding figure, we write

$$\begin{aligned} r_1 &= c_{11}z_1 + c_{12}z_2 \\ r_2 &= c_{21}z_1 + c_{22}z_2 \\ r_3 &= c_{31}z_1 + c_{32}z_2 \end{aligned}$$

and—looking (as a matter of convenience) to the three-body collision points—require that

$$\begin{aligned} -\tfrac{1}{3}s &= -c_{11}\tfrac{1}{2}a + c_{12}\tfrac{1}{2}\sqrt{3}a \\ -\tfrac{1}{3}s &= -c_{21}\tfrac{1}{2}a + c_{22}\tfrac{1}{2}\sqrt{3}a \\ +\tfrac{2}{3}s &= -c_{31}\tfrac{1}{2}a + c_{32}\tfrac{1}{2}\sqrt{3}a \end{aligned} \qquad \text{and} \qquad \begin{aligned} -\tfrac{2}{3}s &= +c_{11}\tfrac{1}{2}a + c_{12}\tfrac{1}{2}\sqrt{3}a \\ +\tfrac{1}{3}s &= +c_{21}\tfrac{1}{2}a + c_{22}\tfrac{1}{2}\sqrt{3}a \\ +\tfrac{1}{3}s &= +c_{31}\tfrac{1}{2}a + c_{32}\tfrac{1}{2}\sqrt{3}a \end{aligned}$$

Working out the implied values of the coefficients c_{pq} (recall in this connection that $s/a = \frac{1}{4}\sqrt{3}$) we obtain

$$\begin{aligned} r_1 &= \tfrac{1}{4\sqrt{3}}(-z_1 - \sqrt{3}z_2) \\ r_2 &= \tfrac{1}{4\sqrt{3}}(\ 2z_1) \\ r_3 &= \tfrac{1}{4\sqrt{3}}(-z_1 + \sqrt{3}z_2) \end{aligned}$$

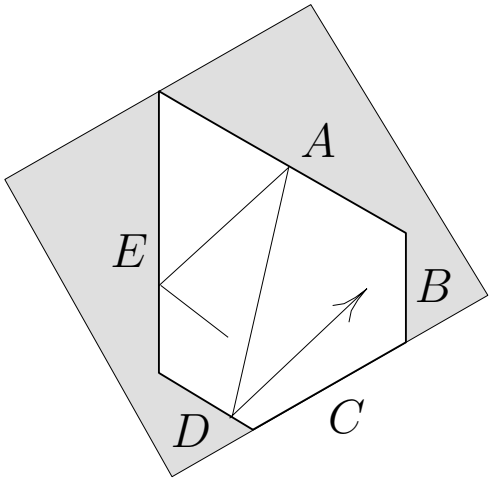

FIGURE 51: *Because all masses have been assumed equal, the law of reflection is automatic.*

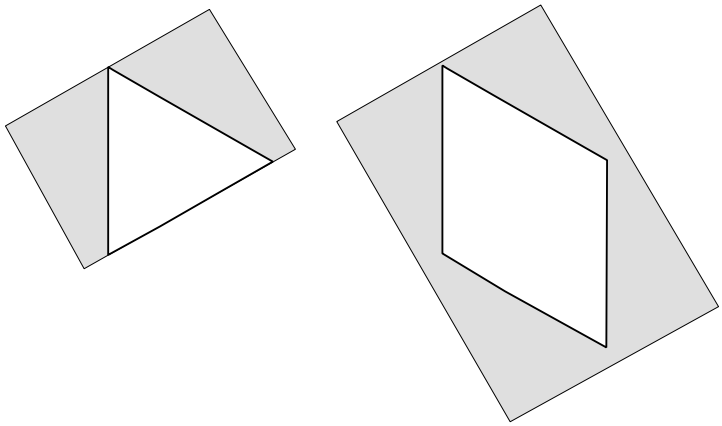

FIGURE 52: *At left is the case* $s_{13} \downarrow s \equiv s_{12} = s_{23}$. *At right* $s_{13} > 2s$, *and it has become impossible for* ① *and* ③ *to anticollide. The quadrilateral box (see again Figure 13) does tesselate the plane, but does not permit unique parity assignments. The equilateral triangular box—which arises from setting all string-lengths equal—is therefore unique in the sense that it alone permits application of the method of images.*

with which we are, in fact, already familiar: a notational adjustment

$$r_1 = \tfrac{a}{4\pi\sqrt{3}} X_2, \quad r_2 = \tfrac{a}{4\pi\sqrt{3}} X_0 \quad \text{and} \quad r_3 = \tfrac{a}{4\pi\sqrt{3}} X_1$$

gives back equations which we encountered already on p. 40.

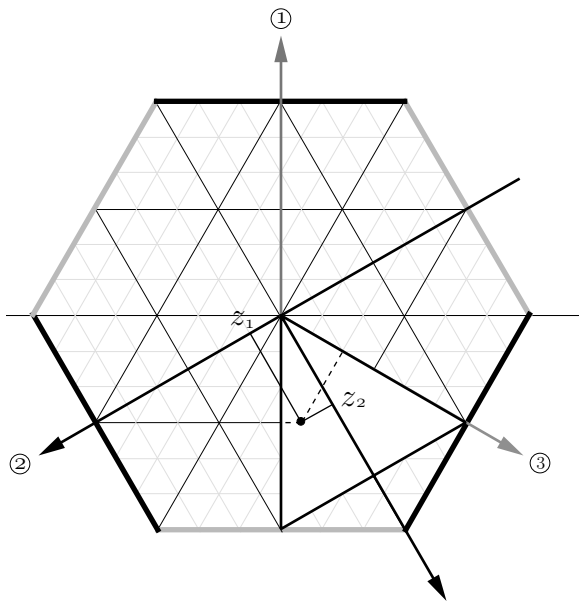

FIGURE 53: *Relationship of the internal molecular coordinates* $\{r_1, r_2, r_3\}$ *to the coordinates* $\{z_1, z_2\}$ *introduced to establish contact with the "particle in an equilateral box problem" (see Figure 23). The size of the triangle is set by the string-length* s*:*

$$\begin{aligned} \textit{height } h &= 2s \\ \textit{base (or side-length) } a &= \tfrac{2}{\sqrt{3}}h = \tfrac{4}{\sqrt{3}}s \\ \textit{area} &= \tfrac{1}{2}ah = \tfrac{4}{\sqrt{3}}s^2 \end{aligned}$$

The special role assigned to r_2 *reflects the physical fact that* ② *is atypical in that it is the only "atom" with neighbors both left and right.*

We have now in hand all we need to obtain an exact account of the internal quantum mechanics of the "one-dimensional string ozone molecule" by direct *reinterpretation* of prior results relating to the "equilateral triangular box problem." We have reproduced precisely the results to which C. Jung was led by a group-theoretic mode of argument.[54] Jung, however, writes without reference to the method of images, or to theta functions, and appears not to have noticed the number-theoretic properties of the spectrum. Concerning the completeness

[54] "An exactly soluble three-body problem in one dimension," Canadian Journal of Physics **58**, 719 (1980). I am indebted to Oz Bonfim for bringing the existence of this paper to my attention.

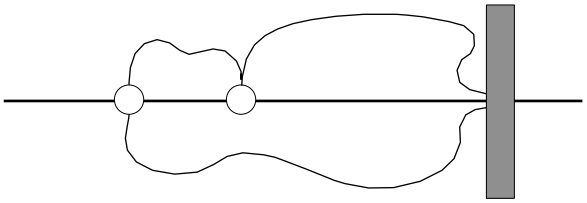

FIGURE 54: *Triatomic string molecule becomes a pinned diatomic string molecule in the limit* $m_3 \to \infty$

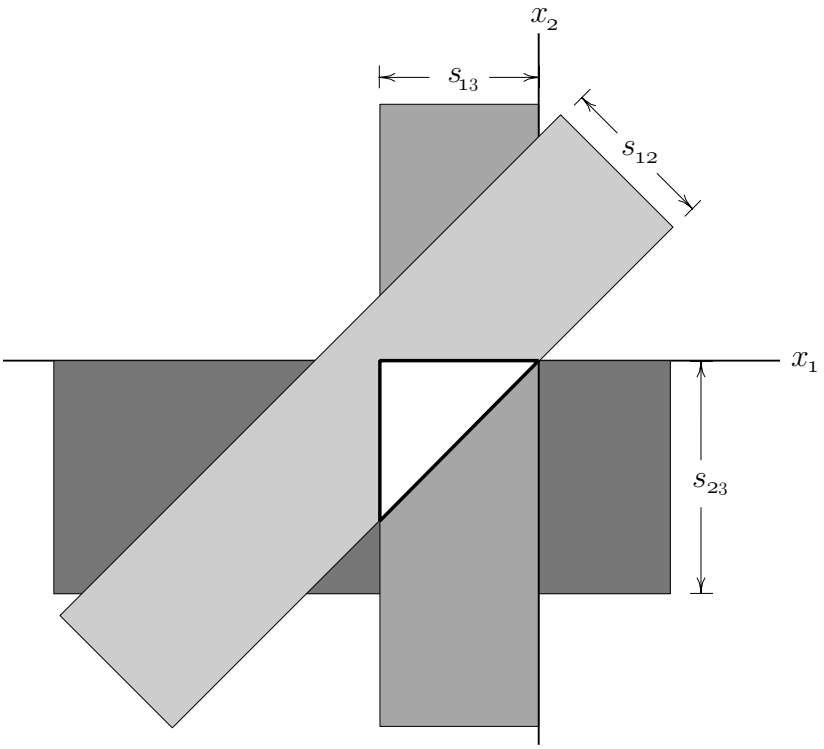

FIGURE 55: *Construction of the configuration space accessible to a pinned diatomic string molecule. It becomes natural to assume as before that all strings have the same length:* $s_{12} = s_{23} = s_{13}$.

of his (non-separable) eigenfunctions (which follows from the fact that they can be assembled to yield the propagator) he advances only the circumstantial spectral evidence (see again (69)) that $\mathcal{N}(E)$ conforms to the "Morse & Feshbach principle" mentioned on p. 67.

Jung does remark the existence of two additional cases that yield also to his group-theoretic mode of analysis. Both of those involve setting $m_3 \to \infty$; the

resulting systems can be thought of as "diatomic molecules bound to points" ("one-dimensional surface chemistry!"), as illustrated in Figure 54. Passage to the limit (equivalently: the presence of the pin or "barrier") serves to break the translational symmetry of the system, and to reduce by one the number of degrees of freedom. Assigning coordinates $x_1 \leq x_2 \leq 0$ to m_1 and m_2, the accessible configuration space is constructed by a variant of Figure 50: see Figure 55 below. Clearly, a two-particle system which is confined to an interval by action of a pin and a string is physically and formally equivalent to a two-particle system confined by the action of two pins. We are brought thus back to precisely the systems studied already in §12. Those are systems—formally equivalent to the 45-45-90 and 30-60-90 box systems studied earlier—which we found yield to the method of images, and which Jung finds yield to the methods of group theory. Notably, Jung appeals not to a group theory but to a result obtained analytically by F. Oberhettinger[55] to identify his tractable cases; Oberhettinger found that "diffraction in a corner of a polygon does not occur whenever the angle of this corner is π divided by an integer." For triangles on has, by this principle, three possibilities and three only:

$$\begin{aligned}
\tfrac{\pi}{4}+\tfrac{\pi}{4}+\tfrac{\pi}{2}=\pi \quad &: \quad \text{the 45-45-90 triangle} \\
\tfrac{\pi}{3}+\tfrac{\pi}{3}+\tfrac{\pi}{3}=\pi \quad &: \quad \text{the 60-60-60 triangle} \\
\tfrac{\pi}{6}+\tfrac{\pi}{2}+\tfrac{\pi}{2}=\pi \quad &: \quad \text{the 30-60-90 triangle}
\end{aligned}$$

One can, by the way, on these grounds understand the "intractability" of the case—otherwise the physically most attractive case—that gives rise to the quadrilateral in Figure 52, wherein two of the angles are $\frac{2}{3}\pi$. It is interesting to notice also that "diffraction physics" and the geometrical "reflective tessellation problem"[56] lead one *via* identical conditions to identical populations of cases. And that the relevant "angles" are in the molecular context set not by the geometry of a literal "box" but (by the mechanism illustrated in Figure 43) by *mass ratios*.

When I remarked that the molecular interpretation of the particle-in-a-box problem "leads naturally to a modest loosening of the constraints that at present so tightly bind us" I had in mind is illustrated in my final figure, and has to do with the imposition of periodic boundary conditions which—though they do arise in connection with the thermal interpretation of our physics (see again the Sommerfeld material mentioned on p. 11)—are not natural to the quantum mechanics of a single particle in a polygonal box. Related topics will be treated in a separate essay, so I will not on this occasion spell out the details, some of which can be found (beginning at p. 238) in FEYNMAN FORMALISM (1971–1976).

Jung himself—proceeding in reverse along the path we have traveled—did not fail to notice that his molecular systems admit of particle-in-a-box

---

[55] J. Res. Natl. Bur. Stand. **61**, 343 (1958).

[56] See again the reference (near the beginning of §6) to work by Wieting.

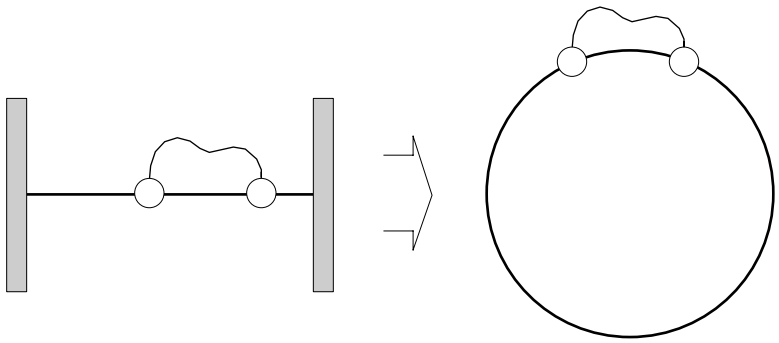

FIGURE 56: *From molecule-in-a-box to molecule-on-a-ring; a reflective phase factor disappears from the analysis, but the method of images survives otherwise intact.*

interpretation, and that they pertain also to the vibration of membranes. It is, I suppose, only "amusing" that our original particle-in-a-box results admit of several alternative lines of physical reinterpretation. More interesting—because more deeply consequential—is the fact which has just emerged: group representation theory and the method of images (at least as they relate to the class of problems which have concerned us) appear to have identical domains of applicability. This, on second thought, is hardly grounds for surprise; the theory of theta functions, particularly in its multivariate formulation, is central to an intensely group-theoretic branch of higher analysis. But it is disquieting news; what I likened at the beginning of §12 to a Mozartian trio has become a quartet. The "rigidity" of group theory would appear (if group theory is an essential member of the ensemble) to diminish the likelihood that I will be successful in my motivating ambition, which is to develop such an enlargement of the theory of theta functions (and, more particularly, of Jacobi's identity) as would permit me to say useful things about (to pick a silly example which lies, however, far beyond my present reach) the 29-62-89 triangle. It remains my hunch—but only a hunch—that Jacobi's beautiful identity is only a symptom of a much deeper mathematics to which the Feynman formalism alludes. In companion essays I will explore details of topics suggested by the preceding (long!) discussion; whatever intrinsic interest may attach to those details, my unspoken objective as I go about the business of patiently "turning over the rocks" will be to find a soft spot in the rigid ediface that stands now before us. My objective will be to lend substance to my hunch—else to expose clearly why it is misguided.